XIAP promotes melanoma growth by inducing tumour neutrophil infiltration

Inaugural-Dissertation

zur

Erlangung des Doktorgrades

der Mathematisch-Naturwissenschaftlichen Fakultät

der Universität zu Köln

vorgelegt von

Mila Daoud

aus Hasaka

Köln, Juni 2022

Berichterstatter: Prof. Dr. Hamid Kashkar
(Gutachter)

Prof. Dr. Manolis Pasparakis

Tag der mündlichen Prüfung: 15.08.2022

Table of contents

Abstract……1

1 Introduction……..2

1.1 Cell death, pro-survival and pro-inflammatory signalling……..2

1.2 Inhibitors of apoptosis proteins (IAPs)……5

1.3 E3 ubiquitin ligase activity……..7

1.4 XIAP……..8

1.4.1 XIAP in inflammatory signalling……...9

1.4.2 Therapeutic targeting of XIAP……13

1.5 Aim of the study……15

2 Material and Methods……..16

2.1 Chemicals……..16

2.2 Antibodies……..16

2.3 DNA constructs……17

2.4 Generation of stable knock-out cell lines……..18

2.5 Subcutaneous injection of B16 cell lines……...18

2.6 Intra-peritoneal injection (IP) of antibodies……...19

2.7 *Hgf-Cdk4*^{R24C} mice……19

2.8 Cell culture……20

2.9 Transfection……...20

2.10 RNA interference (siRNA)……20

2.11 Enzyme-linked immunosorbent assay (ELISA)……21

2.12 RNA isolation……...21

2.13 Reverse transcription and quantitative PCR (qRT-PCR)……21

2.14 PrimePCR^{TM} assay……22

2.15 Western blot……23

2.16 Immunoprecipitation (IP)……24

2.17 Endogenous IP……24

2.18 *In vitro* cell free ubiquitylation assay……25

2.19 Immunofluorescence (IF)……..25

2.20 Immunofluorescence of isolated mice tumours……26

2.21 H&E staining of isolated mice tumours……26

2.22 Immunohistochemistry of isolated mice tumours (IHC)……27

2.23 Immunohistochemistry of human samples……27

2.24 Ethics approval……28

2.25 Cell death assay……28

2.26 Cell proliferation assay……..28

2.27 Statistical analysis……..28

3 Results……30

3.1 XIAP deficiency in B16 mouse melanoma cells reduces tumour growth independently of its anti-apoptotic function……..…30

3.2 XIAP promotes IL8 secretion in melanoma……..32

3.3 RIPK2 and TAB1 act as downstream targets of XIAP……35

3.4 XIAP driven IL8 secretion in melanoma is dependent on interaction with RIPK2 and TAB1……..39

3.5 XIAP supports melanoma growth *via* XIAP-RIPK2-TAB1 signalling complex…42

3.6 XIAP supports melanoma growth by inducing neutrophil infiltration……44

3.7 XIAP supports tumour growth in *Hgf-Cdk4*^{R24C} mouse melanoma model by mediating neutrophil infiltration……50

4 Discussion……54

4.1 XIAP supports melanoma growth independently of its anti-apoptotic function...55

4.2 XIAP mediates IL8 secretion in melanoma……...56

4.3 XIAP mediated IL8 secretion in melanoma is dependent on direct interaction with RIPK2 and TAB1……..……..57

4.4 XIAP supports melanoma tumour growth *via* interaction with RIPK2 and TAB1……..59

4.5 XIAP supports melanoma growth in B16 and *Hgf-Cdk4*^{R24C} mouse melanoma models by inducing neutrophil infiltration……60

4.6 Conclusion……64

5 References……66

6 Appendix……96

6.1 Appendix Table 1: Cytokine/Chemokine transcripts in B16 WT *vs* B16-XIAP^{KO} (clone 1)……96

6.2 Appendix Table 2: Cytokine/Chemokine transcripts in B16 WT *vs* B16-XIAP^{KO} (clone 2)……97

6.3 Appendix Table 3: Intensities of CD177 and XIAP immunostainings in tumour samples derived from melanoma patients……..98

6.4 Appendix Table 4: Cytokine/Chemokine transcripts in *Hgf-Cdk4*^{R24C} *Xiap*^{KO} (mouse 1) *vs Hgf-Cdk4*^{R24C} *Xiap*$^{fl/fl}$……...99

6.5 Appendix Table 5: Cytokine/Chemokine transcripts in *Hgf-Cdk4*^{R24C} *Xiap*^{KO} (mouse 2) *vs Hgf-Cdk4*^{R24C} *Xiap*$^{fl/fl}$……100

6.6 Appendix Table 6: Cytokine/Chemokine transcripts in *Hgf-Cdk4*^{R24C} *Xiap*^{KO} (mouse 3) *vs Hgf-Cdk4*^{R24C} *Xiap*$^{fl/fl}$……101

7 Abbreviation……102

8 Acknowledgments……103

9 Declaration……...104

10 CV……106

Abstract

X-linked inhibitor of apoptosis (XIAP) is a member of the inhibitors of apoptosis proteins (IAPs) and it negatively regulates apoptosis *via* direct interaction and inhibition of caspase activity. XIAP expression is highly increased in malignant melanoma, thus XIAP was considered to mediate apoptosis resistance and therefore promotes melanoma progression. In addition to XIAP anti-apoptotic function, XIAP is involved in inflammatory responses and can induce NFκB activation. However, the inflammatory function of XIAP is still not considered in cancer. Our data show that XIAP supports melanoma tumour growth independently of its anti-apoptotic function. Moreover, XIAP mediates chemokine secretion like IL8, which mediates neutrophil chemo-attraction. Furthermore, our data reveal that XIAP forms a signalling complex with RIPK2 and TAB1. The XIAP-RIPK2-TAB1 complex mediates chemokine secretion and intra-tumoural neutrophil infiltration. Finally, deficiency of XIAP-RIPK2-TAB1 complex or depletion of neutrophils reduced melanoma growth in mice. Collectively, our data revealed a major signalling pathway that mediates melanoma growth and thus, identifies XIAP as a novel therapeutic target in cancer by targeting its inflammatory function.

1 Introduction

1.1 Cell death, pro-survival and pro-inflammatory signalling

Developmental processes, tissue homeostasis, immunity and many other cellular mechanisms require functional cell death. Thus, deregulated cell death is associated with multiple diseases and therefore becomes an interesting therapeutic target. The first described form of cell death was apoptosis (Kerr et al., 1972). Apoptosis is described by several morphological changes leading to DNA fragmentation and the formation of apoptotic bodies (Kerr et al., 1972; Zakeri et al., 1993). Two main pathways mediate apoptosis: the intrinsic and the extrinsic pathways (**Figure 1.1**). The intrinsic pathway is initiated by internal signals like cellular stress leading to mitochondrial outer membrane permeabilisation (MOMP), the release of cytochrome c (Saelens et al., 2004) and the second mitochondria-derived activator of caspase (SMAC or DIABLO) (Fulda et al., 2010). Cytochrome c induces the formation of the apoptosome complex by binding to the apoptotic protease activating factor-1 (Apaf-1) (Zou et al., 1997) and the initiator caspase-9. Within the apoptosome, caspase-9 becomes activated, which in turn activates downstream executioner caspases, caspase-3 and -7 (P. Li et al., 1997). A key regulator of the intrinsic apoptosis is the B cell lymphoma-2 (Bcl-2) proteins family. The Bcl-2 proteins are either pro-apoptotic (like Bad, Bax or Bid), or anti-apoptotic (like Bcl-2 and Bcl-XL) (Ola et al., 2011). Sensitivity of cells to apoptotic stimuli is dependent on the balance between the pro- and anti-apoptotic Bcl-2 proteins (Siddiqui et al., 2015). In particular, MOMP is dependent on Bax and Bak pro-apoptotic Bcl-2 proteins (Green & Kroemer, 2004). Thus, abnormalities in Bcl-2 family function were described to be involved in various diseases like cancer and autoimmune disorders (Siddiqui et al., 2015).

Extrinsic apoptosis is mediated by tumour necrosis factor (TNF) superfamily members like TNF, Fas ligand (FasL) and TNF-related apoptosis-inducing ligand (TRAIL). Interaction of TNF family members with their corresponding receptors leads to the recruitment of Fas associated protein with death domain (FADD). FADD in turn recruits caspase-8 and forms the death inducing signalling complex (DISC) (Medema et al., 1997; Sayers, 2011). Caspase-8 activates itself by oligomerisation-dependent autoproteolytic cleavage leading to the activation of caspase-3 and -7 (Stennicke et al., 1998; Ashkenazi, 2008). Activated caspase-8 can also indirectly activate

caspase-3 *via* BH3-interacting domain death agonist (BID) cleavage and stimulation of MOMP (Ashkenazi, 2008). One major regulator of the extrinsic apoptosis is the cellular FLICE (FADD like IL-1β converting enzyme)-inhibitory protein (c-FLIP). C-FLIP mediates resistance to TNF, FasL and TRAIL induced apoptosis by forming an apoptosis inhibitory complex (AIC) with FADD and/or caspase-8 or -10 and TRAIL receptor 5 (DR5). Thus, preventing the formation of DISC and the subsequent activation of the caspase cascade (Safa 2012).

In addition to cell death, members of the TNF family and their corresponding receptors regulate other cellular processes like cell survival and inflammation by activating the nuclear factor kappa-light-chain-enhancer of activated B cells (NFκB) and mitogen-activated protein kinase (MAPK) signalling pathways. Binding of TNF to TNF receptor 1 (TNFR1) (Bodmer et al., 2002; Wajant & Siegmund, 2019) leads to the recruitment of the TNFR1 associated death domain (TRADD) protein to the cytoplasmic region of the TNFR1 (Hsu et al., 1995). Subsequently, receptor interacting serine/threonine protein kinase 1 (RIPK1) and TNF receptor associated factor 2 (TRAF2) are recruited (Hsu, Huang, et al., 1996; Hsu, Shu, et al., 1996; Ting et al., 1996). Next, cellular inhibitor of apoptosis protein 1 (cIAP1) and cellular inhibitor of apoptosis protein 2 (cIAP2) (cIAP1/2) are recruited to the TNFR1 complex *via* interaction with TRAF2 (Shu et al., 1996; Vince et al., 2009). Following, cIAP1/2 use their E3 ligase activity to mediate poly-ubiquitylation of RIPK1 and other proteins within the TNFR1 complex (Park et al., 2004; Bertrand et al., 2009; Varfolomeev et al., 2008). Thereby, facilitating the binding of the linear ubiquitin chain assembly complex (LUBAC) (Haas et al., 2009; Ikeda et al., 2011). The formed complex consisting of TNFR1, TRADD, TRAF2, RIPK1, cIAP1/2 and LUBAC was described as complex I of the TNFR1 signalling cascade (Pasparakis & Vandenabeele, 2015). LUBAC in turn mediates the formation of linear ubiquitin chains (M1) on several components of complex I like TNFR1, RIPK1 and TRADD (Haas et al., 2009; Ikeda et al., 2011). The formed poly-ubiquitin chain network enables the binding of two kinase complexes: the IκB kinase (IKK) complex and the transforming growth factor β activated kinase 1 (TAK1) complex, which is composed of TAK1 binding protein 1, 2 and 3 (TAB1; TAB2; TAB3). The IKK complex consists of the kinases IKKα and IKKβ in addition to the regulatory subunit IKKγ/NEMO. TAK1 phosphorylates IKKβ

resulting in the activation of the IKKβ kinase domain, which in turn phosphorylates IκBα. Subsequently, IκBα is targeted for ubiquitylation and proteasomal degradation leading to the release of NFκB dimers (p50/p65) that were retained in the cytoplasm. Thus, enabling the NFκB dimers to translocate to the nucleus where these transcription factors mediate the expression of various pro-inflammatory and pro-survival genes (Oeckinghaus et al., 2011). This pathway is termed, the canonical NFκB pathway. The NFκB transcription factor family includes five members in mammals: NFκB1 (p105), NFκB2 (p100), RelA, RelB and cRel (Pahl, 1999; Hayden &Ghosh, 2011). Additionally, TAK1 can activate the MAPK signalling pathway through the extracellular-signal-regulated kinase 1/2 (ERK1/2), Jun N-terminal kinase (JNK), and p38 pathways (Z. Chen et al., 1995; Ghosh & Hayden, 2012; Sabio & Davis, 2014). Besides, activation of NFκB members can be mediated *via* a non-canonical NFκB pathway, in addition to the canonical pathway. The non-canonical pathway induces the activation of a RelB/p52 NFκB complex by processing p100 into p52 in an NFκB inducing kinase (NIK) dependent manner and thus enables the translocation of RelB/p52 heterodimers to the nucleus (S. C. Sun, 2011; Coope et al., 2002; Claudio et al., 2002). The non-canonical pathway was described to regulate various biological functions like bone metabolism, B-cell survival and maturation, and dendritic cell activation (Dejardin, 2006).

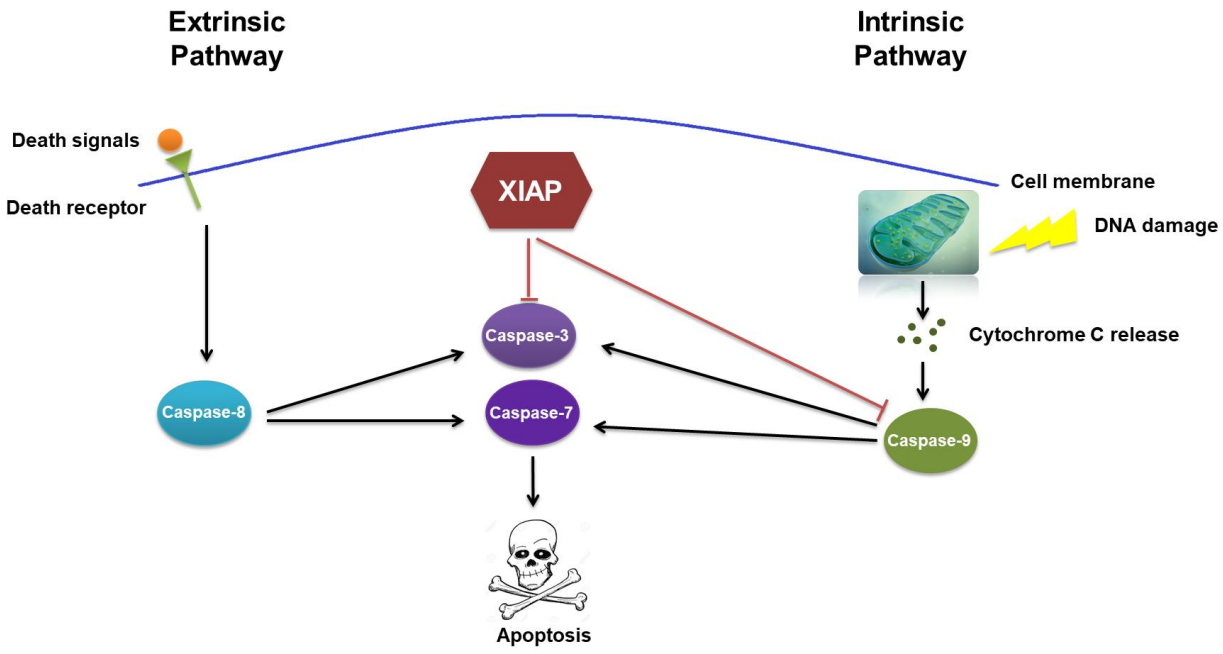

Figure 1.1: Extrinsic and intrinsic apoptosis

Extrinsic apoptosis can be triggered *via* binding of TNF family ligands to their receptors leading to activation of caspase-8, which in turn can activate caspase-3 and -7 resulting in apoptosis. Intrinsic apoptosis can be triggered *via* intracellular stimuli like DNA damage leading to MOMP and cytochrome c release. Subsequently, cytochrome c binds to Apaf-1 leading to caspase-9 activation, which can activate downstream executioner caspases-3 and -7, finally leading to apoptosis. XIAP can inhibit caspase-3, -7 and -9 activities, thereby inhibiting apoptosis.

1.2 Inhibitors of apoptosis proteins (IAPs)

Apoptosis is regulated by various proteins including the inhibitors of apoptosis proteins (IAPs) (Deveraux & Reed, 1999). Viruses have developed strategies to maintain the survival of the infected cells and thus maintain their replication by encoding IAP proteins and here the first IAPs were discovered in the genome of the baculoviruses *Cydia pomonella* granulovirus (CpGV) and *Orgyia pseudotsugata* M nucleopolyhedrovirus (OpMNPV) (Crook et al., 1993; Miller, 1999; Birnbaum et al., 1994). IAP family proteins were found in all metazoans. In humans, eight IAP proteins were discovered: XIAP (also known as inhibitor of apoptosis protein 3 (IAP3), baculoviral IAP repeat-containing protein 4 (BIRC4), and human IAPs like protein (hILP)), neuronal apoptosis inhibitory protein (NAIP or BIRC1), cIAP1 (or BIRC2), cIAP2 (or BIRC3), survivin (BIRC5), ubiquitin-conjugating BIR domain enzyme apollon (BIRC6), melanoma IAP (ML-IAP or BIRC7), and IAP-like protein 2 (ILP2 or BIRC8) (Birnbaum et al., 1994; Ndubaku et al., 2009) (**Figure 1.2**).

IAP proteins are characterised by the presence of one to three N-terminal Baculoviral IAP Repeat (BIR) motifs, mediating protein-protein interaction between IAPs and caspases, IAP antagonists or other proteins (Vaux & Silke, 2005). The BIR domain has a fold consisting of one histidine and three cysteine residues that regulate a zinc ion for stabilisation (Hinds et al., 1999). Most IAPs have a C-terminal really interesting new gene (RING) domain, which has an E3 ligase activity mediating the transfer of ubiquitin to a target substrate (Lorick et al., 1999). XIAP, cIAP1/2 and ILP2 have additionally a ubiquitin associated domain (UBA) mediating the binding of IAP to different ubiquitin chains, which is crucial for different signalling pathways (Gyrd-Hansen et al., 2008; Blankenship et al., 2009). Only cIAP1/2 have a caspase recruitment domain (CARD) mediating protein-protein interactions (Rumble &

Duckett, 2008). NAIP has in addition to the BIR domains, a nucleotide binding oligomerisation domain (NOD) and a C-terminal leucine-rich repeat (LRR) domain, which both regulate the interaction of NAIP-BIR domains with caspase-9 (Davoodi et al., 2004). Survivin has a C-terminal coiled-coil domain that mediates survivin functions in cell cycle (Conway et al., 2000). Whereas, apollon has a C-terminal ubiquitin-conjugating enzyme domain (UBC) (Z. Chen et al., 1999).

Upon MOMP, the mitochondria releases several IAP binding motif (IBM)-containing proteins like SMAC and the high temperature requirement protein A2 (HTRA2 or OMI), which can bind and regulate the IAP family proteins (Du et al., 2000; Miguel Martins et al., 2002). In addition to SMAC and OMI, there were other IAP binding proteins identified like apoptosis-related protein in the TGFβ signalling pathway (ARTS) (Larisch et al., 2000) and XIAP-associated factor 1 (XAF1), which can interact with several IAP proteins and not only XIAP (Liston et al., 2001; Arora et al., 2007).

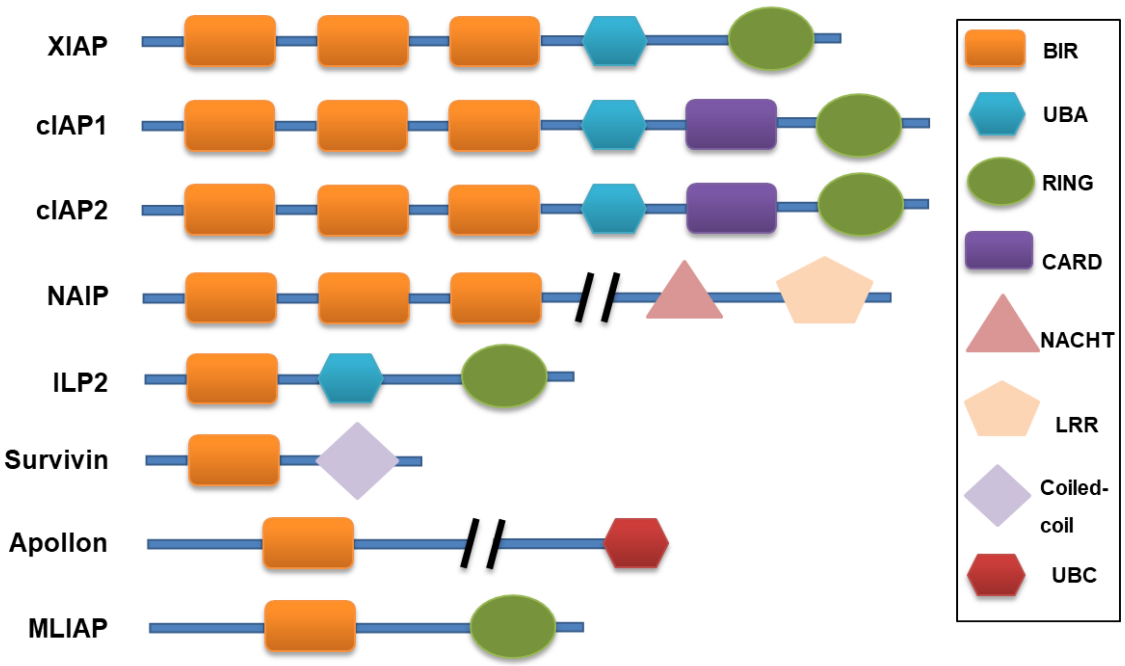

Figure 1.2: Domains of human IAP proteins

Eight IAP proteins were found in humans: XIAP (also known as inhibitor of apoptosis protein 3 (IAP3), baculoviral IAP repeat-containing protein 4 (BIRC4), and human

IAPs like protein (hILP)), cellular IAP1 (c-IAP1 or BIRC2), cellular IAP2 (c-IAP2 or BIRC3), neuronal apoptosis inhibitory protein (NAIP or BIRC1), IAP-like protein 2 (ILP2 or BIRC8), survivin (BIRC5), ubiquitin-conjugating BIR domain enzyme apollon (BIRC6), and melanoma IAP (ML-IAP or BIRC7). Baculoviral IAP repeat (BIR) is conserved in all IAP proteins. XIAP, cIAP1, cIAP2, ILP2 and MLIAP contain a RING domain that has an E3 ubiquitin ligase activity. cIAP1 and cIAP2 have a caspase recruitment domain (CARD). XIAP, cIAP1, cIAP2 and ILP2 contain a ubiquitin associated domain (UBA), which can bind mono-or poly-ubiquitin chains. Apollon has an additional ubiquitin-conjugating domain (UBC). Survivin has a coiled-coil region. NAIP also possesses a nucleotide binding and oligomerisation domain and a leucine rich repeat (LRR) domain (Adapted from Fulda & Vucic, 2012).

1.3 E3 ubiquitin ligase activity

Ubiquitylation is one of the main post-translational protein modifications that regulate protein half-life by targeting them for proteasomal degradation. However, some ubiquitin modifications affect the protein activity instead of targeting them for degradation (Deshaies & Joazeiro, 2009). Ubiquitylation is an enzymatic process resulting in a covalent attachment of a ubiquitin (Ub), a highly conserved protein of 8 kDa, to a lysine (K) residue of target proteins. This process requires the presence of three enzymes including an E1 enzyme mediating ubiquitin activation, an E2 enzyme mediating ubiquitin conjugation and an E3 ubiquitin ligase mediating the transfer of the ubiquitin from E2 to a lysine residue of the substrate (Schulman & Wade Harper, 2009; Deshaies & Joazeiro, 2009) (**Figure 1.3**). The key regulators of the ubiquitylation reaction are the Ub ligases as they specify the timing and the substrate selection of the reaction. Additionally, Ub signals are regulated by deubiquitinating enzymes (DUBs) that can remove or dampen the signal (Hicke & Dunn, 2003). Several Ub modifications can be formed leading to a variety of cellular functions. A single Ub molecule can be attached to form a mono-ubiquitin chain, which was described as a regulatory signal in different processes such as endocytosis and DNA repair (Hicke, 2001; Hoege et al., 2002; Salghetti et al., 2001). Further, poly-ubiquitin chains can be assembled on any of the ubiquitin lysine residues (K6, K11, K27, K29, K33, K48 and K63) (Pickart & Fushman, 2004) or on the methionine at position-1 (M1). The best characterised poly-ubiquitin chains are the ones linked *via* K48 and K63 (Hicke et al., 2005). Poly-ubiquitin chains assembled *via* K48 linkage are known to target proteins for proteasomal degradation (Nath & Shadan, 2009), as well as the

K11 (Baboshina & Haas, 1996; Matsumoto et al., 2010). However, other Ub linkages such as K63 are involved in the regulation of different cellular processes including the TNF signalling cascade and NFκB activation independently of proteolytic degradation (Haglund & Dikic, 2005). Both K27 and K33 linkages could be assembled during stress response (Hatakeyama et al., 2001). Besides, poly-ubiquitin chain assembled *via* K29 was linked to lysosomal degradation (Chastagner et al., 2006). Poly-ubiquitin chain linked *via* M1 also called linear ubiquitylation, is known to mediate immunity and inflammatory signalling *via* TNFR1 and NOD1/2 receptors (Dittmar & Winklhofer, 2020).

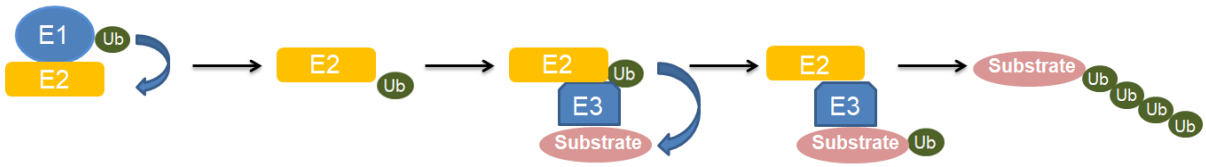

Figure 1.3: The ubiquitylation reaction

A ubiquitin is activated *via* an E1 enzyme, conjugated to an E2 enzyme and finally transferred to a lysine residue of a substrate *via* an E3 ubiquitin ligase.

1.4 XIAP

The name X-linked inhibitor of apoptosis came from the discovery of XIAP after applying a PCR method using IAP homologous sequences from the X chromosome of *Cydia pomonella* granulovirus. The *Xiap* gene is located at chromosome Xq24-25 (Tu & Costa, 2020; Liston et al., 1996). XIAP is ubiquitously expressed in normal tissues but has also been linked to various types of cancer (L. Li et al., 2004; Oost et al., 2004). The structure of XIAP consists of three BIR (BIR 1-3) domains, which can directly bind to and inhibit caspases; therefore it acts as a negative regulator of apoptosis. XIAP can bind and inhibit caspase-3 and -7 *via* interaction of the XIAP linker sequence between BIR1 and BIR2 with the substrate binding site of activated caspase-3 or -7 (Y. Huang et al., 2001; Silke et al., 2001). By contrast, XIAP can inhibit caspase-9 *via* interaction of its BIR3 domain with the caspase-9 IAP binding sequence, thereby preventing caspase-9 homodimerisation (Deveraux et al., 1997; Srinivasula et al., 2001; Shiozaki et al., 2003). Further, it was shown that the BIR1

domain of XIAP binds to TAB1 (Lu et al., 2007) and the BIR2 domain binds to receptor interacting serine/threonine kinase 2 (RIPK2) (Heim et al., 2020). Moreover, XIAP and other IAP proteins such as cIAP1 and cIAP2 contain a C-terminal RING domain, which provides an E3-Ubiquitin ligase activity mediating auto-ubiquitylation or trans-ubiquitylation of corresponding substrates (Vaux & Silke, 2005; Vucic et al., 2011). Additionally, XIAP and cIAP1/2 possess an Ub-binding domain (UBA) that recognises ubiquitylated proteins (Y. Yang et al., 2000; Gyrd-Hansen et al., 2008; Blankenship et al., 2009; Eckelman et al., 2006).

XIAP and IAP proteins have been frequently described to be highly expressed in cancer (Fulda & Vucic, 2012; LaCasse et al., 1998). In particular, high XIAP expression was correlated with diffuse large B cell lymphoma (Hussain et al., 2010), clear-cell renal cell carcinoma (Ramp et al., 2004; Yan et al., 2004), colorectal cancer (Xiang et al., 2009) and hepatocellular carcinoma (Augello et al., 2009). XIAP was also found to be highly expressed in melanoma cell lines as well as, primary and metastatic melanoma tissues (Kluger et al., 2007; Emanuel et al., 2008). Furthermore, high XIAP levels were associated with tumour progression and melanoma thickness. Thus, the anti-apoptotic functions of IAPs, in particular XIAP and its contribution to chemo-resistance and disease progression have been extensively studied (Hunter et al., 2007; Kashkar, 2010; Schiffmann, Göbel, et al., 2019). In contrast, XIAP deficiency causes an immunodeficiency disease called X-linked lymphoproliferative syndrome (XLP type 2/ XLP-2) (Rigaud et al., 2006; Schmid et al., 2011). XLP-2 patients having XIAP mutations show symptoms like fever, splenomegaly, colitis and cytopenia (Schmid et al., 2011). XIAP is known to be an essential ubiquitin ligase in the nucleotide binding and oligomerisation domain (NOD)-like receptors (NLR) such as NOD2-mediated inflammatory signalling. Therefore, XLP-2 pathogenesis was linked to deregulations in the NOD2 signalling (Damgaard et al., 2012).

1.4.1 XIAP in inflammatory signalling

The role of XIAP in the host innate immunity was identified after characterisation of XIAP knock-out (KO) mice, which developed normally with no defects in apoptosis

(Harlin et al., 2001). However, these mice could not mount immunity in response to infection with *Listeria monocytogenes* (Pedersen et al., 2014), *Shigella flexneri* (Andree et al., 2014), *Chlamydophila pneumoniae pulmonary* (Prakash et al., 2010) or after treatment with a peptidoglycans derived from Gram positive or Gram negative bacteria, such as muramyl dipeptide (MDP) (Vucic, 2018).

The inflammatory function of XIAP was described in several signalling pathways including transforming growth factor beta (TGFβ) and bone morphogenetic proteins (BMPs) receptor signalling (Reffey et al., 2001), which were correlated with the role of XIAP in developmental processes (Reffey et al., 2001; Yamaguchi et al., 1999). TGFβ and BMP are cytokines related to the TGFβ superfamily, which mediates various cellular functions (Wrana, 2000; Massague, 2000). In the BMP signalling pathway, XIAP serves as a bridging molecule between the receptor and TAB1 (Yamaguchi et al., 1999). Oncogenic signalling by TGFβ is mediated *via* the E3 ligase activity of XIAP. Upon binding of XIAP to the TGFβ receptor, XIAP ubiquitylates TAK1 and further facilitates NFκB activity (Neil et al., 2009; Reffey et al., 2001; Lewis et al., 2004) (**Figure 1.4**).

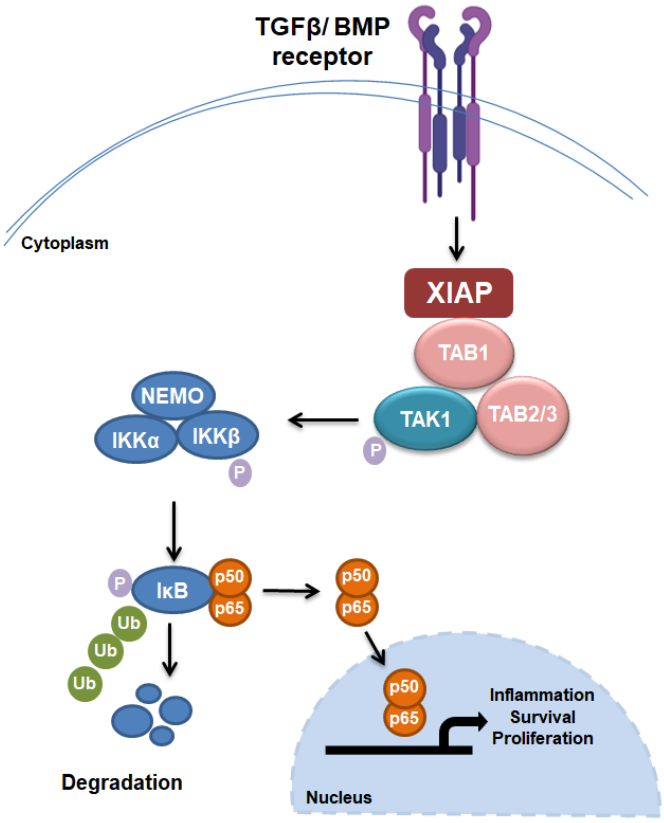

Figure 1.4: XIAP in TGFβ and BMP receptor signalling pathway

Upon TGFβ and BMP receptors activation, XIAP binds to TAB-TAK1 complex leading to the activation of TAK1. TAK1 in turn can activate IKK complex leading to NFκB activation (Adapted from Tu & Costa, 2020 and Oeckinghaus et al., 2011).

Additionally, XIAP can bind to RIPK2 *via* its BIR2 domain (Krieg et al., 2009; Damgaard et al., 2012), which was shown to be essential for NLR signalling *in vitro* and *in vivo* (Bauler et al., 2008; Krieg et al., 2009; Damgaard et al., 2012; Stafford et al., 2018). NOD1 and NOD2 are cytosolic NLR family receptors, which mediate pathogen recognition and are therefore essential factors in the host innate immunity (Caruso et al., 2014; Franchi et al., 2009). Thus, deregulated NOD signalling is associated with inflammatory disorders such as Crohn's disease (Hugot et al., 2001; Ogura et al., 2001). Activation of NOD1 and NOD2 upon bacterial infection or MDP stimulation leads to NOD oligomerisation and recruitment of RIPK2, which gets activated by subsequent auto-phosphorylation. Next, several E3 ligases such as cIAP1/2 and XIAP induce RIPK2 ubiquitylation (Witt & Vucic, 2017), where in deed XIAP was shown to be the main E3 ligase mediating RIPK2 ubiquitylation (Bauler et al., 2008; Damgaard et al., 2012; Goncharov et al., 2018) further recruiting the LUBAC complex (Damgaard et al., 2012; Hasegawa et al., 2008). RIPK2 ubiquitylation is followed by recruitment and activation of TAK1 and IKK complexes (Hasegawa et al., 2008; Inohara et al., 2000; Hrdinka & Gyrd-Hansen, 2017) and finally leading to the activation of the NFκB as well as the MAPK signalling pathways and the secretion of pro-inflammatory cytokines (Damgaard et al., 2012) (**Figure 1.5**). Mutations in XIAP can impair NOD2 mediated inflammatory signalling and cause various immune-deficient disorders such as XLP-2 and inflammatory bowel disease (IBD) (Damgaard et al., 2012; Speckmann et al., 2013; Pedersen et al., 2014).

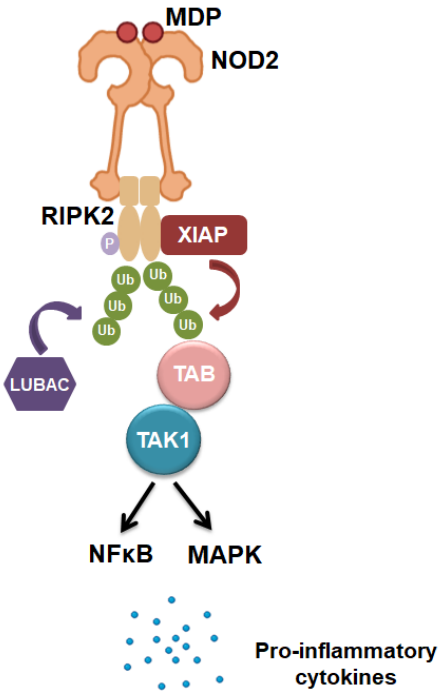

Figure 1.5: XIAP in NOD2 signalling

MDP stimulation leads to NOD2 receptor activation and subsequent activation of RIPK2. XIAP mediates RIPK2 ubiquitylation and recruitment of the LUBAC complex. RIPK2 ubiquitylation can activate the TAK1 complex leading to induction of NFκB and MAPK signalling activation (Adapted from Goncharov et al., 2018).

RIPK2 is a serine–threonine kinase (McCarthy et al., 1998a; Honjo et al., 2021) and is composed of an N-terminal kinase domain (KD), an intermediate domain with unknown function and a C-terminal caspase activation and recruitment domain (CARD), which mediates the engagement with the NOD1/2 receptors through a homotypic CARD-CARD interaction (**Figure 1.6**) (McCarthy et al., 1998b; Chen et al., 2008; Inohara et al., 1998). Thus, RIPK2 acts as an essential adaptor protein for NOD1/2 mediated inflammatory signalling.

RIPK2 is expressed by innate immune cells like antigen-presenting cells (APC) (Chen et al., 2008; Philpott et al., 2014) but also by epithelial cells (G. Chen et al., 2008). Deregulation of RIPK2 expression was shown to mediate IBD (Jun et al., 2013; Garcia-Carbonell et al., 2019). Most RIPK2 inhibitors target the poly-ubiquitylation of RIPK2 rather than the kinase activity by interfering with the interaction between XIAP and RIPK2 such as ponatinib, GSK583 and CSLP37

(Hrdinka et al., 2018; Suebsuwong et al., 2020). Additionally, regions around residues I212 and K209 on the C-lobe of the kinase domain were found to affect the interaction between XIAP and RIPK2. Thus, mutations in I212 or K209 residues can block NOD mediated inflammatory signalling and thereby giving a therapeutic option for diseases associated with excessive NOD signalling (Heim et al., 2020).

Figure 1.6: RIPK2 structure

RIPK2 structure consists of an N-terminal kinase domain (KD), an intermediate domain (INTD) and a C-terminal caspase activation and recruitment domain (CARD). (Adapted from McCarthy et al., 1998).

1.4.2 Therapeutic targeting of XIAP

Resistance to cell death is one of the hallmarks of cancer (Hanahan & Weinberg, 2011a). Therefore, many efforts during the last decades have applied to target the IAP protein family due to their elevated expression in tumour cells and inhibition of apoptosis (Schimmer et al., 2006; Fulda & Vucic, 2012). Most IAP antagonists led to cIAP1 and cIAP2 proteasomal degradation (Fulda & Vucic, 2012). More recently, specific XIAP antagonists were designed but were not sufficient to induce apoptosis in cancer cells (Fulda & Vucic, 2012; Goncharov et al., 2018). Other strategies focused on targeting the physical interaction between the BIR2 domain of XIAP and RIPK2 and thus disrupting NOD2 signalling and the production of inflammatory cytokines by preventing RIPK2 ubiquitylation (Goncharov et al., 2018). Combined treatment of chemo/radio-therapy with death ligands like TRAIL to treat melanoma has faced resistance due to binding of XIAP to caspase-3 (Hörnle et al., 2011).

Endogenously, XIAP is inhibited by SMAC, which is released from the mitochondria upon intrinsic apoptosis. SMAC binds to XIAP through its amino-terminal amino acid residues (Ala-Val-Pro-Ile) (AVPI) preventing XIAP from binding to caspases and accordingly promoting apoptosis (G. Wu et al., 2000; Elsayed et al., 2015). Inhibiting the anti-apoptotic function of XIAP in cancer cells can be done either by targeting XIAP expression through antisense oligonucleotides or by mimicking the IAP binding

motif of SMAC to interrupt the protein-protein interactions using small molecules as pro-apoptotic agents (Sun et al., 2006; Andersen et al., 2005; Schimmer et al., 2006). The antisense oligonucleotide approach is based on 12-30 oligonucleotide stretches of DNA that complement a target mRNA and thus interfere with the translation of a specific gene of interest (Hiscutt et al., 2010). Using antisense oligonucleotides in combination with other cancer treatment showed effectiveness *in vivo* in xenograft models (LaCasse et al., 2006; Shaw et al., 2008) but could not show efficacy in clinical trials (Schimmer et al., 2011).

SMAC mimetics are composed of four amino terminal peptides AVPI derived from SMAC. They can be monovalent having one AVPI motif, or bivalent having two AVPI motifs and thus can bind to both BIR2 and BIR3 domains of XIAP (Ndubaku et al., 2009; Gao et al., 2007; L. Li et al., 2004; Varfolomeev et al., 2007) thereby preventing XIAP from binding to caspases and to SMAC. SMAC mimetic in combination with other cancer treatments have shown efficacy in endorsing cell death in cancer cells as well as in xenograft studies (Arnt et al., 2002; Vucic & Fairbrother, 2007). Nevertheless, SMAC mimetics failed so far to develop as therapeutic agents due to poor pharmacological properties (Vucic et al., 2002; Fulda et al., 2002; Arnt et al., 2002; L. Yang et al., 2003). Additionally, SMAC mimetics have more effects on cIAPs leading to their auto-ubiquitylation followed by proteasomal degradation (Varfolomeev et al., 2007; Vince et al., 2007). Other strategies based on using IAP antagonist in combination with other anti-cancer treatments. For example, a combination of IAP antagonist with chemotherapy was shown to be effective in endorsing apoptosis and thus sensitising different cancers including skin cancer to chemotherapy (Löder et al., 2012; Probst et al., 2010). Additionally, using IAP antagonist in melanoma was considered in combination with death receptor agonist like TRAIL (Fulda & Vucic, 2012). Melanoma treatment is still a challenge due to early metastasis and increasing drug resistance (Hörnle et al., 2011). Therefore, there is a need for the development of new therapeutic strategies for melanoma treatment.

1.5 Aim of the study

XIAP is highly expressed in melanomas and most studies focused on the role of XIAP as an inhibitor of apoptosis. Thus, XIAP was considered to mediate chemo-resistance mainly *via* its anti-apoptotic properties. As deregulated apoptosis is a hallmark of cancer, many therapeutics approaches aimed to target XIAP. However, recent studies showed that XIAP mediates not only inhibition of apoptosis, but also inflammatory responses and NFκB activation. More specifically, XIAP induces TGFβ and BMP signalling pathways through interaction with TAB1. Additionally, XIAP is crucial for NOD1/2 signalling *via* interaction and ubiquitylation of RIPK2. However, the role of XIAP inflammatory function in cancer is still not been considered. Therefore, the current study aimed to investigate the role of enhanced XIAP expression in melanoma and whether its inflammatory function plays a role in this context. We analysed the effect of XIAP, RIPK2 or TAB1 deficiency on melanoma tumour growth in model cell lines, melanoma cells, tumour derived from melanoma patients and two mouse melanoma models. Both apoptosis and inflammatory signalling; *via* analysing cytokine/chemokine secretion and intra-tumoural immune cells infiltration, were examined. Thus, this study would provide novel targeting strategies for melanoma by deciphering one of the signalling pathways that mediate melanoma growth.

2 Materials and methods

2.1 Chemicals

All chemicals used were obtained from Roth, Sigma-Aldrich or Merck, unless indicated elsewhere. TRAIL was purchased from Enzo, m-TNF from R&D, Birinapant from Promocell and Sytox Green from Invitrogen. L18-MDP (MDP) was obtained from Invivogen.

2.2 Antibodies

Table 1: Primary antibodies

Antibody	Isotype	Supplier
TAB1 (#3226)	Rabbit, monoclonal	Cell Signaling
TAB1 (#3387)	Rabbit, polyclonal	ProSci
RIPK2 (#4142)	Rabbit, monoclonal	Cell Signaling
XIAP (#610763)	Mouse, monoclonal	BD Biosciences
XIAP (# M044-3)	Mouse, monoclonal	MBL
Ly6G (#551459)	Rat, monoclonal	BD Pharmingen
Caspase-3 (#9665)	Rabbit, monoclonal	Cell Signaling
Caspase-9 (#ab2014)	Rabbit, polyclonal	Abcam
Caspase-8 (mouse specific) (#4927)	Rabbit, polyclonal	Cell Signaling
c-IAP1 (#ALX-803-335)	Rat, monoclonal	Enzo
RIPK1 (#51-6559GR)	Mouse, monoclonal	BD Biosciences
β-Actin (#A5441)	Mouse, monoclonal	Sigma
c-Myc HRP (#ab62928)	Mouse, monoclonal	Abcam
Ubiquitin (#3936)	Mouse, monoclonal	Cell Signaling
Cleaved caspase-3 (Asp 175) (#9661)	Rabbit, polyclonal	Cell Signaling

Table 2: Secondary antibodies

Antibody	Isotype	Supplier
anti-mouse conjugated to HRP (#A4416)	goat	Sigma
Anti-mouse IgG light chain HRP (#115-035-174)	goat	Jackson ImmunoResearch
Anti-Rabbit IgG HRP linked (#7074)	goat	Cell Signaling
Anti-rat IgG (H+L) HRP (#031470)	goat	ThermoFisher Scientific
Anti-rat Alexa Fluor 488 (#A11006)	goat	life technologies
anti-rabbit Alexa Fluor 594 (#A11012)	goat	life technologies

2.3 DNA constructs

DNA constructs were provided by Dr. Pia Nora Broxtermann. The desired ORF were amplified by PCR and cloned into a pcDNA 3.1+ vector having a myc-tag sequence (Invitrogen) or into a pEGFP-C3 vector (Clontech).

Table 3: DNA constructs

Name	ORF	Vector
GFP	-	pEGFP-C3
GFP-XIAP	XIAPwt	pEGFP-C3
myc-XIAP	XIAPwt	pcDNA3.1+ myc
myc-XIAP$^{\Delta BIR1}$	XIAPΔBIR1	pcDNA3.1+ myc
myc-XIAP$^{\Delta BIR2}$	XIAPΔBIR2	pcDNA3.1+ myc
myc-XIAP$^{\Delta BIR3}$	XIAPΔBIR3	pcDNA3.1+ myc
myc-XIAP$^{\Delta RING}$	XIAPΔRING	pcDNA3.1+ myc

2.4 Generation of stable knock-out cell lines

Gene knock-out in cell lines was carried out by using CRISPR/Cas9 gene editing (Ran et al., 2013). Cells were transfected with the desigend oligonucleotide sgRNAs (purchased from Eurofins Genomics or designed and purchased from Sigma-Aldrich as indicated in **Table 4**), cloned into the pSpCas9(BB)-2A-GFP (PX458) vector (a gift from F. Zhang; Addgene plasmid 48138). Transfected cells, expressing GFP, were sorted according to their expression with a BD Influx™ cell sorter (BD Biosciences). GFP positive cells were cultured for 4 days, followed by diluting cells to a single cell suspension plated on a 96-well plate. Next, the plated cells were grown in an appropriate colony size and analysed *via* Western blot and sequencing.

Table 4: Oligonucleotide sgRNAs sequences

Targeted locus	Sequence (5'-3')
Mouse XIAP (sigma)	CATCAACATTGGCGCGAGC
	AAGCCAAGTGAAGACCCTT
Human XIAP (sigma)	ATCAACACTGGCACGAGCAGGG
	GACTCTATACACAGGTATTGG
Mouse TAB1	AACCGCAGCTACTCTGCTGA
	GCGCCACAAAGTTGGTCACG
Human TAB1	TGCCATCAGCAGAGTAGCTG
	AACCGCAGCTACTCTGCTGA
Mouse RIPK2	GGTCGGCGAGCTTGTGGTA
	GCAGGATGCGGAATCTAA
Human RIPK2	GAATTTTTGGGAATAGTTAC
	TTGAGATTTCGCATCCTGCA

2.5 Subcutaneous injection of B16 cell lines

BL/6 mice were recieved from the CECAD animal facility. At age of 8-12 weeks, mice were subcutaneously injected into the flank region with 100 µl of 1 x 10^7 cells/ml of B16 WT cells or *in vitro* generated B16 knock-out (KO) cells (This was done by Dr. Jens Seeger). Tumour growth was measured in 2 dimensions every second day. When reaching a tumour size of 15 mm in diameter, the mice were sacrificed. Tumour volume was calculated as length × width^2 × π/6 (Schiffmann et al., 2020; Witt

et al., 2015). For *in vivo* experiments, the majority of analyses included at least 3 mice per group in a simple experiment. Mouse experiments were repeated in independent experimental replicates. Sample size estimate was based on our previous studies and the approval by the German Regulations for Welfare of Laboratory Animals.

2.6 Intra-peritoneal injection (IP) of antibodies

IP injection of IgG2a (InVivo plus, clone C1.18.4) or Ly6G (InVivo plus, clone 1A8) was performed 1 day prior to the injection of tumour cells until the end of the experiment in a dose of 100 µg antibody in 100 µl PBS per mouse per day (Coffelt et al., 2015; Schiffmann et al., 2019; Szczerba et al., 2019).

2.7 *Hgf-Cdk4^{R24C}* mice

Xiap^{KO} and *Hgf-Cdk4^{R24C}* mice were described previously (Andree et al., 2014). For carcinogen-induced tumour growth, neonates were treated with 160 nmol neonatal carcinogen (7,12-dimethylbenz[a]anthracene (DMBA)) treatment in acetone 4 days after birth. Development of melanocytic neoplasms and other skin tumours in both, untreated and DMBA-treated animals was monitored weekly. Nevi and melanomas were counted and tumour size was measured in two dimensions using a calliper (tumour size is given in mm^2). When a single tumour reached a size of approx. 1.5 cm, or the sum of tumours was exceeding 3.0 cm in diameter, the animals were sacrificed (This analysis was done by Dr. Fabian Schorn). Animals were housed in the animal care facility of the University of Cologne under standard pathogen-free (SPF) conditions with a 12 h light/dark schedule and provided with food and water ad libitum. Animal experiments were performed following German Regulations for Welfare of Laboratory Animals and with approval by LANUV NRW (NRW authorization for generation of the line 84-02.04.2015.A471 and 84-02.04.2016.A012 to analyse tumour development).

2.8 Cell culture

HeLa, HEK293T, B16 cells were purchased from ATCC. HCT116 and HCT-XIAP^{KO} were a kind gift from Prof. Dr. Mads Gyrd-Hansen (University of Oxford, Great Britan) and have been previously described (Cummins et al., 2004). M5, BLM, Colo38 and SK-Mel28 have been previously described (Zigrino et al., 2005). HeLa, HEK293T and B16 cells were cultured in DMEM (Merck) supplemented with 10% FCS (Biowest), 100 µg/ml streptomycin and 100 unit/ml penicillin (Merck). HCT116 cells (human colon cancer cell line) were cultured in McCoy's 5A (Merck) supplemented with 10% FCS (Biowest). M5, BLM, Colo38 and SK-Mel28 melanoma cells were cultured in RPMI (Merck) supplemented with 10% FCS (Biowest), 100 µg/ml streptomycin, 100 unit/ml penicillin (Biochrom) and non-essential amino acids (Biochrom). Cells were cultured at 37°C and a CO2 saturation of 5%. Cells were routinely tested for mycoplasma contaminations by PCR.

2.9 Transfection

Cells were transfected with respective constructs for 16 h using Lipofectamine® 2000 (Invitrogen) or Polyethylenimin (PEI) (Polysciences Europe GmbH) according to the manufacturer's instructions.

2.10 RNA interference (siRNA)

Cells were transfected with 50 nM of the respective siRNA for 48 h using Lipofectamine® RNAi MAX™ (Invitrogen) according to the manufacturer's instructions.

Table 5: siRNA sequences

siRNA	Sequence
siXIAP	5'-GGAAUAAAUUGUUCCAUGCTT- 3'
siTAB1	5'-GGAUGAGCUCUUCCGUCUUUU- 3'
siRIPK2	5'-GUAUGAUCUCUCUAAUAGA- 3'
siScr	5'-GGA UUA CUU GAU AAC GCU AUU- 3'

2.11 Enzyme-linked immunosorbent assay (ELISA)

Human melanoma cells were seeded on 12-well plates and transfected with siRNA either alone for 48 h or additionally treated with TNF 20 ng/ml (Biomol) for 8 h. Medium was changed and collected after 48 h. HEK293T, HCT116-TAB1^{KO} and HCT116-RIPK2^{KO} cells were seeded on 12-well plates and transfected with indicated plasmids for 16 h. Medium was changed and collected after 24 h. HCT116 cells were treated with MDP (1 µg/ml) for 24 h. Supernatant was collected and frozen at -20°C. Human melanoma cells were treated with Birinapant 20 µM (Biozol), BV6 2 µM (Universal Biologicals) or XB2d89 (d89) 2 µM (Genentech, USA). Analysis of secreted IL8 was performed using human CXCL8/IL8 DuoSet ELISA (R&D Systems, Minneapolis, USA) according to the manufacturer´s instructions.

2.12 RNA isolation

RNA was isolated using either RNeasy Kit (Qiagen) according to the manufacturer's instructions or standard phenol-chloroform-method (Chomczynski & Sacchi, 1987). Cells were resuspended in TRIzol® (Ambion, Life Technologies) and afterwards homogenised using QIAshredder columns (Qiagen). Chloroform was added to the homogenate of cells, incubated on ice and centrifuged to separate the homogenate into a lower organic layer containing DNA and proteins, an interphase and an upper aqueous layer containing the RNA. Aqueous layer was collected; RNA was precipitated by adding isopropanol, washed with 70% Ethanol and resolved in nuclease free water. RNA was quantified by measuring at wavelength 260nm with a spectral photometer (NanoDrop®) and stored at -80°C. To purify RNA from single- and double-stranded DNA, RNA was digested with DNaseI (Thermo Scientific) according to the manufacturer´s instructions. Level of purity was checked by agarose gel electrophoresis.

2.13 Reverse transcription and quantitative PCR (qRT-PCR)

RevertAid^{TM} Premium First Strand cDNA Synthesis Kit (ThermoFisher) was used to synthesis the cDNA from the RNA with oligo dT-primers according to the manufacturer´s instructions. qRT-PCR was performed with specific primers. LightCycler® SYBR-Green I Mix (Roche Applied Sciences) was used with a 96-well-

plate Multicolor Real-Time PCR Detection System (iQTM5, BIO-RAD). Data were further evaluated as previousely described (Schiffmann et al., 2020) and target gene expression was normalised to the reference gene Actin.

Table 6: qRT-PCR primers sequence

Primer	Sequence
Cxcl10	Fwd: AGTGCTGCCGTCATTTTCTG Rev: ATTCTCACTGGCCCGTCAT
Cxcl1	Fwd: ACTGCACCCAAACCGAAGTC Rev: TGGGGACACCTTTTAGCATCTT
Actin	Fwd: CTGAGAGGGAAATCGTGCGT Rev: AACCGCTCGTTGCCAATAGT
Il6	Fwd: CTGCAAGAGACTTCCATCCAG Rev: AGTGGTATAGACAGGTCTGTTGG
Il1b	Fwd: CCTGAACTCAACTGTGAAATGC Rev: GATGTGCTGCTGCGAGATT
Tnf	Fwd: TGGCCTCCCTCTCATCAGT Rev: CTTGGTGGTTTGCTACGACG
Ccl5	Fwd: AGATCTCTGCAGCTGCCCTCA Rev: GGAGCACTTGCTGCTGGTGTAG
Ccl19	Fwd: TTCACCACACTAAGGGGCTA Rev: GCCACAGAGAGATGGTGTTC
Vegfa	Fwd: CCTGGTGGACATCTTCCAGGAGTA Rev: GAAGCTCATCTCTCCTATGTGCTGG

2.14 PrimePCR™ assay

To determine the transcription level of different cyto- and chemokine, Bio-Rad PrimePCR™ Assay Plate Cytochemokine Tier 1 H96 or M96 were used. The assay

was performed according to the manufacturer´s instructions. Data analysis was carried out with Bio-Rad PrimePCR analysis software.

2.15 Western blot

Whole cell lysates were prepared using either CHAPS lysis buffer (10mM HEPES pH 7.4, 150 mM NaCl, 1% (w/v) CHAPS, protease inhibitor (complete Mini, Roche, Germany)), or RIPA lysis buffer (1% Triton X100, 150 mM NaCl, 50 mM Tris pH 7.4, 0.1% SDS, 0.5% Na-deoxycholat, protease inhibitor (complete Mini, Roche, Germany)). Collected cell pellets were resuspended in 1 pellet volume lysis buffer, incubated for 20 min on ice, followed by centrifugation at 20,000xg for 20 min at 4°C. Proteins concentrations of cell lysates were measured using a Pierce BCA Protein Assay (Thermo Fisher Scientific, Waltham, U.S) according to the manufacturer's instructions. Proteins were separated by SDS–PAGE and transferred to a nitrocellulose membrane (GE healthcare). Membranes were developed using a ChemiDoc MP Imaging System (BioRad).

Table 7: Buffers for Western Blotting

Buffer	Ingredients
Laemmli sample buffer (5x)	25% glycerol 0.6 M Tris-HCl 144 mM SDS 0.1% brome phenol blue
SDS Running buffer	14.4% (w/v) Glycin 3% (w/v) Tris Base 0.1% (w/v) SDS
Transfer buffer (Blot)	25 mM Tris Base, pH 8.3 192 mM Glycin 20% (v/v) Methanol
Blocking buffer	10 mM Tris-HCl, pH 7.4 – 7.6 150 mM NaCL 5% (w/v) Skim milk powder

	2% (w/v) BSA 0.1% (v/v) Tween-20
Washing buffer	50 mM Tris-HCl, pH 7.5 150 mM NaCl Optional: +0,1% Tween for TBS-T buffer

2.16 Immunoprecipitation (IP)

HCT116 cells were transfected with respective constructs for 24 h. Cells were collected and lysed using IP-lysis buffer from µMACS c-myc Isolation Kit (Miltenyi Biotec), incubated 20 min on ice and centrifuged at 20,000xg for 20 min at 4°C. Lysates were magnetically labeled with µMACS c-myc MicroBeads. Immunoprecipitation was performed according to the manufacturer's instructions and analysed by Western blot.

2.17 Endogenous IP

Immunoprecipitation of endogenous proteins analysis was done as described previously (Albert et al., 2020). In brief, cells were washed with chilled PBS and centrifuged at 700xg for 3 min. The cell pellet was resuspended in lysis buffer (Miltenyi Biotec) in addition to *N*-ethylmaleimide (NEM) (Sigma-Aldrich) and 1× complete protease inhibitor cocktail (Roche) followed by 30 min incubation on ice and centrifugation for 20 min at 20,000×g at 4°C. Supernatant was collected and incubated first 1 h with a respective antibody against XIAP (#14334, Cell Signaling) at 4°C on a rotating wheel followed by overnight incubation with Protein A/G Plus agarose beads (sc-2003, Santa Cruz). Beads were washed 3× with PBST (PBS + 0.1% Tween 20).

Immunoprecipitation of endogenous ubiquitylated RIPK2 was carried out as described above. The cell pellet was resuspended in RIPA buffer (1% Triton, 150 mM NaCl, 50 mM Tris, 1% SDS, 0.5% deoxycholate) in addition to *N*-ethylmaleimide (NEM) (Sigma-Aldrich) and 1× complete protease inhibitor cocktail (Roche) followed by 30 min incubation on ice and centrifugation for 20 min at 20,000×g at 4°C. SDS concentration was diluted to 0.1% SDS prior to antibody incubation. Lysates were

incubated first 1 h with a respective antibody against RIPK2 (#4142, Cell Signaling) at 4°C on a rotating wheel followed by overnight incubation with Protein A/G Plus agarose beads (sc-2003, Santa Cruz). Beads were washed 3× with PBST (PBS + 0.1% Tween 20).

2.18 *In vitro* cell free ubiquitylation assay

The following recombinant proteins were used: UBE1, His-UbcH7, ubiquitin (Boston Biochem), flag-XIAP (BPS Bioscience) and GST-RIPK2 (technical novusbio). Ubiquitin assay was performed in 10× E3 ubiquitin ligase buffer (Enzo) and 10× activation buffer (Enzo) for 2 h at 37°C followed by 5 min on ice. The reaction was done using 2 µg ubiquitin, 1 µg E2 (UbcH7), 0.4 µg E1 (UBE1), 0.5 µg substrate (RIPK2), and 0.78 µg E3 (XIAP) in a total amount of 25 µl reaction.

2.19 Immunofluorescence (IF)

Immunofluorescence analysis was performed as described previously (Albert et al., 2020). In brief, HCT116 or HeLa cells were seeded on coverslips in 12-well plate and transfected with GFP-XIAP for 16 h. Cells were washed with PBS and subsequently fixed with 3% paraformaldehyde in PBS for 20 min. Cells were blocked and permeabilised with blocking buffer for 30 min and later incubated with primary antibodies (**Table 1**) in a humid chamber overnight at 4°C. After incubation, coverslips were washed with washing buffer three times and incubated with secondary antibody (**Table 2**) for 1 h at room temperature. Subsequently, cells were stained with 300 nM DAPI (Molecular Probes, Lifetechnologies) for 10 min and washed three times and embedded with mowiol overnight. For imaging, Fluoview FV1000 confocal microscope (Olympus GmbH) was used (objective: Olympus PlanApo, 60x/1.40 oil, ∞/0.17).

Table 8: Buffers for immunoflourescence sample preparation

Buffer	Ingredients
Washing buffer	0.1% Saponin in PBS
Blocking buffer	0.1% Saponin

	3% BSA in PBS
Mowiol	10% Mowiol 25% Glycerol 0.1 M Tris 2.5% DABCO in H2O

2.20 Immunoflourecense of isolated mice tumours

Tumours were embedded in O.C.T. compound, Tissue-Tek, and stored at −80 °C. To analyse neutrophils infiltration, cryosections (10 µm) were fixed in aceton, washed with PBS, blocked with 10% normal goat serum in addition to 5% BSA and stained with a monoclonal rat anti-mouse Ly6G (**Table 1**). Secondary Alexa Fluor 488 goat anti-rat antibody (**Table 2**) was used. To analyse active caspase-3, cryosections (10 µm) were fixed in 10% PFA, washed with PBS, blocked with 10% normal goat serum and stained with a polyclonal rabbit anti-cleaved caspase-3 (Asp 175) (**Table 1**). Secondary Alexa Fluor 594 goat anti-rabbit antibody (**Table 2**) were used (Günther et al., 2020). Immune cell phenotyping was performed using IHC Antibody Sampler Kit (#37495, Cell Signaling). All antibodies were used in a 1:200 dilution. Secondary Alexa Fluor 488 goat anti-rabbit antibody (1:1000, #A11008, life technologies) was used. Tumour cells nuclei were stained with 4,6-diamidin-2-phenylindol (DAPI). Imaging was conducted on a motorized inverted Olympus IX81 microscope (CellR Imaging Software) or Fluoview FV1000 confocal microscope (Olympus GmbH) was used (objective: Olympus PlanApo, 60x/1.40 oil, ∞/0.17). Cl-Caspase-3+ areas were calculated using ImageJ software (http://imagej.nih.gov/ij). Number of Ly6G+ infiltrates were counted manually (L. M. Schiffmann et al., 2019).

2.21 H&E staining of isolated mice tumours

Cryosections from B16 tumours were incubated for 10 min in tap water, 3.5 min in Hematoxylin, shortly washed with tap water followed by 15 min incubation with tap water and then 1 min in demineralised water. Next, sections were incubated for 1 min in Eosin followed by dehydration in a serial of ethanol dilutions and Xylol. Sections were fixed with Entellan.

2.22 Immunohistochemistry of isolated mice tumours (IHC)

Paraffin sections were deparaffinised in alcohol series, washed with demineralised water followed by bleaching which was done as following: 20 min incubation with 30% H2O2 and 0,5% KOH at 37°C, 20 sec incubation with 1% acetic acid and washed with demineralised water. Antigen unmasking was done using Citrate buffer (pH 6) with 0.05% Tween 20, heated 4x in the microwave and cooled down at RT for 20 min. Next, blocking was done using 10% BSA in TBS for 30 min. After that, sections were stained with a monoclonal rat anti-mouse Ly6G primary antibody (1:500, #551459, BD Pharmingen) diluted in 1% BSA and TBS at 4°C overnight. Chromogen staining was done as following: incubation with goat anti-rat biotin conjugated secondary antibody (1:500, #112-065-003, JacksonImmunoResearch) for 45 min at RT, 3x washing with TBS for 5 min, 15 min incubation with Alkaline phosphatase (Fa.DCS #AD000RP) followed by 3x washing with TBS. Sections were incubated with Chromogen (Fast Red Substrate Pack, Fa. BioGenex #HK182-5KE) for 5 min. Nuclear staining was done by incubating the sections with Hematoxylin for 1 min, followed by 3x washing in warm tap water and finally washed with demineralised water.

2.23 Immunohistochemistry of human samples

Paraffin-embedded sections (7 µm) of human melanoma specimens from patients diagnosed at the University Hospital of Cologne were obtained using a Thermo Shandon Finesse Microtome, collected on microscope slides (Gerhard Menzel GmbH) and dried overnight at 37°C. Sections were deparaffinised by incubation of the slides in xylene (20 min) followed by a graded alcohol series (1 min each): isopropyl alcohol, 96% EtOH, 75% EtOH, distilled water.

Antigen retrieval was performed using Target Retrieval System pH 6.0 (TRS, Dako) in a preheated water bath at 95°C for 20 min. Slides were cooled at RT before immersing in wash buffer for the next step. Sections were washed three times in TBS blocked for 1 h with 10% BSA in TBS. Primary antibodies diluted in TBS, 1% BSA were added to the sections and incubated overnight at 4°C in a humidified chamber. The following antibodies were used: rabbit-anti-CD177 (1:400, #PA5-83575, Invitrogen) and rabbit-anti-XIAP (1:100, #ab21278, Abcam). After 2x5 min washes in

TBS, bound antibodies were detected using the DAKO REAL kit (K5005) and fast red (#HK182-5KE, Fa. BioGenex) as a substrate. Nuclei were counterstained with hematoxylin solution for 1 min (Shandon). Stained sections were viewed and recorded using Leica DM 4000B microscope (Leica) equipped with Diskus program version 4.50.1638 - #393. Expression of XIAP and amount of CD177 positive cells were qualitatively estimated according to the intensity of specific staining and were arbitrarily set as the following: -, not expressed; +, low; ++, moderate; +++, strong.

2.24 Ethics approval

Human materials were obtained according to the study protocol confirmed to the ethical guidelines of the 1975 Declaration of Helsinki and were approved by the Ethics Committee of the Medical Faculty of the University of Cologne (Approval No. 21-1006). Informed consent has been obtained.

2.25 Cell death assay

20,000 cells were seeded on 96-well plate and treated with either 100 ng/ml TNF (R&D), 50 ng/ml TRAIL (Enzo), DMSO (Roth) or 2 mM H_2O_2 (Roth) for 24 h. Treatments were done in the presence of 5 µM Sytox Green (Invitrogen). Analysis of cell death was performed using an IncuCyte system (SARTORIUS). Scanning was done every 1 or 2 h over 24 h with 20x magnification. Cell death was determined as Sytox positive cells and quantified with the software supplied by the manufacturer.

2.26 Cell Proliferation assay

Cell proliferation assay of generated CRISPR/Cas9 cell lines was assessed *in vitro* by using Incucyte Live-Cell-Analsis according to the manufacturer's instructions.

2.27 Statistical analysis

Data are presented as mean ± SD or ± s.e.m. *In vitro* experiments were repeated at least two times. The respective tests or analyses are listed in the figure's legend. Significances were indicated as *P < 0.05, **P < 0.01, ***P < 0.001, ****P < 0.0001,

and ns, not significant. GraphPad Prism 7.0 and Excel were used to analyse the data in this study.

3 Results

3.1 XIAP deficiency in B16 mouse melanoma cells reduces tumour growth independently of its anti-apoptotic function

XIAP is highly expressed in melanoma patients and was described to be associated with melanoma progression (Emanuel et al., 2008). Therefore, to understand the exact mechanism how XIAP is involved in melanoma tumour growth, XIAP knock-out ($XIAP^{KO}$) B16 mouse melanoma cell lines were generated using CRISPR/Cas9. Two independent single guide RNAs (sgRNAs) targeting the *Xiap* gene at different sites were used (**Table 4**). Western blot analysis showed the successful deletion of XIAP in two different cell clones (clone 1 and 2) (**Figure 3.1A**). Expression levels of other proteins were not affected in both $XIAP^{KO}$ lines (**Figure 3.1A**). Next, we employed a syngenic melanoma mouse model involving immune-competent mice bearing cutaneous B16 melanomas (Schiffmann et al., 2020; Witt et al., 2015). Two independent clones of B16-$XIAP^{KO}$ or B16 wild type (WT) melanoma cells were subcutaneously injected in BL/6 mice. Both WT and $XIAP^{KO}$ B16 cells formed palpable tumours and the tumours volume was measured over 14 days. The tumour volume was significantly reduced in the $XIAP^{KO}$ tumours (**Figure 3.1B**), indicating a crucial role for XIAP in melanoma tumour growth.

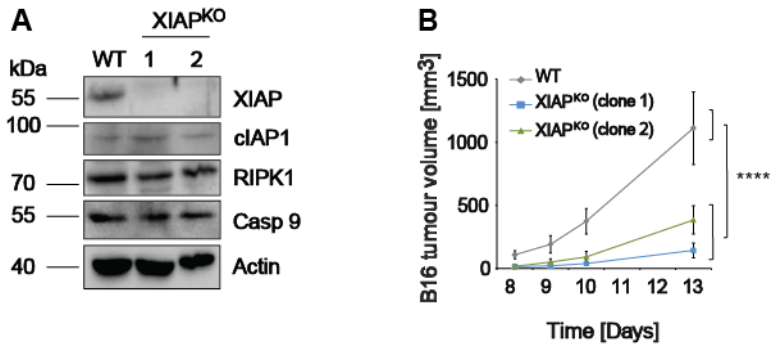

Figure 3.1: XIAP deficiency in B16 mouse melanoma cells reduces tumour growth

A Western blot analysis of B16 WT and two independent $XIAP^{KO}$ cell lines. Actin was used as a loading control. **B** Subcutaneous melanoma growth in BL/6 WT mice (n=5) using B16 WT and $XIAP^{KO}$ (clone1 and 2) cells. Data are presented as mean ± s.e.m. Two-way analysis of variance (ANOVA) followed by Dunnett's post-analysis. ****P < 0.0001 (this analysis was done by Dr. Pia Nora Broxtermann).

Various melanoma cells overexpress XIAP to resist apoptosis (Hartman & Czyz, 2013). To examine whether the reduced tumour volume in XIAP^{KO} melanomas was due to a higher susceptibility towards apoptotic cell death, we analysed the activation of the apoptotic machinery in B16 WT and XIAP^{KO} tumours. A staining for cleaved caspase-3 (cl-caspase-3) showed no differences in both B16 WT and XIAP^{KO} tumours (**Figure 3.2A**). Next, the apoptotic properties of B16-XIAP^{KO} cells were analysed *in vitro* in response to various cell death-inducing stimuli. Incucyte analysis was performed after treating B16 WT and XIAP^{KO} cells with TNF or TRAIL. Both, B16 WT and XIAP^{KO} melanoma cells were resistant towards cell death induced by TNF treatment in addition to TRAIL (**Figure 3.2B** and **C**), which was previously described (Zeise et al., 2004). Additionally, there was no difference in proliferation in both B16 WT and XIAP^{KO} cells (**Figure 3D**). Taken together, these data suggest that cell death is not the underlying mechanism behind the reduced tumour volume in the B16-XIAP^{KO} melanomas.

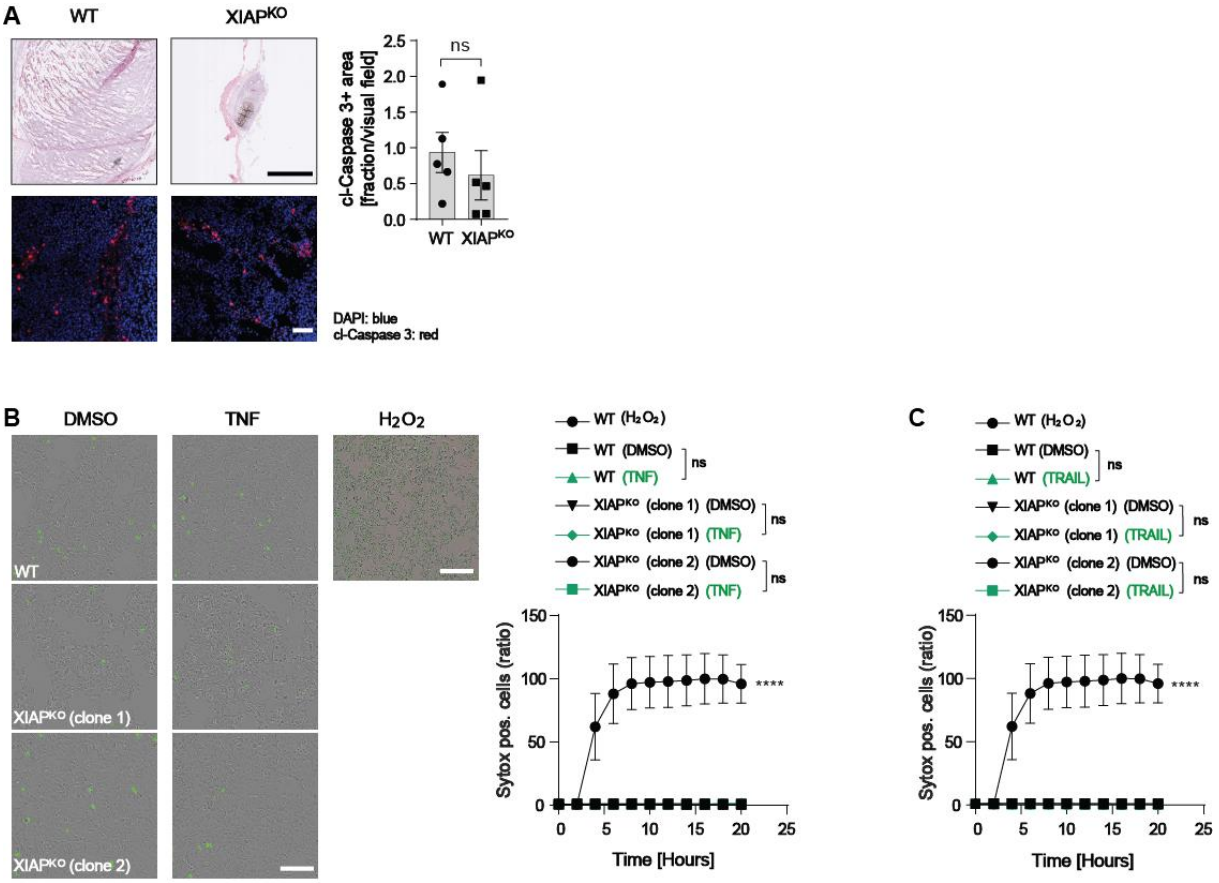

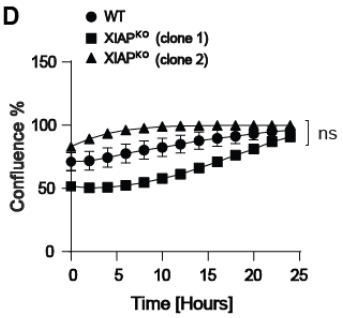

Figure 3.2: XIAP deficiency in B16 mouse melanoma cells reduces tumour growth independently of its anti-apoptotic function

A Representative H&E (scale bar 50 µm) and fluorescent (Scale bar 100 µm) images of cl-Caspase-3 staining in B16 WT and XIAP^{KO} tumours (left panel). Nuclei were stained with DAPI (blue). Quantification thereof (right panel). Dots represent individual mice (n=5). Data are presented as mean ± s.e.m. Mann-Whitney, two-tailed test analysis. **B** Representative Incucyte images and cell death measurements using Sytox Green in B16 WT and XIAP^{KO} (clone 1 and 2) cells after 24 h treatment with 100 ng/ml TNF. DMSO was used as a negative control. Scale bar 200 µm. 2 mM H_2O_2 was used as a positive control. Scale bar 400 µm. **C** Incucyte cell death measurements using Sytox Green in B16 WT and XIAP^{KO} (clone 1 and 2) cells after 24 h treatment with 50 ng/ml TRAIL. DMSO was used as a negative control. 2 mM H_2O_2 was used as a positive control. **D** Cell proliferation analysis of B16 WT and XIAP^{KO} CRISPR/Cas9 clones using Incucyte Live-Cell-Analysis. In **B**, **C** and **D**, data are presented as mean ± s.e.m; two-way analysis of variance (ANOVA) followed by Tukey's post-analysis. Data derived from three individual biological replicates. ****P < 0.0001 and ns, not significant.

3.2 XIAP promotes IL8 secretion in melanoma

XIAP was shown to be crucial for inflammatory signalling and cytokine secretion (Damgaard et al., 2012, Goncharove 2018). To investigate whether the inflammatory function of XIAP was involved in melanoma tumour progression, different cytokines and chemokines were analysed in B16-XIAP^{KO} versus WT cell lines. Transcripts of C-X-C motif chemokine ligands (CXCL) including CXCL1 (also called keratinocytes-derived chemokine (KC) in mice) and CXCL10 were downregulated in B16-XIAP^{KO} melanoma cells (**Figure 3.3A**) (also see **Appendix Table 1 and 2**).

Serum levels of Interleukin-8 (IL8), a member of the CXCL chemokine family, were reported to be increased in patients with melanoma metastases indicating a role for

IL8 in melanoma progression and metastasis (Bar-Eli, 1999). CXCL1 was also described to be involved in melanoma progression and tumour growth (Dhawan & Richmond, 2002). To further examine the association between XIAP and IL8 secretion in human melanoma cells, IL8 secretion was measured in different melanoma cell lines after XIAP knock-down (**Figure 3.3B**). Efficient knock-down of XIAP using specific siRNAs (**Table 5**) (J. M. Seeger et al., 2010a; J. M. Seeger et al., 2010b) was confirmed by Western blot analysis (**Figure 3.3B** lower panel). Compared to the negative control (siScr), IL8 secretion was reduced when XIAP was knocked-down in all tested melanoma cell lines. Additionally, we generated different human melanoma cell lines with a knock-out of XIAP. Human colorectal cancer cell line HCT116 and HCT-XIAP^{KO} were a kind gift from Prof. Dr. Mads Gyrd-Hansen and have been previously described (Cummins et al., 2004). Western blot analysis was performed to confirm the deletion of XIAP (**Figure 3.3C**). IL8 secretion was measured in WT and XIAP^{KO} cells. The secretion of IL8 was significantly reduced in all tested XIAP^{KO} cell lines (**Figure 3.3D**). In addition to analysing IL8 secretion under steady state conditions (**Figure 3.3B** and **D**), human melanoma cells BLM, SK-Mel28 and M5 were exposed to inflammatory conditions by TNF administration (Abreu-Martin et al., 1995) after XIAP knock-down or knock-out (**Figure 3.3E** and **F**). Both, XIAP knock-down and knock-out could reduce the IL8 secretion induced by TNF but could not completeley block it. Thus, IL8 secretion induced by TNF is probably not completely dependent on XIAP. Collectively, these data indicate that XIAP expression is crucial for inflammation mediated by CXCL family members and that inflammatory conditions within the tumour environement could enhance the IL8 secretion.

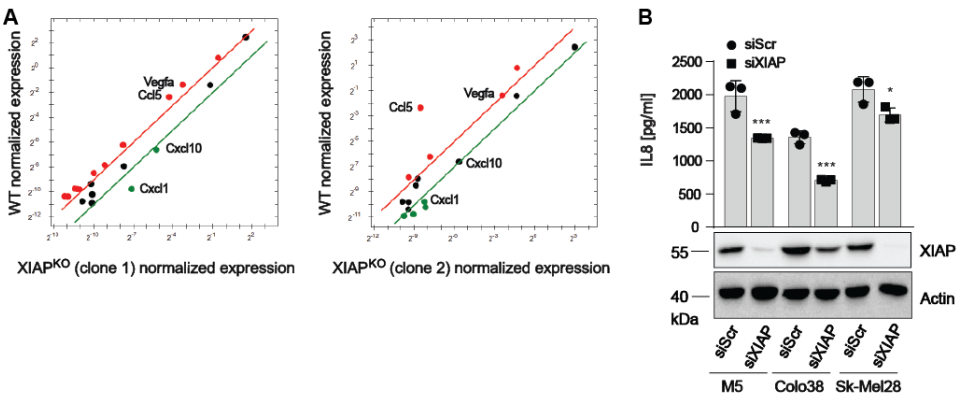

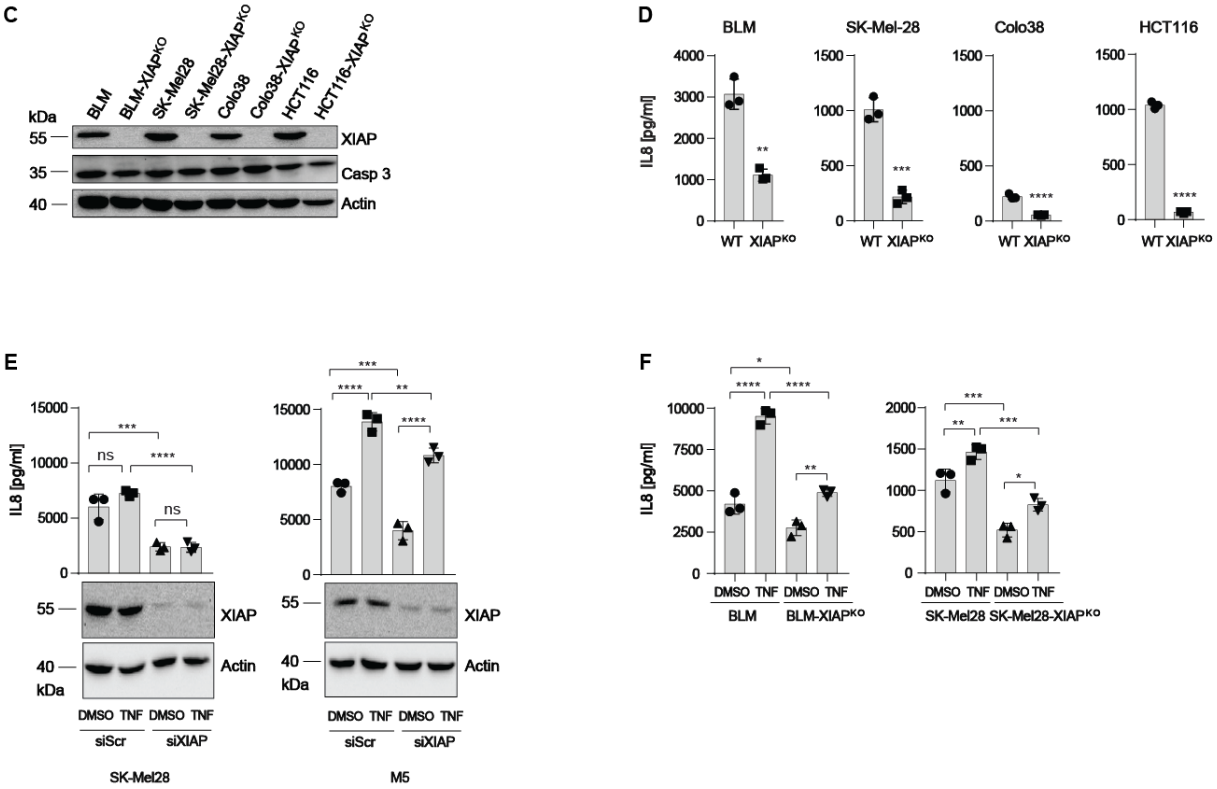

Figure 3.3: XIAP mediates IL8 secretion in melanoma

A qRT-PCR analysis (PrimePCR^{TM} Assay) of different cytokine/chemokine transcripts in B16 WT cells plotted *vs* B16-XIAP^{KO} cells (clone1 and 2). Samples that are at least 2-fold up-regulated are shown in red, samples that are at least 2-fold down-regulated are shown in green (Done by Dr. Pia Nora Broxtermann). **B** IL8 measurement in the supernatant of the indicated cell lines after 48 h transfection with siScr (control) or siXIAP and Western blot analysis of the corresponding cell lysates (bottom). One-way analysis of variance (ANOVA) followed by Dunnett's post-analysis. **C** Western blot analysis of cell lysates of BLM WT, XIAP^{KO}, SK-Mel28 WT, SK-Mel28-XIAP^{KO}, Colo38 WT, Colo38-XIAP^{KO}, HCT116 WT and HCT116-XIAP^{KO} after CRISPR/Cas9 gene editing. **D** IL8 measurement in the supernatant of the indicated cell lines after 24 h of seeding the cells. Unpaired t test, two-tailed analysis. **E** and **F** IL8 measurement in the supernatant of SK-Mel28 and M5 after 48 h siRNA transfection (**E**) or after 24 h of seeding BLM, BLM-XIAP^{KO}, SK-Mel28, and SK-Mel28-XIAP^{KO} cells (**F**). Cells were treated with 20 ng/ml TNF for 8 h. In **E** and **F**, data are presented as mean ± SD. One-way analysis of variance (ANOVA) followed by Dunnett's post-analysis. In **B**, **C**, **E** and **F**, dots represent individual biological replicates. *P < 0.05; **P < 0.01; ***P < 0.001; ****P < 0.0001 and ns, not significant.

3.3 RIPK2 and TAB1 act as downstream targets of XIAP

To investigate other target proteins which might be involved in XIAP mediated inflammatory response in melanoma, IL8 secretion was measured in human embryonic kidney 293 cells containing SV40 T-antigen (HEK293T) after ectopically expressing myc-XIAP full length or single domain deletion variants (**Figure 3.4A**). Ectopic myc-XIAP expression as well as myc-XIAP$^{\Delta BIR3}$ could induce IL8 secretion. In contrast, ectopically expressing myc-XIAP$^{\Delta BIR1}$, myc-XIAP$^{\Delta BIR2}$ and myc-XIAP$^{\Delta RING}$ could not induce IL8 secretion (**Figure 3.4B**). These data indicate an important role of BIR1 and BIR2 domains in XIAP mediated inflammatory signalling in addition to its E3 ligase activity.

Previous studies have shown that XIAP-BIR1 and -BIR2 domains are required for the interaction with TAB1 and RIPK2, respectively, which can result in NFκB activation (Lu et al., 2007; Yamaguchi et al., 1999). To investigate the role of TAB1 and RIPK2 in XIAP mediated inflammatory response in melanoma, we first studied the interaction between XIAP, TAB1 and RIPK2. Immunoprecipitation (IP) analysis showed that ectopically expressed myc-XIAP in HCT116 cell lines (**Figure 3.4C**) or endogenous XIAP in BLM human melanoma cell line (**Figure 3.4D**) can directly interact with TAB1 and RIPK2. Moreover, immunoflourescence (IF) analysis showed that ectopically expressed GFP-XIAP in HCT116 cells (**Figure 3.4E**) and in HeLa cells (**Figure 3.4F**) co-localises with TAB1 and RIPK2. The co-localisation of GFP-XIAP with TAB1 was BIR1 dependent (Lu et al., 2007; Yamaguchi et al., 1999), whereas the co-localisation of GFP-XIAP with RIPK2 was BIR2 dependent (Ramp et al., 2004; Krieg et al., 2009) (**Figure 3.4F**).

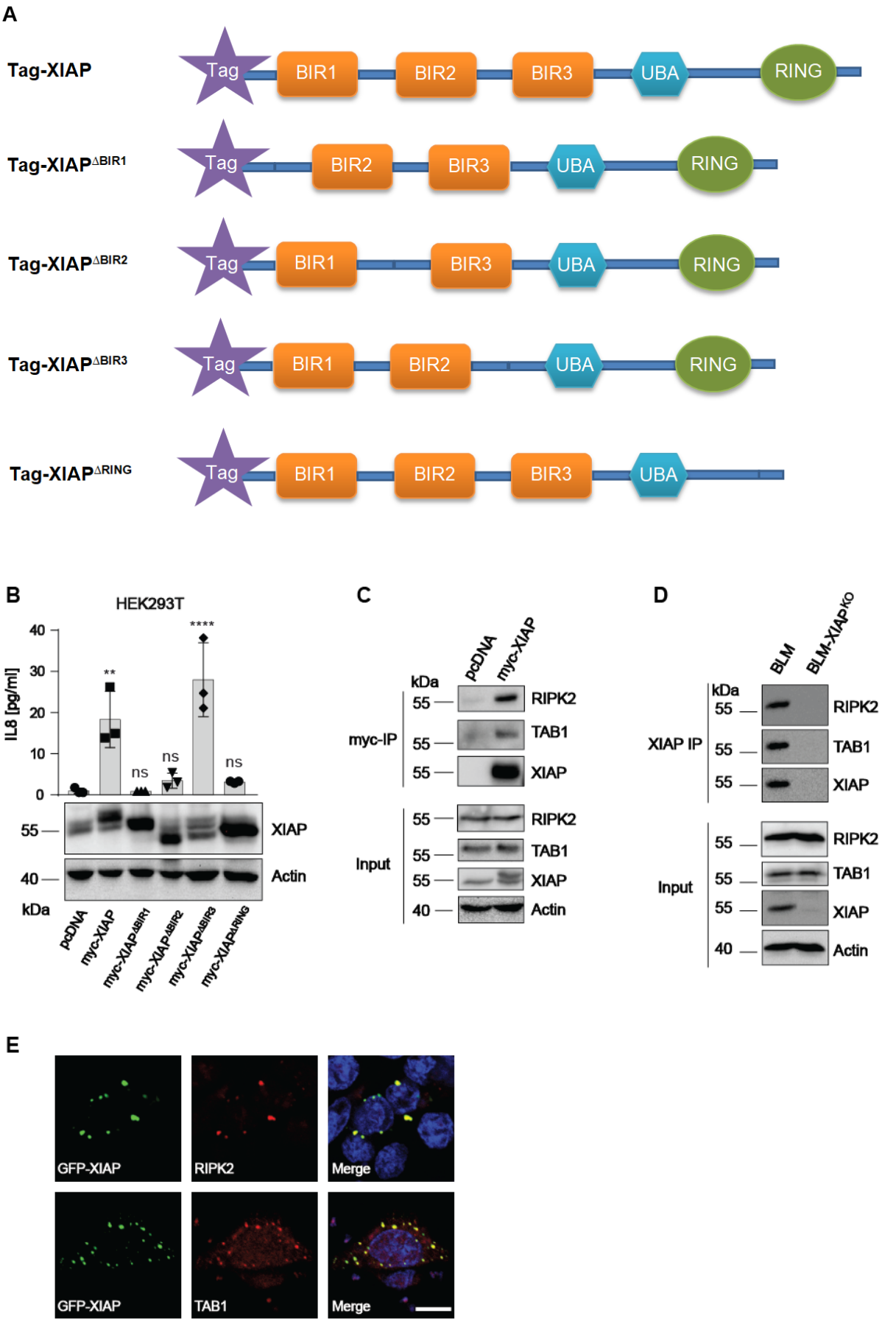
A
Tag-XIAP
Tag-XIAP^ΔBIR1
Tag-XIAP^ΔBIR2
Tag-XIAP^ΔBIR3
Tag-XIAP^ΔRING
Tag
BIR1
BIR2
BIR3
UBA
RING
B
HEK293T
IL8 [pg/ml]
ns
**
****
XIAP
Actin
kDa
pcDNA
myc-XIAP
myc-XIAP^ΔBIR1
myc-XIAP^ΔBIR2
myc-XIAP^ΔBIR3
myc-XIAP^ΔRING
C
pcDNA
myc-XIAP
myc-IP
Input
RIPK2
TAB1
XIAP
Actin
D
BLM
BLM-XIAP^KO
XIAP IP
Input
E
GFP-XIAP
RIPK2
Merge
TAB1

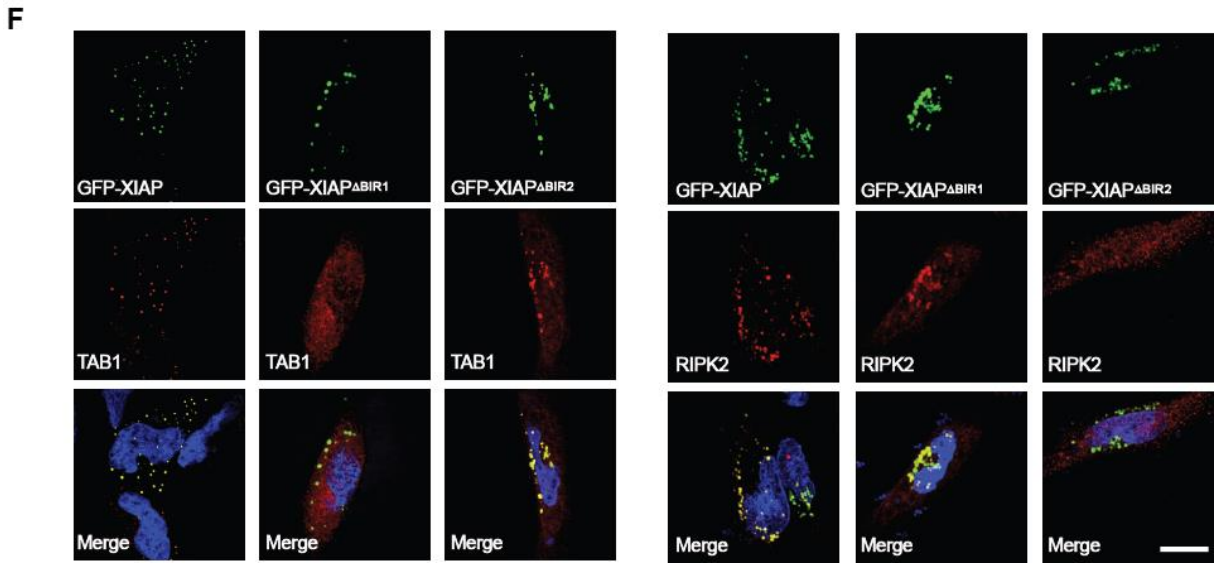

Figure 3.4: XIAP interacts and co-localises with RIPK2 and TAB1

A Illustration of XIAP full length and single domain deletion constracts. Tag represents myc or GFP. **B** IL8 measurement in the supernatant of transfected HEK293T cells after 24 h. Western blot analysis of cell lysates of HEK293T cells transfected with the indicated plasmids (bottom). Data are presented as mean ± SD. One-way analysis of variance (ANOVA) followed by Dunnett's post-analysis. Dots represent individual biological replicates. **C** Western blot analysis of cell lysates (input) and myc-IP of HCT116 cells transfected with pcDNA as a negative control or myc-XIAP for 24 h. **D** Western blot analysis of cell lysates of BLM and BLM-XIAP^{KO} cells (input) and XIAP-IP. **E** Confocal microscopic analysis of transfected HCT116 cells with GFP-XIAP for 16 h and stained for TAB1 or RIPK2 (red). Nuclei were stained with DAPI (blue). Scale bar 20 µm. **F** Confocal microscopic analysis of HeLa cells transfected with the indicated plasmids for 16 h and stained for TAB1 or RIPK2 (red). Nuclei were stained with DAPI (blue). Scale bar 20 µm. **P < 0.01; ****P < 0.0001 and ns, not significant.

XIAP E3 ligase activity was shown to be essential for RIPK2 ubiquitylation during NOD1 and NOD2 signalling (Goncharov, Hedayati, Mulvihill, Izrael-Tomasevic, et al., 2018). However, whether the enhanced XIAP expression in melanoma cells can induce RIPK2 ubiquitylation has not been studied. To analyse the ability of XIAP to ubiquitylate RIPK2 indepentendly of an upstream signal, we first performed a cell-free ubiquitylation assay using recombinant proteins required for the ubiquitylation reaction (Albert et al., 2020). The ubiquitylation reaction was performed using a ubiquitin, an E1 enzyme (UBE1) to mediate the ubiquitin activation, an E2 enzyme

(His-UbcH7) to mediate the ubiquitin conjucation, and flag-XIAP as the E3 ubiquitin ligase to mediate the transfer of ubiquitin from E2 to a lysine residue of a substrate, here GST-RIPK2 was used (**Figure 3.5A**). This assay clearly showed that XIAP can auto-ubiquitylate itself in addition to RIPK2. To analyse whether XIAP alone in melanoma cells can ubiquitylate RIPK2, RIPK2 IP was performed in human BLM, SK-Mel28 melanoma cells and in murine B16 WT *vs* XIAP^{KO} melanoma cells. Enhanced XIAP expression in human and mouse melanoma cell lines induced RIPK2 ubiquitylation and XIAP^{KO} could effeciently diminish ubiquitylation of RIPK2 (**Figure 3.5B**). Taken together, enhanced XIAP expression in melanoma cells without any further upstream stimuli can mediate the ubiquitylation of itself in addition to RIPK2.

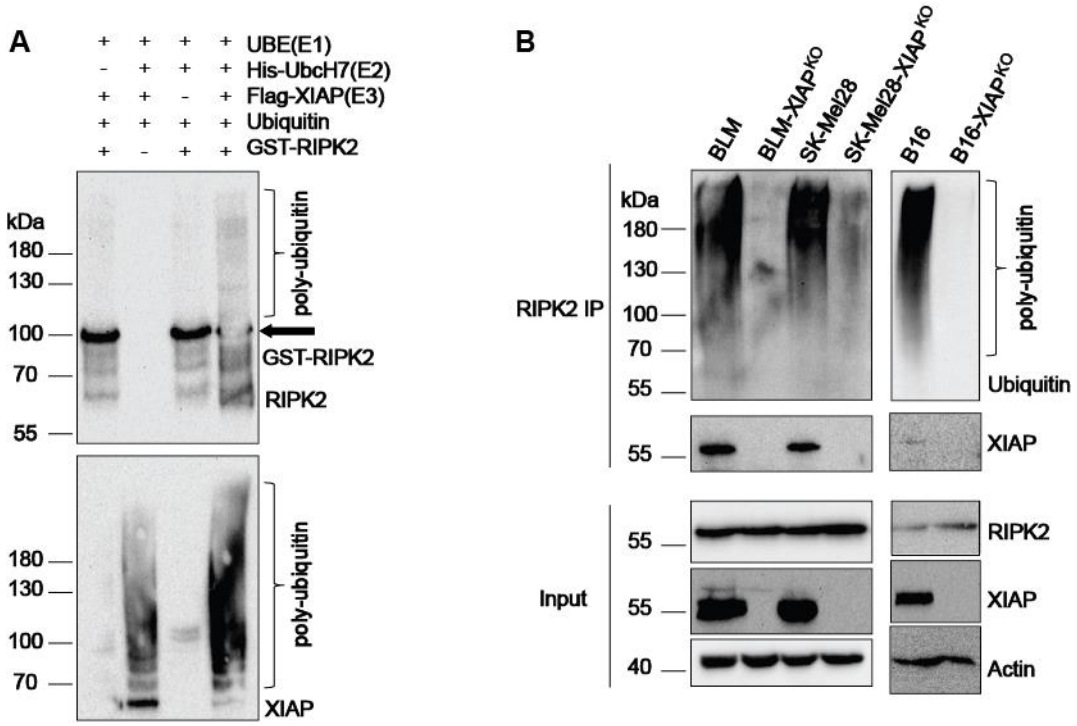

Figure 3.5: XIAP ubiquitylates RIPK2

A Cell-free ubiquitylation assay of recombinant GST-RIPK2 by Flag-XIAP after addition of respective E1/E2 and recombinant ubiquitin. Poly-ubiquitylated RIPK2 and XIAP were detected by Western blotting. **B** Western blot analysis of cell lysates of BLM, BLM-XIAP^{KO}, SK-Mel28, SK-Mel28-XIAP^{KO}, B16, and B16-XIAP^{KO} cells (input) and RIPK2-IP. Poly-ubiquitin was detected using anti-ubiquitin antibody.

3.4 XIAP driven IL8 secretion in melanoma is dependent on interaction with RIPK2 and TAB1

As RIPK2 and TAB1 are down-stream targets of XIAP, we analysed whether they play a role in XIAP mediated inflammation and IL8 secretion. Using CRISPR/Cas9 technology, we generated HCT116 cell lines lacking either TAB1 or RIPK2. IL8 secretion was measured following ectopic expression of myc-XIAP in HCT116 WT, $XIAP^{KO}$, $RIPK2^{KO}$ and $TAB1^{KO}$ cell lines. Ectopically expressed myc-XIAP could induce IL8 secretion in HCT116 WT and $XIAP^{KO}$ cell lines (**Figure 3.6A**). In contrast, there was no difference in IL8 secretion upon overexpressing myc-XIAP or the empty vector pcDNA in both $RIPK2^{KO}$ and $TAB1^{KO}$ cell lines. Ectopically expressing HA-RIPK2 together with an empty vector pcDNA or with myc-XIAP in HCT116-$RIPK2^{KO}$ cells could induce IL8 secretion (**Figure 3.6B**). Similarly, TAB1-HA overexpression together with an empty vector pcDNA or with myc-XIAP in HCT116-$TAB1^{KO}$ cells could induce IL8 secretion (**Figure 3.6C**). To further study the role of RIPK2 and TAB1 in XIAP mediated IL8 secretion in melanoma, IL8 secretion was measured in BLM and SK-Mel28 melanoma cells after specific knock-down of TAB1 or RIPK2 (**Figure 3.6D**). TAB1 and RIPK2 knock-down was confirmed by Western blot analysis (**Figure 3.6D** lower panel). IL8 secretion was efficiently reduced after knock-down of TAB1 or RIPK2 similar to XIAP (**Figure 3.6D** upper panel). Taken together, these data indicate that TAB1 and RIPK2 are crucial for XIAP mediated inflammatory signalling and IL8 secretion in melanoma cells.

In order to block IL8 secretion mediated by XIAP, we used different XIAP inhibitors, which were previously described (Goncharov et al., 2018). Compound XB2d89 (d89), which specifically targets the XIAP-RIPK2 interaction (Goncharov et al., 2018), could efficiently reduce IL8 secretion in BLM and SK-Mel28 human melanoma cells (**Figure 3.6E**). Additionally, other XIAP inhibitors such as Birinapant (Bir) and BV6, both targeting the BIR3 domain of XIAP, were tested. However, both Birinapant and BV6 could not reduce and even induced higher levels of IL8 secretion (**Figure 3.6F**). This further indicate that XIAP-RIPK2 interaction is essential for XIAP mediated IL8 secretion.

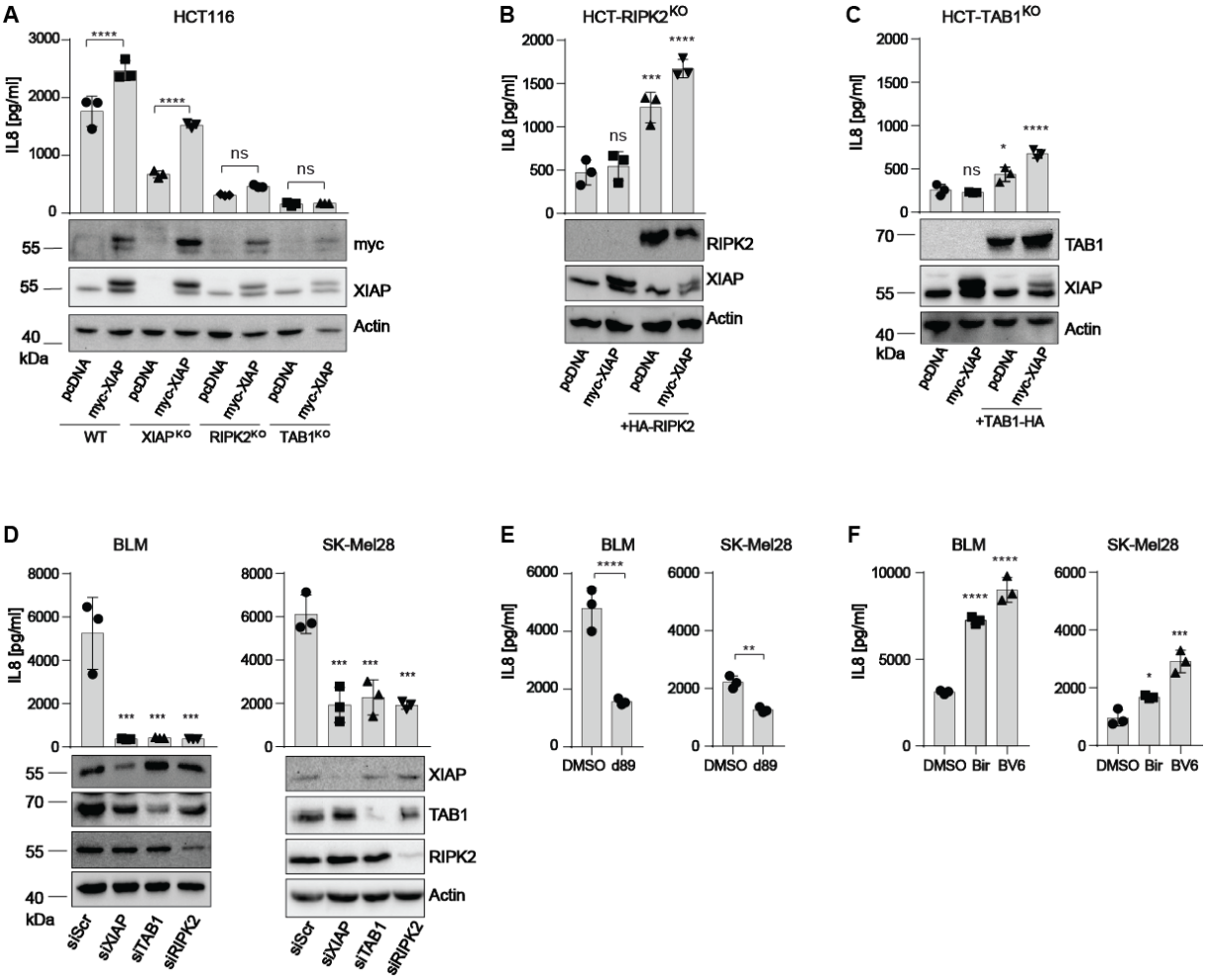

Figure 3.6: XIAP mediates IL8 secretion *via* interaction with RIPK2 and TAB1

A IL8 measurement in the supernatant of transfected HCT116 WT, XIAP^{KO}, RIPK2^{KO} and TAB1^{KO} cells after 24 h. One-way analysis of variance (ANOVA) followed by Sidak's post-analysis. Western blot analysis of cell lysates of the respective cell lines transfected with the indicated plasmids (bottom). **B** and **C** IL8 measurement in the supernatant of transfected HCT-RIPK2^{KO} (**B**) or HCT-TAB1^{KO} (**C**) cells after 24 h. Western blot analysis of cell lysates of HCT-RIPK2^{KO} and HCT-TAB1^{KO} cells transfected with the indicated plasmids (bottom). **D** IL8 measurement in the supernatant of transfected BLM (left panel) or SK-Mel28 (right panel) cells with siScr (control), siXIAP, siTAB1 or siRIPK2 after 48 h. Western blot analysis of the respective cell lysates of BLM cells (left bottom) or SK-Mel28 cells (right bottom) transfected with the indicated siRNA. **E** IL8 measurement in the supernatant of BLM or SK-Mel28 treated with 2 µM d89 (BIR2 antagonist) or DMSO as a negative control for 24 h. Unpaired t test, two-tailed test analysis. **F** IL8 measurement in the supernatant of BLM or SK-Mel28 treated with 20 µM birinapant (Bir), 2 µM BV6 (both BIR3 antagonist) or DMSO as a negative control for 24 h. In **A**, **B**, **C**, **D**, **E** and **F**, data are presented as mean ± SD. In **B**, **C**, **D** and **F**, one-way analysis of variance

(ANOVA) followed by Dunnett's post-analysis. In **A**, **B**, **C**, **D**, **E** and **F**, dots represent individual biological replicates. *P < 0.05; **P < 0.01; ***P < 0.001; ****P < 0.0001 and ns, not significant.

Recent studies have shown that XIAP is essential for the activation of NFkB upon inflammatory responses mediated by NOD2/RIPK2 signalling (Andree et al., 2014; Krieg et al., 2009). Therefore, the impact of RIPK2 on XIAP inflammatory function upon NOD2 stimulation was analysed. HCT116 cells were transfected with siScr, siTAB1, siRIPK2 or siXIAP for 48 h and treated with L18-muramyl dipeptide (MDP, NOD2 ligand) for 24 h. MDP treatment could induce IL8 secretion. XIAP or RIPK2 knock-down could significantly moderate the IL8 secretion as expected. Interestingly, TAB1 knock-down could also reduce the IL8 secretion (**Figure 3.7A**), indicating an essential role of TAB1 downstream XIAP-RIPK2 in mediating IL8 secretion. Analysis of IL8 mRNA level (**Figure 3.7B**) additionally confirmed that IL8 is transcriptionally down-regulated upon XIAP, RIPK2 or TAB1 knock-down. These results concealed that IL8 secretion upon MDP treatment was dependent on the expression of XIAP, RIPK2 and TAB1.

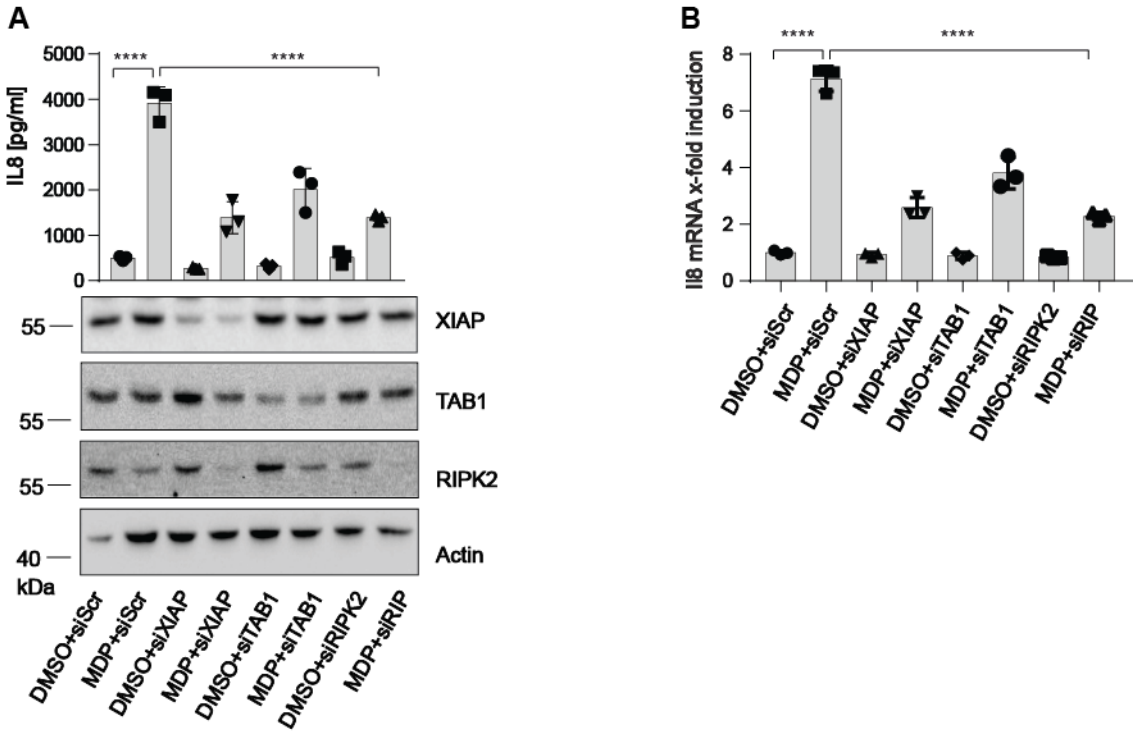

Figure 3.7: XIAP mediates IL8 secretion upon MDP stimulation

A IL8 measurement in the supernatant of HCT116 cells transfected with the indicated siRNA for 48 h and treated with DMSO (control) or MDP for 24 h. Western blot analysis of cell lysates of HCT116 cells (bottom). **B** mRNA expression level of Il8 in HCT116 cells transfected with the indicated siRNA for 48 h and treated with DMSO (control) or MDP for 24 h. In **A** and **B**, dots represent individual biological replicates. Data are presented as mean ± SD. One-way analysis of variance (ANOVA) followed by Dunnett's post-analysis. ****P < 0.0001.

3.5 XIAP supports melanoma growth *via* XIAP-RIPK2-TAB1 signalling complex

To study the involvement of RIPK2 and TAB1 in melanoma tumour growth, we generated B16 melanoma cell lines lacking RIPK2 ($RIPK2^{KO}$) or TAB1 ($TAB1^{KO}$) using CRISPR/Cas9 technology. Western blot analysis showed the successful deletion of RIPK2 and TAB1 in these cells (**Figure 3.8A**). The $RIPK2^{KO}$ and $TAB1^{KO}$ did not affect the expression level of other proteins (**Figure 3.8A**). Next, B16 WT, $XIAP^{KO}$, $RIPK2^{KO}$ or $TAB1^{KO}$ melanoma cells were subcutaneously injected into BL/6 mice. All B16 melanoma cell lines formed palpable tumours. However, $RIPK2^{KO}$ or $TAB1^{KO}$ could significantly reduce B16 melanoma tumour growth in mice similar to $XIAP^{KO}$ (**Figure 3.8B**). Together indicating that XIAP forms a signalling complex with RIPK2 and TAB1 that supports melanoma tumour growth.

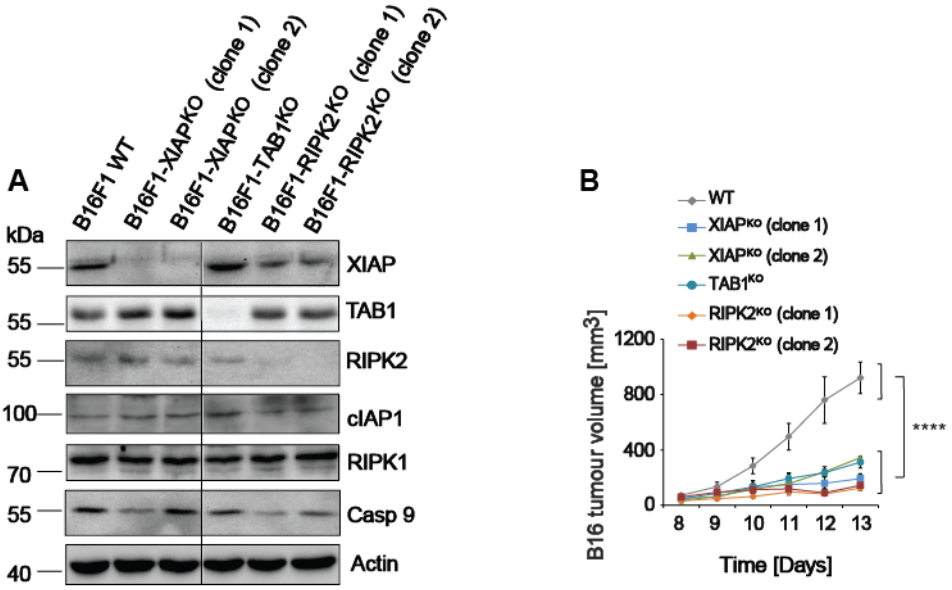

Fig 3.8: XIAP supports melanoma tumour growth *via* XIAP-RIPK2-TAB1 signalling complex

A Western blot analysis of cell lysates of B16 WT, B16-XIAP^{KO} (clone 1 and 2), B16-TAB1^{KO} and B16-RIPK2^{KO} (clone 1 and 2) after CRISPR–Cas9 gene editing. **B** B16 WT, B16-XIAP^{KO} (clone 1 and 2), B16-TAB1^{KO} and B16-RIPK2^{KO} (clone 1 and 2) subcutaneous melanoma tumour growth in BL/6 WT mice (n=5 each genotype). This analysis was done in association with Dr. Jens Seeger. Data are presented as mean ± s.e.m; two-way analysis of variance (ANOVA) followed by Dunnett's post-analysis. ****P < 0.0001.

To examine whether the reduced tumour volume in RIPK2^{KO} or TAB1^{KO} was due to changes in apoptosis, we analysed the activation of apoptosis in the B16 tumours isolated from the mice. There was no difference in cl-Caspase-3 staining in B16 RIPK2^{KO} or TAB1^{KO} tumours similar to B16 WT and XIAP^{KO} tumours (**Figure 3.9A**). Next, we analysed the apoptotic propensity of RIPK2^{KO} or TAB1^{KO} B16 cells in culture. Incucyte analysis was performed after treating the cells with TNF. Similar to our observation in XIAP^{KO} (**Figure 3.2B** and **D**), RIPK2^{KO} and TAB1^{KO} melanoma cells were resistant to cell death induced by TNF treatment and the apoptotic propensity of RIPK2^{KO} or TAB1^{KO} B16 cells was similar to WT (**Figure 3.9B**). Additionally, there was no difference in proliferation in both RIPK2^{KO} and TAB1^{KO} compare to B16 WT (**Figure 3.9C**). Thus, apoptosis is not the underlying molecular mechanism behind the reduced tumour volume in TAB1^{KO} or RIPK2^{KO} tumours similar to XIAP^{KO}.

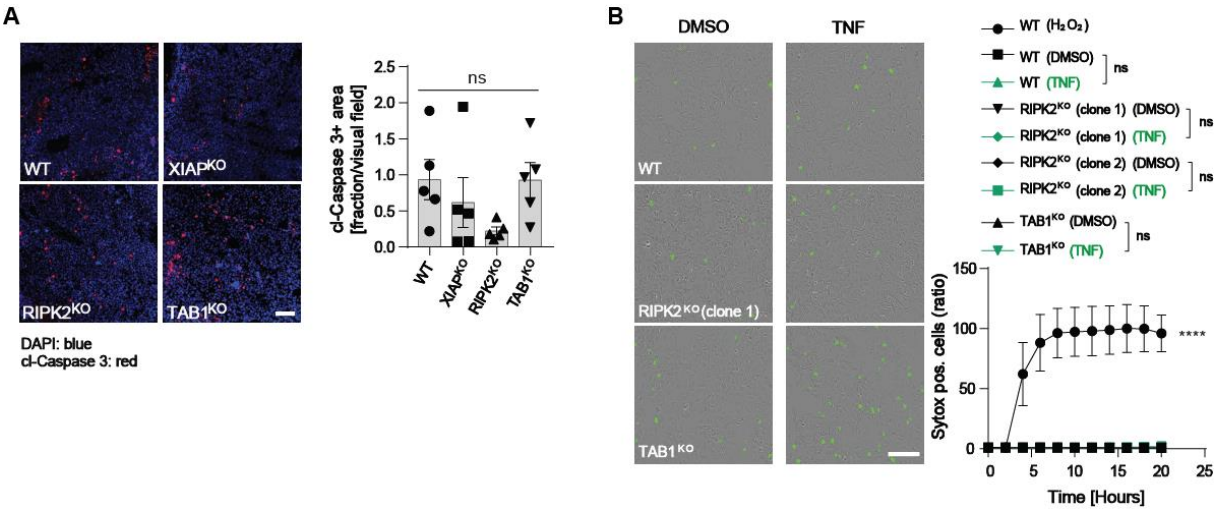

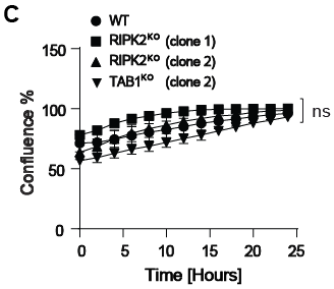

Figure 3.9: XIAP, RIPK2 or TAB1 deficiency in B16 mouse melanoma cells reduces tumour growth independently of apoptosis

A Representative fluorescent images of cl-Caspase-3+ cells in B16 WT, $XIAP^{KO}$, $TAB1^{KO}$ or $RIPK2^{KO}$ melanoma tumours. Nuclei were stained with DAPI (blue). Scale bar 100 µm. Quantification thereof (right panel). Dots represent individual mice (n=5). Data are presented as mean ± s.e.m. One-way analysis of variance (ANOVA) followed by Dunnett's post-analysis. **B** Cell death measurement of B16 WT, $TAB1^{KO}$ and $RIPK2^{KO}$ (clone 1 and 2) cells using Incucyte analysis after 24 h treatment with DMSO as a negative control or 100 ng/ml TNF. H_2O_2 treatment serves as a positive control. Scale bar 200 µm. **C** Proliferation assay using Incucyte Live-Cell-Analysis assay. In **B** and **C,** data are presented as mean ± s.e.m; two-way analysis of variance (ANOVA) followed by Tukey's post-analysis. Data derived from three individual biological replicates. ****P < 0.0001 and ns, not significant.

3.6 XIAP supports melanoma growth by inducing neutrophil infiltration

Previews studies have shown increased IL8 serum level, a neutrophil chemo-attractant, in patients with melanoma metastases providing a role of IL8 in melanoma progression and metastasis (Bar-Eli, 1999; Payne & Cornelius, 2002b). Together with our observation that inflammatory responses mediated CXCL family secretion is dependent on XIAP expression, we examined the correlation between XIAP expression and neutrophils intra-tumour infiltration. First, the correlation was analysed by co-staining XIAP and CD177 (a neutrophil marker) in tumour samples derived from melanoma patients (**Figure 3.10A, B and Appendix Table 3**). The signal intensity of XIAP and CD177 staining showed that increased XIAP expression in tumour cells was tightly associated with intra-tumoural neutrophil infiltration.

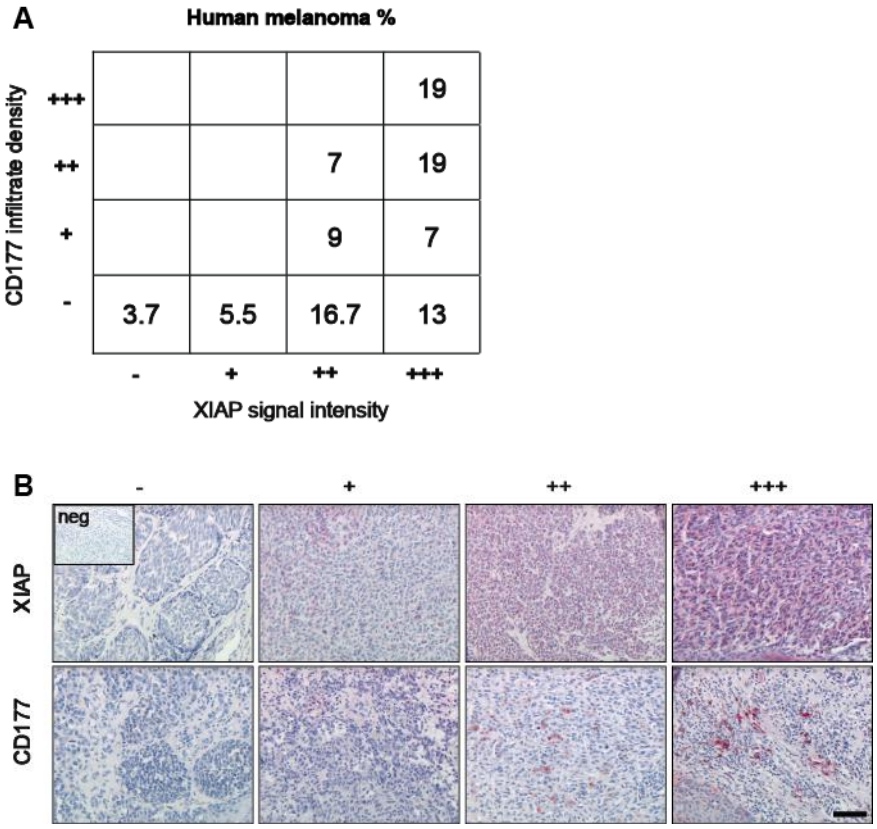

Figure 3.10: Increased XIAP expression in melanoma patient's tissues is correlated with intra-tumoural neutrophil infiltration

A Intensities of CD177 and XIAP immunostainings in tumour sections from 55 patients were visually scored. The numbers of melanomas with different intensities were plotted into the table as a percentage of the total. Specific staining intensity for XIAP and CD177, corresponding to relative amounts of infiltrated neutrophils, was arbitrarily set as the following: -, not expressed; +, low; ++, moderate; and +++, strong expression. **B** Representative IHC pictures from A. Scale bar 100 µm. **A** and **B** were done by Dr. Paola Zigrino.

Next, the correlation between XIAP, RIPK2, TAB1 expression and intra-tumoural neutrophil infiltration in murine B16 melanoma tumours was studied. Different cytokines and chemokines were analysed in B16 tumours isolated from mice after injection of different B16 mouse melanoma cells (**Figure 3.11A**). Cxcl1 and Cxcl10 were significantly reduced in $RIPK2^{KO}$ and $TAB1^{KO}$ B16 tumours similar to $XIAP^{KO}$. Additionally, IHC staining (**Figure 3.11B**) or IF staining (**Figure 3.11C**) of the B16 tumours was performed using Ly6G (a neutrophil marker). The number of intra-tumoural Ly6G+ was quantified (**Figure 3.11C** right panel). Taken together, lack of

XIAP, RIPK2 or TAB1 could sufficiently reduce neutrophil infiltration in B16 tumours. To exclude a correlation between XIAP, RIPK2, TAB1 expression and infiltration of other immune cells in the B16 melanoma tumours, we performed an immunophenotyping of B16 tumours (WT, XIAP^{KO}, RIPK2^{KO}, and TAB1^{KO}) by using specific antibodies detecting different immune cells (**Figure 3.11D**). CD3 (cluster of differentiation 3), a T cells marker (Kuhns et al., 2006); CD4 (cluster of differentiation 4), a marker for T helper cells, regulatory T cells, monocyte, macrophages and dendritic cells (DC) (Zamoyska, 1994); CD8 (cluster of differentiation 8), a marker for cytotoxic T cells and subsets of DC (Zamoyska, 1994; Shortman & Heath, 2010); F4/80, a marker for macrophages (McKnight et al., 1996); CD11c, a marker for DC, activated natural killer (NK) cells, subsets of B and T cells, monocyte, granulocyte, and some B cell malignancies (Kohrgruber et al., 1999; Qualai et al., 2016); CD19, a B cell marker (Tedder et al., 1997; Scheuermann & Racila, 1995); FoxP3 (Forkhead box P3), a marker for regulatory T cells (Ochs et al., 2007) and Granzyme B, a marker for CD8+ cytotoxic T cells and NK cells (Trapani, 2001). Immunophenotyping of B16 tumours revealed that lack of XIAP, RIPK2 or TAB1 could sufficiently reduce neutrophil infiltration in B16 tumours but did not affect the infiltration of other tested immune cells.

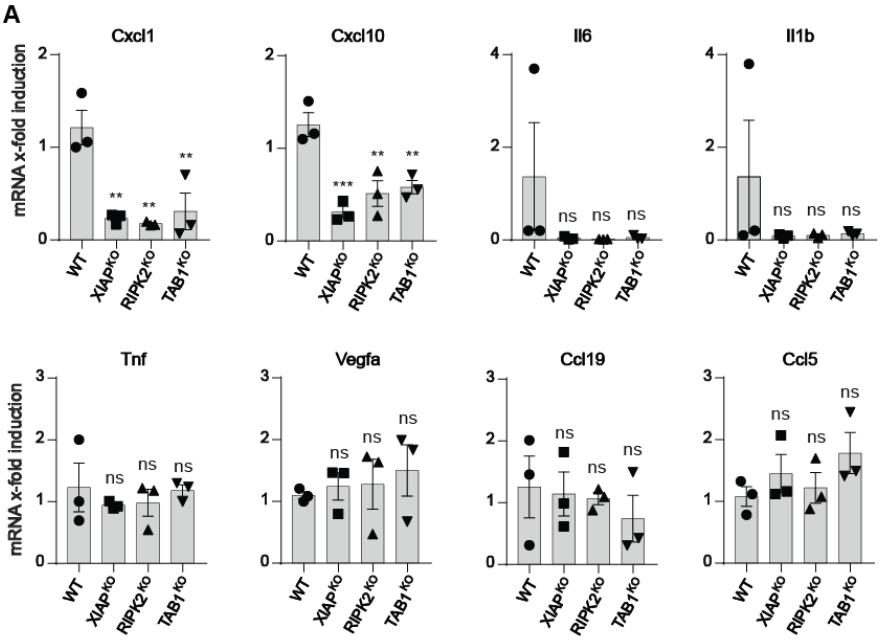

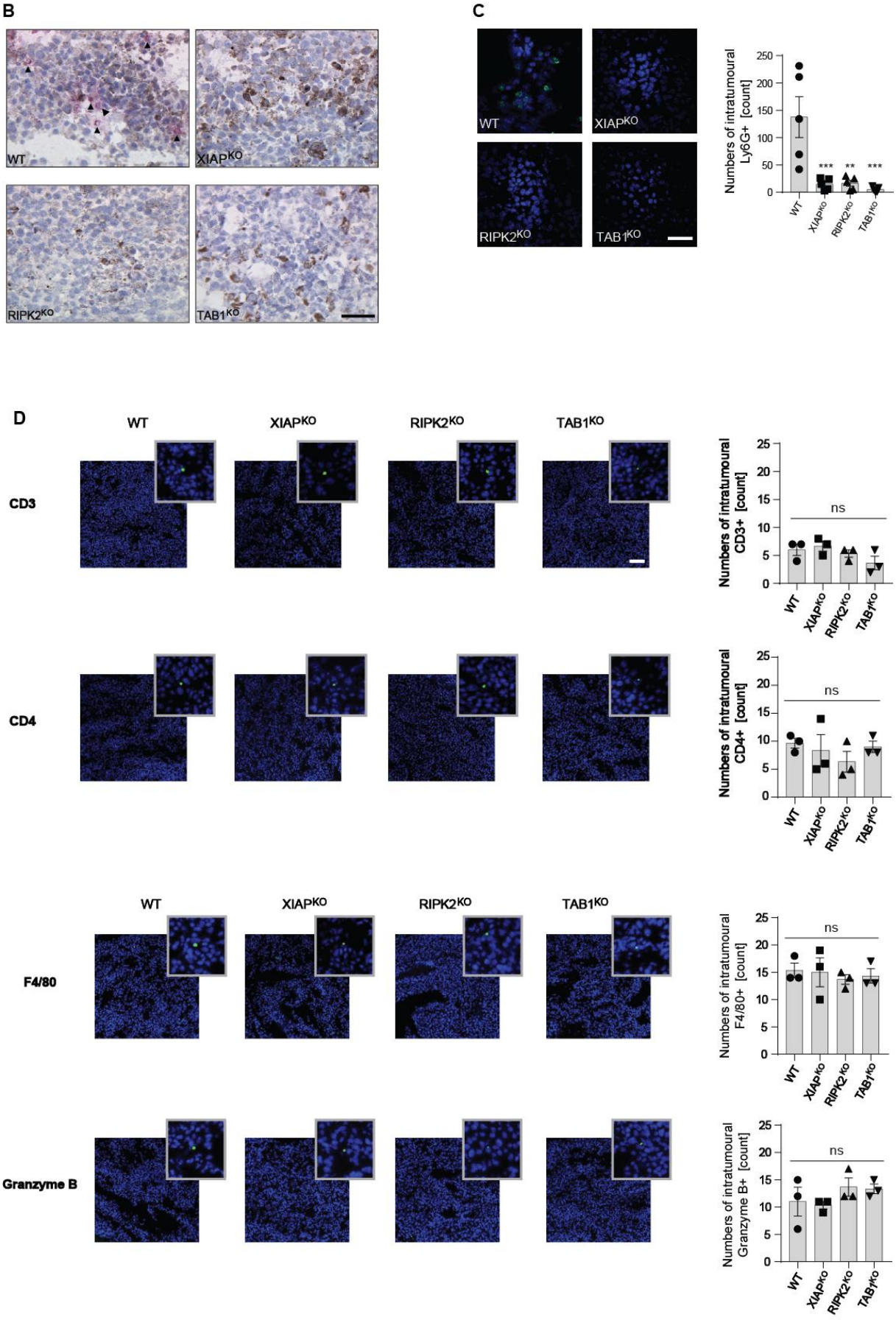
B
WT
XIAP^KO
RIPK2^KO
TAB1^KO
C
WT
XIAP^KO
RIPK2^KO
TAB1^KO
Numbers of intratumoural Ly6G+ [count]
***
**
***
D
WT
XIAP^KO
RIPK2^KO
TAB1^KO
CD3
Numbers of intratumoural CD3+ [count]
ns
CD4
Numbers of intratumoural CD4+ [count]
ns
F4/80
Numbers of intratumoural F4/80+ [count]
ns
Granzyme B
Numbers of intratumoural Granzyme B+ [count]
ns

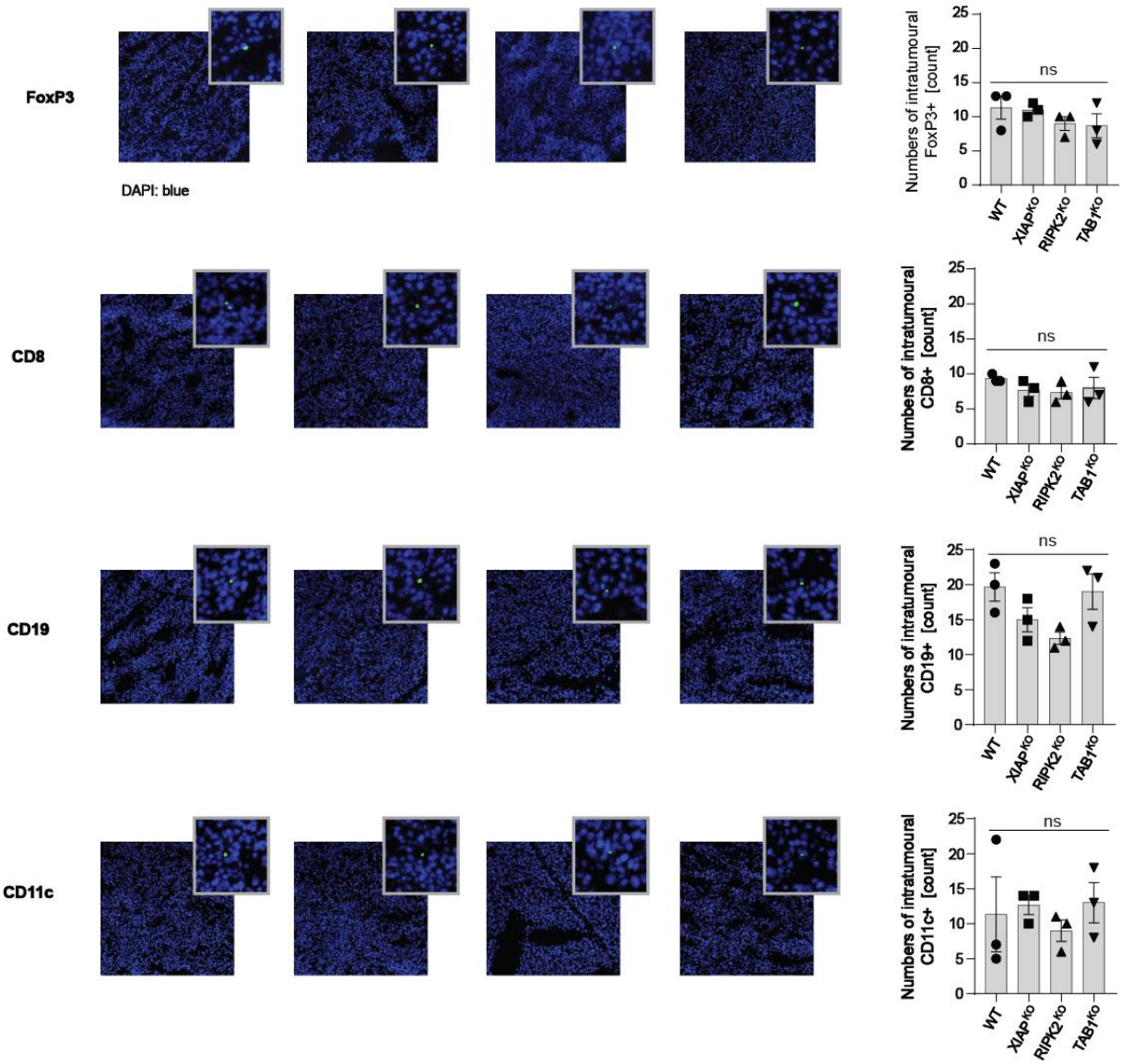

Figure 3.11: XIAP supports melanoma growth in B16 tumours by inducing neutophil infiltration

A qRT-PCR analysis of different cytokines/chemokines in the indicated melanoma tumours in mice. Dots represent individual mice (n=3). Data are presented as mean ± SD. One-way analysis of variance (ANOVA) followed by Dunnett's post-analysis. **B** Representative IHC staining of neutrophil in B16 tumours. Scale bar 50 µm (Done by Dr. Paola Zigrino). **C** Representative IF (neutrophil staining) in B16 WT, $XIAP^{KO}$, $TAB1^{KO}$ or $RIPK2^{KO}$ tumours (Scale bar 50 µm) and quantification of Ly6G+ cells. The sum of Ly6G+ cells from 5 randomly selected areas of the tumour (5 mice per genotype) were represented. Dots represent individual mice (n=5). Data are presented as mean ± s.e.m. One-way analysis of variance (ANOVA) followed by Dunnett's post-analysis. **D** Representative fluorescent images (Scale bar: 100 µm) and quantification of different immune cells in B16 melanoma tumours as indicated by using specific antibodies. Dots represent individual mice (n=3). Data are

presented as mean ± s.e.m. One-way analysis of variance (ANOVA) followed by Dunnett's post-analysis. **P < 0.01; ***P < 0.001 and ns, not significant.

To investigate whether the reduced tumour growth in B16-XIAP^{KO} melanoma tumours was due to the reduction in neutrophils infiltration, neutrophils were experimentally depleted in mice using Ly6G specific antibodies (**Figure 3.12A** and **B**). WT or XIAP^{KO} B16 melanoma cells were subcutaneously injected into BL/6 mice. The mice were treated with either IgG antibodies as a negative control or with Ly6G antibodies. Neutralizing the neutophils in B16 WT tumours could significantly reduce the tumour growth. In contrast, there was no difference in tumour growth between B16-XIAP^{KO} tumours treated with IgG or B16-XIAP^{KO} tumours treated with Ly6G neutralizing antibodies (**Figure 3.12A**). Depletion of the neutrophils after treatment was tested by IHC staining (**Figure 3.12B**) or IF staining (**Figure 3.12C**) using Ly6G antibody. Quantification of the number of intra-tumoural Ly6G+ (**Figure 3.12C right panel**) showed that depletion of neutrophils could sufficiently reduce neutrophil infiltration in B16 WT tumours similar to XIAP^{KO}. Taken together, these data indicate that XIAP promotes melanoma tumour growth by activating a down-stream signalling cascade resulting in intra-tumoural neutrophil infiltration.

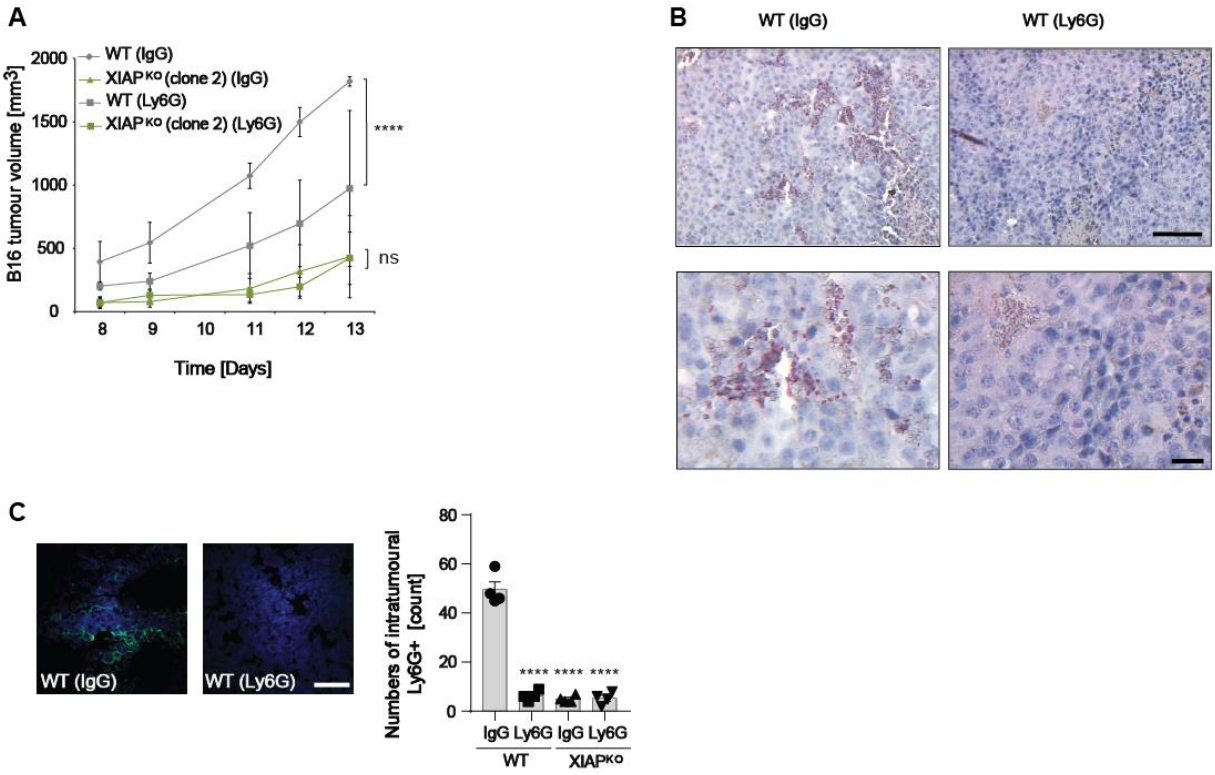

Figure 3.12: Neutrophil depletion reduces B16 tumour growth

A B16 WT, XIAP^{KO} (clone 2) subcutaneous melanoma tumour growth in BL/6 WT mice (n=5). Mice were intra-peritoneal injected with IgG antibody as a negative control or Ly6G antibody 1 day prior to the subcutaneous injection of the B16 WT or XIAP^{KO} cells. Data are presented as mean ± s.e.m. Two-way analysis of variance (ANOVA) followed by Dunnett's post-analysis (Done by Dr. Pia Nora Broxtermann). **B** Representative IHC staining of neutrophil in B16 tumours derived from mice treated either with control IgG or Lys6G antibodies. Scale bar 100 µm (upper panel) and 10 µm (lower panel) (Done by Dr. Paola Zigrino). **C** Representative IF (neutrophil) scale bar 50 µm and quantification of Ly6G+ cells in tumours from **A.** The sum of Ly6G+ cells from 5 randomly selected areas of the tumour (4 mice per genotype) was represented. Dots represent individual mice (n=4). Data are presented as mean ± s.e.m. One-way analysis of variance (ANOVA) followed by Dunnett's post-analysis. ****P < 0.0001 and ns, not significant.

3.7 XIAP supports tumour growth in *Hgf-Cdk4^{R24C}* mouse melanoma model by mediating neutrophil infiltration

In order to support our data obtained in B16 melanoma, we used another mouse melanoma model called *Hgf-Cdk4^{R24C}*. This mouse model overexpresses the hepatocyte growth factor (Hgf) and has knock-in mutation in the cycline dependent kinase 4. The *Hgf-Cdk4^{R24C}* mouse model is known to develop spontaneous melanomas that match melanoma development in humans (Tormo et al., 2006; Giebeler et al., 2017). To study the impact of XIAP on melanoma development in the *Hgf-Cdk4^{R24C}* mouse model, *Hgf-Cdk4^{R24C}* mice were crossed with *Xiap^{KO}* mice (described in Andree et al., 2014). *Hgf-Cdk4^{R24C}Xiap$^{fl/fl}$* mice were used as controls. In addition to the spontaneous tumour model and in order to promote rapid melanoma growth, some neonates were treated with carcinogen (7,12-dimethylbenz[a]anthracene (DMBA)). DMBA treatment is known to induce primary melanomas in the skin during the first 3 months of life in *Hgf-Cdk4^{R24C}* mouse melanoma model (Tormo et al., 2006). Both *Hgf-Cdk4^{R24C}Xiap$^{fl/fl}$* and *Hgf-Cdk4^{R24C}Xiap^{KO}* mice developed melanomas on the back skin (**Figure 3.13A**), however the tumour size was markedly reduced in the *Hgf-Cdk4^{R24C}Xiap^{KO}* mice (**Figure 3.13A** and **B**), indicating a role of XIAP in melanoma tumour growth. Analysis of cl-Caspase-3 activation revealed that *Xiap^{KO}* tumours have similar apoptosis activation level compared to the control mice *Hgf-Cdk4^{R24C}Xiap$^{fl/fl}$* (**Figure 3.13C**).

Moreover, we analysed the transcription of different cytokines/chemokines in *Hgf-Cdk4*^{R24C}*Xiap*$^{fl/fl}$ *vs* *Hgf-Cdk4*^{R24C}*Xiap*^{KO} mice. Transcripts of the CXCL chemokine family members like Cxcl1 and Cxcl10 were down-regulated in the *Xiap*^{KO} tumours (**Figure 3.13D** and **Appendix Table 4, 5, 6**).

To investigate the correlation between XIAP expression and intra-tumoural neutrophil infiltration in the *Hgf-Cdk4*^{R24C} mouse melanoma model, IHC and IF staining of Ly6G in small and large tumours from *Hgf-Cdk4*^{R24C}*Xiap*$^{fl/fl}$ and *Hgf-Cdk4*^{R24C}*Xiap*^{KO} mice was performed. Lack of XIAP could sufficiently reduce neutrophil infiltration not only in early small tumours (**Figure 3.13E** and **F**) but also in large melanomas at later stages (**Figure 3.13G** and **H**). Thus, XIAP supports melanoma tumour growth in *Hgf-Cdk4*^{R24C} mouse model by mediating intra-tumoural neutrophil infiltration similar to B16 mouse model.

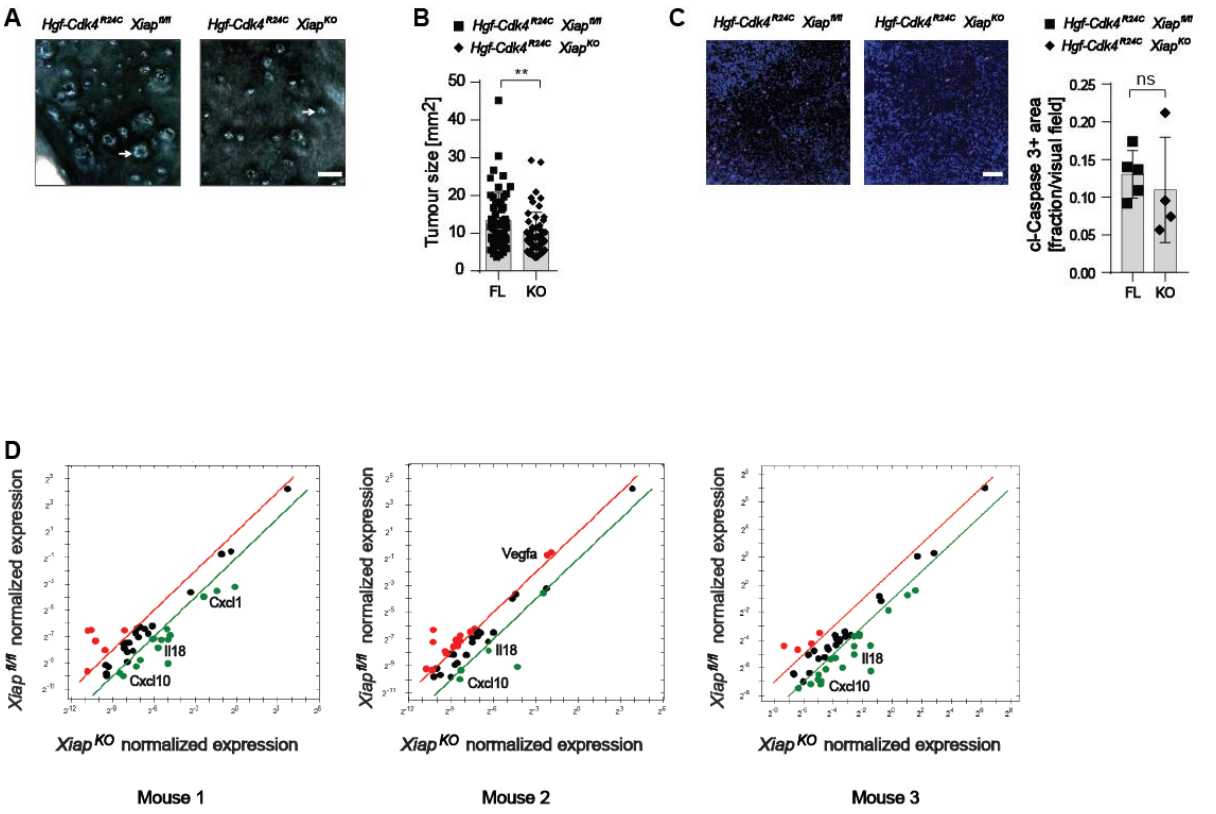

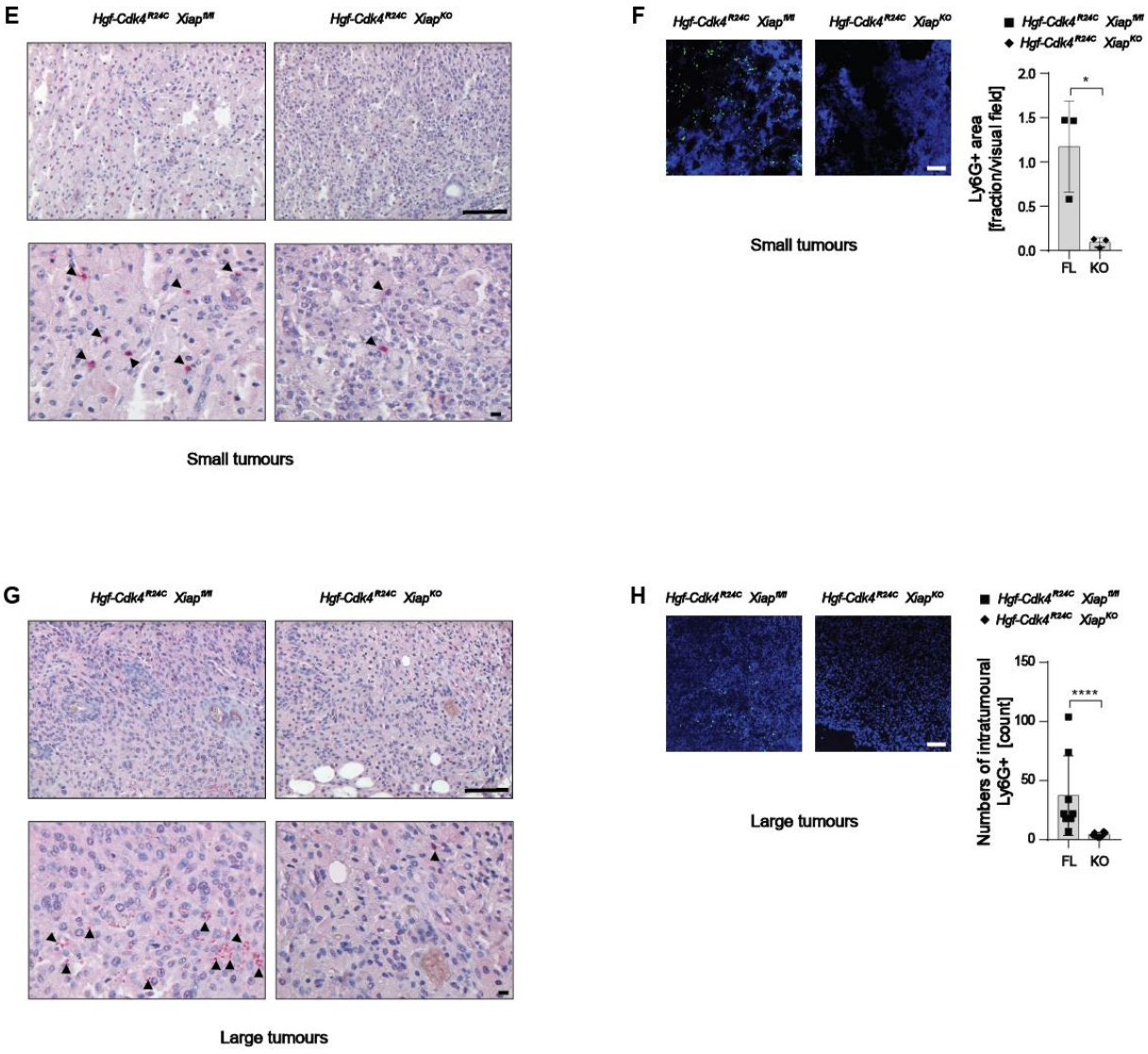

Figure 3.13: XIAP supports tumour growth in *Hgf-Cdk4^{R24C}* mouse melanoma model by mediating neutrophil infiltration

A Representative images of back skin from the DMBA-treated *Hgf-Cdk4^{R24C}Xiap$^{fl/fl}$* and *Hgf-Cdk4^{R24C}Xiap^{KO}* mice at 8 weeks of age. Arrows indicate individual tumour. Scale bar 5 mm. **B** Tumour size in the DMBA-treated *Hgf-Cdk4^{R24C}Xiap$^{fl/fl}$* and *Hgf-Cdk4^{R24C}Xiap^{KO}* mice at 8 weeks of age (n=3). Dots represent an individual tumour. Data are presented as mean ± SD. Mann-Whitney, two-tailed test analysis. (A and B were done by Dr. Fabian Schorn). **C** Representative IF staining (Scale bar 100 µm) and quantification of cl-Caspase-3+ cells within the melanoma tumours in DMBA-treated mice (n=3). The average of cl-Caspase-3+ cells from 5 randomly selected areas of the tumour (3 mice per genotype) was represented. **D** qRT-PCR analysis (PrimePCR^{TM} Assay) of different cytokine/chemokine transcripts in *Hgf-Cdk4^{R24C}Xiap$^{fl/fl}$* mice plotted *vs* 3 independent *Hgf-Cdk4^{R24C}Xiap^{KO}* mice. Samples that are at least 2-fold up-regulated are shown in red, samples that are at least 2-fold down-regulated are shown in green. **E** and **G** Representative IHC staining of

neutrophil in small (early time points) (**E**) and large (late time points) (**G**) tumours. Scale bar 100 µm (upper panel) and 10 µm (lower panel). Arrows show neutrophil (Done by Dr. Paola Zigrino). **F** and **H** Representative IF (neutrophils) staining and quantification of intra-tumoural neutrophil in small (early time points) (**F**) and large (late time points) (**H**) tumours. Scale bar 100 µm. In **F**, the average of Ly6G+ cells from 5 randomly selected areas of the tumour (3 mice per genotype) was represented. In **H**, the sum of Ly6G+ cells from 5 randomly selected areas of the tumour (3 mice per genotype) was represented. In **C**, **F** and **H**, dots represent individual tumour (3 mice per genotype) and data are presented as mean ± SD; Mann Whitney, two-tailed test analysis. *P < 0.05; **P < 0.01; ****P < 0.0001 and ns, not significant.

4 Discussion

XIAP is highly expressed in various cancer entities (Kashkar, 2010; Fulda & Vucic, 2012) and many studies aimed to investigate the role of XIAP in this context. Hence, resistance to apoptosis is a hallmark of cancer as it facilitates tumour growth and metastasis (Hanahan & Weinberg, 2011a), most studies focused on the role of XIAP as an efficient inhibitor of apoptosis (Takahashi et al., 1998; Silke et al., 2002), identifying XIAP as a potential therapeutic target for cancer treatment. Accumulating body of evidence showed that XIAP has in addition to its anti-apoptotic function, a crucial role in innate immunity and inflammatory responses (Bauler et al., 2008; Krieg et al., 2009). However, the inflammatory function of XIAP has not yet been considered in tumourgenesis.

Cutaneous melanoma is an aggressive form of skin cancer, which causes high death rates worldwide. Melanoma can be surgically treated leading to a favourable prognosis but only if detected early (Soengas & Lowe, 2003). Nevertheless, patients might develop resistance to chemotherapy or immunotherapy leading to a disease progression and metastasis (Ayachi et al., 2019). Most chemotherapies are based on inducing apoptosis in the malignant cells, thus defects in apoptosis signalling lead to chemo-resistance (Emanuel et al., 2008; Hiscutt et al., 2010). One major apoptotic defect in melanoma is elevated XIAP expression, which was described to be associated with melanoma thickness and tumour progression (Emanuel et al., 2008). The present study investigated the mechanism underlying enhanced melanoma growth mediated by elevated XIAP expression. Our data demonstrate for the first time that XIAP supports melanoma tumour growth through interaction with RIPK2 and TAB1. The XIAP-RIPK2-TAB1 signalling complex induces the expression and secretion of chemokines, especially the CXCL family members such as IL8, which mediates intra-tumoural neutrophil infiltration and thus supports melanoma progression. These results reveal one of the main signalling pathways that mediate melanoma tumour growth and thus shed additional light on XIAP as a novel therapeutic target in cancer by targeting its inflammatory function.

4.1 XIAP supports melanoma growth independently of its anti-apoptotic function

In this study, we analysed the contribution of XIAP in supporting melanoma tumour growth. Our data revealed that tumour volumes were significantly reduced in B16-XIAP^{KO} tumours compared to B16 WT tumours (**Figure 3.1**). Although, XIAP was previously described to promote tumour growth and survival when it is highly expressed due to enhanced cell death resistance of the malignant cells (Deveraux & Reed, 1999), we were not able to detect any difference in apoptosis in both WT and XIAP^{KO} B16 tumours (**Figure 3.2A**). Nevertheless, in other types of cancer like acute pancreatitis, XIAP deletion was shown to moderate the severity of acute pancreatitis due to increased caspase activity and elevated apoptosis in addition to reduced NFκB activation and inflammation (Liu et al., 2017). Different apoptosis level in different tumours is not surprising as cancer cells can use different mechanisms to escape apoptosis through affecting the transcription, translation or post-translation modifications of different apoptotic pathways (Fulda et al., 2010; Goldar et al., 2015). Thus, although XIAP was deleted, melanoma cells might escape apoptosis by mechanisms other than direct inhibition through XIAP. One example could be the disbalanced expression of pro- and anti-apoptotic BCL-2 proteins, which was previously shown to induce cancer cell survival (Kang & Reynolds, 2009; Galluzzi et al., 2010). In addition, deletion of XIAP alone might not be sufficient to promote apoptosis, as cIAP1 and cIAP2 are still present. This can be further addressed by analysing the effect of cIAP1/2 knock-out on melanoma tumour growth.

Moreover, B16 WT and XIAP^{KO} melanoma cells showed similar proliferation and were both resistant to TNF and TRAIL induced cell death (**Figure 3.2 B** and **C**). Resistance against TRAIL induced apoptosis has already been described for many human melanoma cell lines such as IGR-37, IPC-298, SK-Mel-30, WM-9, and WM-902B (Zeise et al., 2004). Furthermore, human melanoma cells with resistance to TRAIL were shown to have a cross-resistance to different apoptotic stimuli like FasL (X. D. Zhang et al., 2006). Melanoma resistance to members of the TNF receptor superfamily like TNF, FasL and TRAIL was linked to genetic alterations of protein kinases like Ras and B-Raf in addition to their corresponding transcription factors like c-Jun and NFκB (Ivanov et al., 2003). Although XIAP was mainly considered to

exhibit apoptosis resistance when being highly expressed in tumour tissues (Kashkar, 2010), our data revealed that XIAP promotes melanoma growth independently of its anti-apoptotic function. This suggests an additional function of XIAP that contributes to melanoma tumour growth.

4.2 XIAP mediates IL8 secretion in melanoma

CXCL8 (interleukine-8, IL8) is expressed by several cell types and mainly triggers neutrophil chemo-attraction and activation (Teijeira et al., 2021; Kulke et al., 1998; David et al., 2016). IL8 produced by melanoma cells can promote tumour growth and progression, as IL8 can facilitate angiogenesis and induce epithelial to mesenchymal transition (EMT) phenotypic switch in the tumour cells. EMT in turn can enhance metastasis and resistance to immune responses (Schaider et al., 2003; RM et al., 1995; David et al., 2016; Hölzel & Tüting, 2016). Besides, neutralizing IL8 or CXCL1 was shown to decrease melanoma cells proliferation *in vitro* suggesting a role of these chemokines in melanoma growth (Schadendorf et al., 1993; Fujisawa et al., 1999). Therefore, we analysed whether XIAP can induce inflammation and cytokine/chemokine secretion in melanoma that could contribute to XIAP mediated tumour growth. Our data showed that members of the C-X-C chemokine ligands (CXCL) family, mainly Cxcl1 (or KC in mice which is homologue to human IL8) and Cxcl10 expression were dependent on XIAP in B16 melanoma cells (**Figure 3.3A**).

XIAP knock-down using siRNA was previously shown to reduce NFκB activation following NOD1 or NOD2 stimulation in different cell lines. In particular, IL8 secretion upon MDP stimulation in THP1 cells was diminished when XIAP was silenced (Bielig et al., 2014). In line with previous studies indicating that elevated XIAP expression alone can induce cytokine secretion without further stimulation (Hofer-Warbinek et al., 2000), our data clearly showed that XIAP knock-down or knock-out in human cancer cells could markedly abolished IL8 secretion under steady state conditions (**Figure 3.3B** and **D**). To analyse the potential involvement of additional extrinsic stimuli within the tumour microenvironment that might additionally enhance cytokine secretion, we treated human melanoma cells with TNF (**Figure 3.3E** and **F**). Our data indicated that TNF could promote higher IL8 secretion levels and showed that XIAP knock-down or knock-out could not completely block TNF mediated IL8 secretion.

Thus, TNF can promote IL8 secretion in human melanoma cells but not solely through XIAP dependent signalling pathways. This is in line with previous studies indicating that cancer cells facilitate proliferation by inducing inflammation in the tumour microenvironment. This can be achieved by producing TNF, which in turn can activate NFκB transcription factors to induce gene transcription that promotes cell survival and proliferation (Waters et al., 2013). These data can also help to explain the resistance of melanoma cells to TNF induced cell death. It was previously described that TNF mediated NFκB activation drives c-FLIP overexpression and thus inhibits apoptosis induced by TNFR1, Fas and TRAIL receptors (Micheau et al., 2001; Travert et al., 2008). Furthermore, TNF induced IL8 secretion opens the question whether there is an upstream signal of XIAP that could be involved in XIAP mediated IL8 secretion. To address this question, further investigations need to be done like analysing the effect of TNF or TRAIL receptor knock-out on melanoma tumour growth and IL8 secretion.

4.3 XIAP mediated IL8 secretion in melanoma is dependent on direct interaction with RIPK2 and TAB1

Our data showed that enhanced XIAP expression induced increased IL8 secretion (**Figure 3.4B**). XIAP mediated IL8 secretion was dependent on its BIR1, BIR2 and RING domains but not the BIR3 domain. The importance of these XIAP domains in mediating inflammatory responses was described previously. XIAP-TAB1 interaction through the binding of TAB1 to the BIR1 domain of XIAP is crucial for TGFβ signalling and NFκB activation (Lu et al., 2007; Yamaguchi et al., 1999). In addition, interaction of RIPK2 to the BIR2 domain of XIAP was described to mediate NFκB activation upon NOD1/2 stimulation (Krieg et al., 2009; Damgaard et al., 2012). Furthermore, the E3 ligase activity of XIAP was shown to be indispensable for XIAP mediated IL8 secretion (Goncharov et al., 2018). In this study, we were able to reproduce these data and could show that ectopically expressed XIAP or endogenous XIAP can directly interact with TAB1 and RIPK2 (**Figure 3.4C** and **D**). Additionally, XIAP driven IL8 secretion was dependent on both TAB1 and RIPK2 (**Figure 3.6A**, **B**, **C** and **D**).

Next, we analysed whether the direct interaction between XIAP and RIPK2 is followed by RIPK2 ubiquitylation. The crucial role of RIPK2 poly-ubiquitylation mediated by XIAP in NOD2 signalling was extensively studied using different approaches by applying either specific inhibitors or by mutating critical lysine residues of RIPK2, which were shown to be major sites of XIAP-mediated ubiquitylation (Goncharov et al., 2018). Studies using site directed mutagenesis in the RIPK2 kinase domain could block RIPK2 ubiquitylation through interfering with the XIAP-RIPK2 interaction (Heim et al., 2020). In line with these studies, our data revealed that enhanced XIAP expression in human and mouse melanoma cells could promote RIPK2 ubiquitylation (**Figure 3.5 A** and **B**). This further strengthens the theory that enhanced XIAP expression in melanoma can induce RIPK2 ubiquitylation and subsequent IL8 secretion.

As previously described, NOD1/2 stimulation leads to RIPK2 auto-phosphorylation and subsequent ubiquitylation *via* different E3 ligases like XIAP and cIAP1/2 (Bertrand et al., 2009). XIAP was shown to be the main E3 ligase (Heim et al., 2020; Krieg et al., 2009; Damgaard et al., 2012; Goncharov et al., 2018; Nachbur et al., 2015) mediating K63 poly-ubiquitylation and recruitment of the LUBAC complex (Damgaard et al., 2012). The ubiquitin chains on RIPK2 facilitate the interaction with IKK and TAK1 complexes, which eventually results in NFκB activation and IL8 secretion (Heim et al., 2020; Hofer-Warbinek et al., 2000; Hasegawa et al., 2008). In line with these studies, our data showed that MDP mediated IL8 expression and secretion was dependent not only on XIAP and RIPK2 expression but also on TAB1 (**Figure 3.7A** and **B**). This further supports our hypothesis that XIAP mediated IL8 secretion in melanoma is dependent on RIPK2 ubiquitylation and subsequent interaction with TAK1 complex through TAB1, which finally leads to NFκB activation.

To further address that XIAP induced IL8 secretion in melanoma cells is mediated by XIAP-RIPK2 signalling, we used d89, an antagonist that was described to specifically target the BIR2 domain of XIAP and thus disrupts the interaction between XIAP and RIPK2 (Goncharov et al., 2018). Our data showed that d89 antagonist could sufficiently block IL8 secretion in melanoma cells (**Figure 3.6E**), unlike antagonists targeting the BIR3 domain of XIAP like Birinapant and BV6, which could not block IL8

secretion but instead induced even higher level of IL8 (**Figure 3.6E**). Increased IL8 levels upon TNF treatment (**Figure 3.3E and F**), which might be due to the inflammatory microenvironment in melanoma that potentially boosted the effect of exogenous TNF (Coussens & Werb, 2002; Balkwill, 2002), could be induced by TNF-driven NFκB activation through TNFR signalling. Although, SMAC mimetics were described to switch the TNF receptor signalling cascade from NFκB activation and cell survival to apoptosis by mediating cIAP1/2 degradation (Gyrd-Hansen & Meier, 2010; Dueber, 2011; Feltham et al., 2011; Gaither et al., 2007), our data showed that SMAC mimetics induced higher level of IL8 secretion. A potential explanation could be the activation of the non-canonical NFκB signalling pathway due to cIAP1/2 degradation upon treatment with SMAC mimetics (Goncharov et al., 2018; Varfolomeev & Vucic, 2008) resulting in NIK accumulation (S. C. Sun, 2011). This could be further investigated by analysing the processing of p100 into p52. Collectively, our data show a promising therapeutic strategy for targeting melanomas by abrogating the XIAP-RIPK2 axis.

4.4 XIAP supports melanoma growth *via* interaction with RIPK2 and TAB1

Tumour progression in different cancers including colon adenocarcinoma, lung squamous cell carcinoma, breast invasive carcinoma and cutaneous melanomas was shown to be associated with high RIPK2 expression levels, which was accompanied by an increased infiltration of the tumour tissues with different immune cell types such as T cells or cancer associated fibroblasts (H. Zhang et al., 2022). Additionally, RIPK2 expression in colorectal cancer was shown to be positively associated with IL8 expression (R. F. Jaafar et al., 2021). The role of RIPK2 in different malignant tumours was linked to different signalling pathways such as NOD and NFκB signalling pathways in addition to other binding proteins like ubiquitin ligases (H. Zhang et al., 2022).

Based on our data showing the involvement of RIPK2 and TAB1 in XIAP mediated IL8 secretion, we further analysed whether the reduced tumour volume in the B16-XIAP^{KO} tumours was also dependent on RIPK2 and TAB1. Our data revealed that

RIPK2^{KO} and TAB1^{KO} could also reduce melanoma growth in mice (**Figure 3.8B**). This is in line with other studies showing reduced tumour volume in a RIPK2 knock-out background in a breast cancer mouse model (R. Jaafar et al., 2018). Additionally, RIPK2 was described to enhance tumour cell progression in triple negative breast cancer by activating NFκB pathway (Singel et al., 2014). The involvement of RIPK2 in tumour growth *via* activation of the NFκB pathway was also described in gastric cancers (Maloney et al., 2020). Collectively, RIPK2-NFκB signalling was shown to be associated with different malignant tumours suggesting RIPK2 as a promising target for cancer therapy. Furthermore, TAB1 was also described to be involved in cancer development. Reduced tumour growth of 4T1 breast cancer in syngeneic BALB/c mice was found upon expression of truncated TAB1. The role of TAB1 in mediating progression of breast cancer was linked to the activation of NFκB mediated by TGFβ *via* the TAB1, TAK1, IKKβ signalling (Neil & Schiemann, 2008). In non-small cell lung carcinoma (NSCLC), TAB1 was shown to be highly expressed in addition to TAK1. However, the enhanced protein expression of TAK1 and TAB1 in NSCLC tissues was not correlated with tumour size but was rather related to patient prognosis and metastasis. This suggested TAK1 and TAB1 as therapeutic targets for NSCLC (Zhu et al., 2015). In this study, we could show that there were no differences in apoptosis in both RIPK2^{KO} and TAB1^{KO} B16 tumours in addition to cultured cells similar to XIAP^{KO} (**Figure 3.9**). Our data indicated for the first time that XIAP forms a signalling complex with RIPK2 and TAB1 that initiates inflammation by inducing the expression and secretion of IL8. Thus, XIAP-RIPK2-TAB1 complex supports melanoma tumour growth *via* activation of the NFκB pathway and independently of the anti-apoptotic function of XIAP.

4.5 XIAP supports melanoma growth in B16 and *Hgf-Cdk4^{R24C}* mouse melanoma models by inducing neutrophil infiltration

Accumulating studies focused on the association between inflammation and tumour progression. Tumour cells make use of the innate immune cells, chemokines and their corresponding receptors to support their microenvironment (Coussens & Werb, 2002). One of the major tumour promoting inflammatory cells are neutrophils (Coffelt et al., 2010; DeNardo et al., 2010; Egeblad et al., 2010; Murdoch et al., 2008;

Emanuel et al., 2008; De Palma et al., 2007). Neutrophils are chemo-attracted to the tumour sites through chemokines produced by the tumour cells (Coussens & Werb, 2002; Gregory & Houghton, 2011). Chemokines are chemotactic molecules, which have a specific role in leukocyte chemo-attraction and initiation of the inflammatory response (Payne & Cornelius, 2002a; Sherwood & Toliver-Kinsky, 2004). Chemokines were shown to be associated with tumour progression and metastasis in addition to tumour growth, cell proliferation and angiogenesis (Payne and Cornelius, 2002). Melanoma cells produce chemokines like CXCL1 and IL8 to recruit immune cells like neutrophils. Additionally, melanoma cells use their secreted chemokines to promote tumour growth and proliferation (Schaider et al., 2003; Payne & Cornelius, 2002a). Besides, poor prognosis in primary melanoma is associated with intra-tumoural neutrophil infiltration (Jensen et al., 2012). Targeting neutrophils for cancer therapy was previously proposed (Keane et al., 2004) but faced several difficulties as neutrophil depletion might disrupt the host defence (Fulda & Vucic, 2012). Hence, other approaches were studied like targeting the CXCL8 axis or targeting specific substrates that mediate tumour growth (Gregory & Houghton, 2011). Together, neutrophil infiltration is an important tumour biomarker (Masucci et al., 2019). Therfore, we analysed whether melanoma growth is associated with neutrophils not only in B16 mouse melanoma model but also in *Hgf-Cdk4*^{R24C} mouse melanoma model.

A key genetic abnormality usually observed in melanoma patients is the insufficient control of the G1 phase in the cell cycle. This could be due to loss of function of the cyclin-dependent kinase inhibitor or CDK4 gain of function (Chudnovsky et al., 2005; Chin, 2003; Curtin et al., 2005). Depletion of the cyclin-dependent kinase inhibitor (Paul Krimpenfort et al., 2011; Sharpless et al., 2001) or mutation in the CDK4 gene mainly the CDK4^{R24C} promotes melanoma development in mice. Additionally, CDK4^{R24C} mutation was detected in some rare melanoma cases (Wölfel et al., 1995; Zuo et al., 1996). Mice overexpressing Hgf serve as suitable mouse model as the resulting melanomas spread in the skin in a way similar to human which is not found in other mouse melanoma models (Noonan et al., 2001). Taken together, the *Hgf-Cdk4*^{R24C} mouse melanoma model represents an experimental mouse model that can be used to study the biology of melanoma, as it closely resembles melanoma

development in humans. We used this mouse model in addition to the B16 mouse model to study the impact of XIAP in a more close resembled model to the melanoma development in humans. Similar to B16 mouse model, tumour volume was markedly reduced in the *Hgf-Cdk4*^{R24C} *XIAP*^{KO} mouse model (**Figure 3.13A and B**). Additionally, in line with XIAP^{KO}, RIPK2^{KO} or TAB1^{KO} B16 mouse melanoma tumours (**Figure 3.11A**), we could detect reduction in the expression levels of Cxcl1 and Cxcl10 in tumours isolated from the *Hgf-Cdk4*^{R24C} *XIAP*^{KO} mouse model (**Figure 3.13D**). Thus, XIAP mediates chemokines secretion and supports melanoma growth in *Hgf-Cdk4*^{R24C} mouse model similar to the B16 mouse model.

Our data showed an association between neutrophil infiltration and enhanced XIAP expression in tumour samples derived from melanoma patients (**Figure 3.10**). Leucocyte infiltration in various tumour tissues was previously described (Vakkila & Lotze, 2004; Hanahan & Weinberg, 2011b). The tumour can promote its growth by releasing chemokines and cytokines that recruit leukocyte to the tumour microinvironment. Recruited leucocyte in turn increase the production of different components that promote tumour growth by secreting growth factors and angeogenic factors (Arenberg et al., 2000; Mantovani et al., 2002; Vakkila & Lotze, 2004). Human and mouse chemokines like IL8 and KC (Cxcl1) can attract and activate neutrophils (Opdenakker & Van Damme, 2004; Gijsbers et al., 2005). Thus, we investigated whether XIAP-RIPK2-TAB1 complex mediated chemokine secretion is important for neutrophils infiltration first in B16 melanoma tumours. Our data revealed for the first time that depletion of XIAP, RIPK2 or TAB1 in B16 tumours resulted in reduced neutrophil infiltration (**Figure 3.11B** and **C**) but did not affect other immune cells (**Fig 3.11D**). Reduced neutrophil infiltration was also found in tumours isolated from the *Hgf-Cdk4*^{R24C} *XIAP*^{KO} mouse model (**Figure 3.13E, F, G and H**). Monocytes were also described to be attracted to the tumour tissues *via* chemokines released from the tumour. The monocytes can be differentiated into macrophages, which in turn can promote tumour growth (Vakkila & Lotze, 2004; Jerrells et al., 1979; Mantovani et al., 1979). In contrast, infiltration of other immune cells like T cells, natural killer cells or myeloid dentritic cells into tumour tissues was described to induce an immunological response and thus improve patients prognosis (Vakkila & Lotze, 2004) in ovarian cancer (L. Zhang et al., 2003) and gastric cancer (Ishigami et al., 2000). This further

showing that in melanoma, neutrophil infiltration was the main factor involving tumour growth as there were no differences in other immune cells like macrophages, T cells or dentritic cells (**Figure 3.11D**).

To further investigate whether neutrophils are the main dirver of melanoma growth in our mouse model, we depleted neutrophils experimentally using a Ly6G specific antibody, which was previously described (Lakritz et al., 2015). Indeed, neutrophil depletion resulted in reduced tumour volume in B16 WT melanoma to the same level as XIAP^{KO} melanoma tumours (**Figure 3.12**). This indicates that the reduced tumour growth in B16-XIAP^{KO} melanomas was mediated by reduced neutrophil recruitment (**Figure 3.1**). Taken together, our data could show for the first time that the XIAP-RIPK2-TAB1 complex stimulates the expression and secretion of chemokines that are responsible for intra-tumoural neutrophil infiltration and therby facilitates tumour growth. Thus, disrupting the signalling cascade might present an additional strategy to therapeutically target melanomas in the future.

4.6 Conclusion

XIAP was mainly studied as an inhibitor of apoptosis protein due to its ability to directly interact and block caspase activity. In line, resistance to apoptosis in cancer was considered as a result of enhanced XIAP expression in tumour tissues (Kashkar, 2010). However, accumulating evidence indicated that XIAP plays a crucial role in inflammatory signalling. The involvement of XIAP in inflammation was shown in the TGFβ/BMP signalling pathway through interaction with TAB1. Moreover, XIAP interaction with RIPK2 is essential for RIPK2 ubiquitylation and NOD1/2 signalling leading to NFκB activation and cytokine secretion (Heim et al., 2020; Krieg et al., 2009). Therefore, XIAP is considered as a therapeutic target in immune diseases and recently developed small molecules could successfully disrupt the XIAP-RIPK2 interaction and thus abrogate the inflammatory signalling (Goncharov et al., 2018; Hrdinka et al., 2018; Nachbur et al., 2015).

By using human melanoma cell lines, model cell lines, tumour tissues derived from patients and two mouse melanoma models, our study conclusively demonstrates that XIAP supports melanoma tumour growth through interaction with RIPK2 and TAB1. The XIAP-RIPK2-TAB1 signalling complex in turn induced the expression and secretion of chemokines, especially the CXCL members including IL8, which mediates intra-tumoural neutrophil infiltration and thus supports melanoma progression (**Figure 4.1**).

Targeting neutrophils in cancer was previously described either by blocking the IL8 receptor axis or by blocking neutrophil derived substances (Masucci et al., 2019; Gregory & Houghton, 2011). In our study, we observed that XIAP-RIPK2-TAB1 signalling complex mediated tumour neutrophil infiltration and melanoma tumour growth. Thus, XIAP-RIPK2-TAB1 complex represents a novel and valuable therapeutic target for cancer therapies.

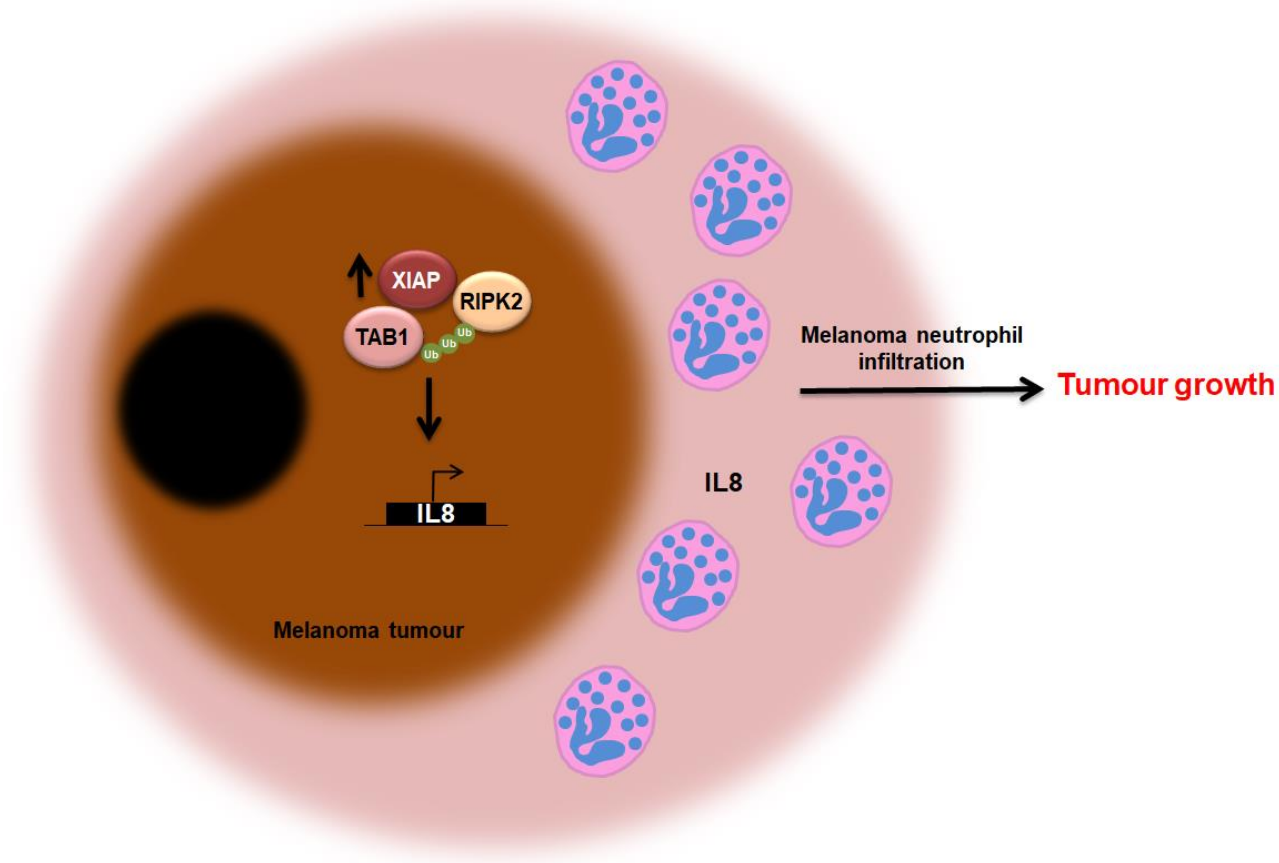

Figure 4.1: XIAP supports melanoma tumour growth through interaction with RIPK2 and TAB1

Enhanced XIAP expression in melanoma can form a complex with RIPK2 and TAB1. XIAP-RIPK2-TAB1 signalling complex induces the expression and secretion of chemokines, especially the CXCL family like IL8, which mediates intra-tumoural neutrophil infiltration and thus supports melanoma progression.

5 References

Abreu-Martin, M. T., Vidrich, A., Lynch, D. H., & Targan, S. R. (1995). Divergent induction of apoptosis and IL-8 secretion in HT-29 cells in response to TNF-alpha and ligation of Fas antigen. *Journal of Immunology (Baltimore, Md.-: 1950)*, *155*(9), 4147–4154. http://www.ncbi.nlm.nih.gov/pubmed/7594569

Albert, M. C., Brinkmann, K., Pokrzywa, W., Günther, S. D., Krönke, M., Hoppe, T., & Kashkar, H. (2020). CHIP ubiquitylates NOXA and induces its lysosomal degradation in response to DNA damage. In *Cell Death and Disease* (Vol. 11, Issue 9). https://doi.org/10.1038/s41419-020-02923-x

Andersen, M. H., Becker, J. C., & Straten, P. T. (2005). Regulators of apoptosis: Suitable targets for immune therapy of cancer. *Nature Reviews Drug Discovery*, *4*(5), 399–409. https://doi.org/10.1038/nrd1717

Andree, M., Seeger, J. M., Schüll, S., Coutelle, O., Wagner-Stippich, D., Wiegmann, K., Wunderlich, C. M., Brinkmann, K., Broxtermann, P., Witt, A., Fritsch, M., Martinelli, P., Bielig, H., Lamkemeyer, T., Rugarli, E. I., Kaufmann, T., Sterner-Kock, A., Wunderlich, F. T., Villunger, A., … Kashkar, H. (2014). BID -dependent release of mitochondrial SMAC dampens XIAP -mediated immunity against Shigella . *The EMBO Journal*, *33*(19), 2171–2187. https://doi.org/10.15252/embj.201387244

Arenberg, D. A., Keane, M. P., DiGiovine, B., Kunkel, S. L., Strom, S. R. B., Burdick, M. D., Iannettoni, M. D., & Strieter, R. M. (2000). Macrophage infiltration in human non-small-cell lung cancer: The role of CC chemokines. *Cancer Immunology Immunotherapy*, *49*(2), 63–70. https://doi.org/10.1007/s002620050603

Arnt, C. R., Chiorean, M. V., Heldebrant, M. P., Gores, G. J., & Kaufmann, S. H. (2002). Synthetic Smac/DIABLO peptides enhance the effects of chemotherapeutic agents by binding XIAP and cIAP1 in situ. *Journal of Biological Chemistry*, *277*(46), 44236–44243. https://doi.org/10.1074/jbc.M207578200

Arora, V., Cheung, H. H., Plenchette, S., Micali, O. C., Liston, P., & Korneluk, R. G. (2007). Degradation of survivin by the X-linked Inhibitor of Apoptosis (XIAP)-XAF1 complex. *Journal of Biological Chemistry*, *282*(36), 26202–26209. https://doi.org/10.1074/jbc.M700776200

Ashkenazi, A. (2008). Targeting the extrinsic apoptosis pathway in cancer. *Cytokine and Growth Factor Reviews*, *19*(3–4), 325–331. https://doi.org/10.1016/j.cytogfr.2008.04.001

Augello, C., Caruso, L., Maggioni, M., Donadon, M., Montorsi, M., Santambrogio, R., Torzilli, G., Vaira, V., Pellegrini, C., Roncalli, M., Coggi, G., & Bosari, S. (2009). Inhibitors of apoptosis proteins (IAPs) expression and their prognostic significance in hepatocellular carcinoma. *BMC Cancer*, *9*, 1–10. https://doi.org/10.1186/1471-2407-9-125

Ayachi, O., Barlin, M., Broxtermann, P. N., Kashkar, H., Mauch, C., & Zigrino, P. (2019). The X-linked inhibitor of apoptosis protein (XIAP) is involved in melanoma invasion by regulating cell migration and survival. *Cellular Oncology*, 319–329. https://doi.org/10.1007/s13402-019-00427-1

Baboshina, O. V., & Haas, A. L. (1996). Novel multiubiquitin chain linkages catalyzed by the conjugating enzymes E2EPF and RAD6 are recognized by 26 S proteasome subunit 5. *Journal of Biological Chemistry*, *271*(5), 2823–2831. https://doi.org/10.1074/jbc.271.5.2823

Balkwill, F. (2002). Tumor necrosis factor or tumor promoting factor? *Cytokine and Growth Factor Reviews*, *13*(2), 135–141. https://doi.org/10.1016/S1359-6101(01)00020-X

Bar-Eli, M. (1999). Role of AP-2 in tumor growth and metastasis of human melanoma. *Cancer and Metastasis Reviews*, *18*(3), 377–385. https://doi.org/10.1023/A:1006377309524

Bauler, L. D., Duckett, C. S., & O'Riordan, M. X. D. (2008). XIAP regulates cytosol-specific innate immunity to listeria infection. *PLoS Pathogens*, *4*(8). https://doi.org/10.1371/journal.ppat.1000142

Bertrand, M. J. M., Doiron, K., Labbé, K., Korneluk, R. G., Barker, P. A., & Saleh, M. (2009). Cellular Inhibitors of Apoptosis cIAP1 and cIAP2 Are Required for Innate Immunity Signaling by the Pattern Recognition Receptors NOD1 and NOD2. *Immunity*, *30*(6), 789–801. https://doi.org/10.1016/j.immuni.2009.04.011

Bielig, H., Lautz, K., Braun, P. R., Menning, M., Machuy, N., Brügmann, C., Barisic, S., Eisler, S. A., Andree, M., Zurek, B., Kashkar, H., Sansonetti, P. J., Hausser, A., Meyer, T. F., & Kufer, T. A. (2014). The Cofilin Phosphatase Slingshot Homolog 1 (SSH1) Links NOD1 Signaling to Actin Remodeling. *PLoS Pathogens*, *10*(9). https://doi.org/10.1371/journal.ppat.1004351

Birnbaum, M. J., Clem, R. J., & Miller, L. K. (1994). An apoptosis-inhibiting gene from a nuclear polyhedrosis virus encoding a polypeptide with Cys/His sequence motifs. *Journal of Virology*, *68*(4), 2521–2528. https://doi.org/10.1128/jvi.68.4.2521-2528.1994

Blankenship, J. W., Varfolomeev, E., Goncharov, T., Fedorova, A. V., Kirkpatrick, D. S., Izrael-Tomasevic, A., Phu, L., Arnott, D., Aghajan, M., Zobel, K., Bazan, J. F., Fairbrother, W. J., Deshayes, K., & Vucic, D. (2009). Ubiquitin binding modulates IAP antagonist-stimulated proteasomal degradation of c-IAP1 and c-IAP21. *Biochemical Journal*, *417*(1), 149–160. https://doi.org/10.1042/BJ20081885

Bodmer, J. L., Schneider, P., & Tschopp, J. (2002). The molecular architecture of the TNF superfamily. *Trends in Biochemical Sciences*, *27*(1), 19–26. https://doi.org/10.1016/S0968-0004(01)01995-8

Caruso, R., Warner, N., Inohara, N., & Núñez, G. (2014). NOD1 and NOD2: Signaling, host defense, and inflammatory disease. *Immunity*, *41*(6), 898–908. https://doi.org/10.1016/j.immuni.2014.12.010

Chastagner, P., Israël, A., & Brou, C. (2006). Itch/AIP4 mediates Deltex degradation through the formation of K29-linked polyubiquitin chains. *EMBO Reports*, *7*(11), 1147–1153. https://doi.org/10.1038/sj.embor.7400822

Chen, G., Shaw, M. H., Kim, Y.-G., Nuñez, G., & Nuñez, N. (2008). *NOD-Like Receptors: Role in Innate Immunity and Inflammatory Disease*. https://doi.org/10.1146/annurev.pathol.4.110807.092239

Chen, Z., Hagler, J., Palombella, V. J., Melandri, F., Scherer, D., Ballard, D., & Maniatis, T. (1995). Signal-induced site-specific phosphorylation targets IκBα to the ubiquitin-proteasome pathway. *Genes and Development*, *9*(13), 1586–1597. https://doi.org/10.1101/gad.9.13.1586

Chen, Z., Naito, M., Hori, S., Mashima, T., Yamori, T., & Tsuruo, T. (1999). A human IAP-family gene, Apollon, expressed in human brain cancer cells. *Biochemical and Biophysical Research Communications*, *264*(3), 847–854. https://doi.org/10.1006/bbrc.1999.1585

Chin, L. (2003). The genetics of malignant melanoma: Lessons from mouse and man. *Nature Reviews Cancer*, *3*(8), 559–570. https://doi.org/10.1038/nrc1145

Chomczynski, P., & Sacchi, N. (1987). Single-step method of RNA isolation by acid guanidinium thiocyanate-phenol-chloroform extraction. *Analytical Biochemistry*, *162*(1), 156–159.

https://doi.org/10.1016/0003-2697(87)90021-2

Chudnovsky, Y., Khavari, P. A., & Adams, A. E. (2005). Melanoma genetics and the development of rational therapeutics. *Journal of Clinical Investigation*, *115*(4), 813–824. https://doi.org/10.1172/JCI24808

Claudio, E., Brown, K., Park, S., Wang, H., & Siebenlist, U. (2002). BAFF-induced NEMO-independent processing of NF-κB2 in maturing B cells. *Nature Immunology*, *3*(10), 958–965. https://doi.org/10.1038/ni842

Coffelt, S. B., Kersten, K., Doornebal, C. W., Weiden, J., Vrijland, K., Hau, C. S., Verstegen, N. J. M., Ciampricotti, M., Hawinkels, L. J. A. C., Jonkers, J., & De Visser, K. E. (2015). IL-17-producing γδ T cells and neutrophils conspire to promote breast cancer metastasis. *Nature*, *522*(7556), 345–348. https://doi.org/10.1038/nature14282

Coffelt, S. B., Lewis, C. E., Naldini, L., Brown, J. M., Ferrara, N., & De Palma, M. (2010). Elusive identities and overlapping phenotypes of proangiogenic myeloid cells in tumors. *American Journal of Pathology*, *176*(4), 1564–1576. https://doi.org/10.2353/ajpath.2010.090786

Conway, E. M., Pollefeyt, S., Cornelissen, J., DeBaere, I., Steiner-Mosonyi, M., Ong, K., Baens, M., Collen, D., & Schuh, A. C. (2000). Three differentially expressed survivin cDNA variants encode proteins with distinct antiapoptotic functions. *Blood*, *95*(4), 1435–1442. https://doi.org/10.1182/blood.v95.4.1435.004k01_1435_1442

Coope, H. J., Atkinson, P. G. P., Huhse, B., Belich, M., Janzen, J., Holman, M. J., Klaus, G. G. B., Johnston, L. H., & Ley, S. C. (2002). CD40 regulates the processing of NF-κB2 p100 to p52. *EMBO Journal*, *21*(20), 5375–5385. https://doi.org/10.1093/emboj/cdf542

Coussens, L. M., & Werb, Z. (2002). Inflammation and cancer. *Nature 2002 420:6917*, *420*(6917), 860–867. https://doi.org/10.1038/nature01322

Crook, N. E., Clem, R. J., & Miller, L. K. (1993). An apoptosis-inhibiting baculovirus gene with a zinc finger-like motif. *Journal of Virology*, *67*(4), 2168–2174. https://doi.org/10.1128/jvi.67.4.2168-2174.1993

Cummins, J. M., Kohli, M., Rago, C., Kinzler, K. W., Vogelstein, B., & Bunz, F. (2004). X-Linked Inhibitor of Apoptosis Protein (XIAP) Is a Nonredundant Modulator of Tumor Necrosis Factor-Related Apoptosis-Inducing Ligand (TRAIL)-Mediated Apoptosis in Human Cancer Cells. *Cancer Research*, *64*(9), 3006–3008.

https://doi.org/10.1158/0008-5472.CAN-04-0046

Curtin, J. A., Fridlyand, J., Kageshita, T., Patel, H. N., Busam, K. J., Kutzner, H., Cho, K.-H., Aiba, S., Bröcker, E.-B., LeBoit, P. E., Pinkel, D., & Bastian, B. C. (2005). Distinct Sets of Genetic Alterations in Melanoma. *New England Journal of Medicine*, *353*(20), 2135–2147. https://doi.org/10.1056/nejmoa050092

Damgaard, R. B., Nachbur, U., Yabal, M., Wong, W. W. L., Fiil, B. K., Kastirr, M., Rieser, E., Rickard, J. A., Bankovacki, A., Peschel, C., Ruland, J., Bekker-Jensen, S., Mailand, N., Kaufmann, T., Strasser, A., Walczak, H., Silke, J., Jost, P. J., & Gyrd-Hansen, M. (2012). The Ubiquitin Ligase XIAP Recruits LUBAC for NOD2 Signaling in Inflammation and Innate Immunity. *Molecular Cell*, *46*(6), 746–758. https://doi.org/10.1016/j.molcel.2012.04.014

David, J. M., Dominguez, C., Hamilton, D. H., & Palena, C. (2016). The IL-8/IL-8R axis: A double agent in tumor immune resistance. *Vaccines*, *4*(3). https://doi.org/10.3390/vaccines4030022

Davoodi, J., Lin, L., Kelly, J., Liston, P., & MacKenzie, A. E. (2004). Neuronal apoptosis-inhibitory protein does not interact with Smac and requires ATP to bind caspase-9. *Journal of Biological Chemistry*, *279*(39), 40622–40628. https://doi.org/10.1074/jbc.M405963200

De Palma, M., Murdoch, C., Venneri, M. A., Naldini, L., & Lewis, C. E. (2007). Tie2-expressing monocytes: regulation of tumor angiogenesis and therapeutic implications. *Trends in Immunology*, *28*(12), 519–524. https://doi.org/10.1016/j.it.2007.09.004

Dejardin, E. (2006). The alternative NF-κB pathway from biochemistry to biology: Pitfalls and promises for future drug development. *Biochemical Pharmacology*, *72*(9 SPEC. ISS.), 1161–1179. https://doi.org/10.1016/j.bcp.2006.08.007

DeNardo, D. G., Andreu, P., & Coussens, L. M. (2010). Interactions between lymphocytes and myeloid cells regulate pro-versus anti-tumor immunity. *Cancer and Metastasis Reviews*, *29*(2), 309–316. https://doi.org/10.1007/s10555-010-9223-6

Deshaies, R. J., & Joazeiro, C. A. P. (2009). RING domain E3 ubiquitin ligases. *Annual Review of Biochemistry*, *78*, 399–434. https://doi.org/10.1146/annurev.biochem.78.101807.093809

Deveraux, Q. L., & Reed, J. C. (1999). IAP family proteins - Suppressors of apoptosis. *Genes and Development*, *13*(3), 239–252. https://doi.org/10.1101/gad.13.3.239

Deveraux, Q. L., Takahashi, R., Salvesen, G. S., & Reed, J. C. (1997).

40901-2. *388*(July), 300–304.

Dhawan, P., & Richmond, A. (2002). Role of CXCL1 in tumorigenesis of melanoma. *Journal of Leukocyte Biology*, *72*(1), 9–18. http://www.ncbi.nlm.nih.gov/pubmed/12101257%0Ahttp://www.pubmedcentral.nih.gov/articlerender.fcgi?artid=PMC2668262

Dittmar, G., & Winklhofer, K. F. (2020). Linear Ubiquitin Chains: Cellular Functions and Strategies for Detection and Quantification. *Frontiers in Chemistry*, *7*(January), 1–16. https://doi.org/10.3389/fchem.2019.00915

Du, C., Fang, M., Li, Y., Li, L., & Wang, X. (2000). Smac, a mitochondrial protein that promotes cytochrome c-dependent caspase activation by eliminating IAP inhibition. *Cell*, *102*(1), 33–42. https://doi.org/10.1016/S0092-8674(00)00008-8

Dueber, E. C. (2011). *Antagonists Induce a Conformational*. *376*(October). https://doi.org/10.1126/science.1207862

Eckelman, B. P., Salvesen, G. S., & Scott, F. L. (2006). Human inhibitor of apoptosis proteins: Why XIAP is the black sheep of the family. *EMBO Reports*, *7*(10), 988–994. https://doi.org/10.1038/sj.embor.7400795

Egeblad, M., Nakasone, E. S., & Werb, Z. (2010). Tumors as organs: Complex tissues that interface with the entire organism. *Developmental Cell*, *18*(6), 884–901. https://doi.org/10.1016/j.devcel.2010.05.012

Elsayed, N. M. Y., Abou El Ella, D. A., Serya, R. A. T., & Abouzid, K. A. M. (2015). Targeting apoptotic machinery as approach for anticancer therapy: Smac mimetics as anticancer agents. *Future Journal of Pharmaceutical Sciences*, *1*(1), 16–21. https://doi.org/10.1016/j.fjps.2015.05.005

Emanuel, P. O. M., Phelps, R. G., Mudgil, A., Shafir, M., & Burstein, D. E. (2008). Immunohistochemical detection of XIAP in melanoma. *Journal of Cutaneous Pathology*, *35*(3), 292–297. https://doi.org/10.1111/j.1600-0560.2007.00798.x

Feltham, R., Bettjeman, B., Budhidarmo, R., Mace, P. D., Shirley, S., Condon, S. M., Chunduru, S. K., McKinlay, M. A., Vaux, D. L., Silke, J., & Day, C. L. (2011). Smac mimetics activate the E3 ligase activity of cIAP1 protein by promoting RING domain dimerization. *Journal of Biological Chemistry*, *286*(19), 17015–17028. https://doi.org/10.1074/jbc.M111.222919

Franchi, L., Warner, N., Viani, K., & Nuñez, G. (2009). Function of Nod-

like receptors in microbial recognition and host defense. *Immunological Reviews*, *227*(1), 106–128. https://doi.org/10.1111/j.1600-065X.2008.00734.x

Fujisawa, N., Hayashi, S., & Miller, E. J. (1999). A synthetic peptide inhibitor for alpha-chemokines inhibits the tumour growth and pulmonary metastasis of human melanoma cells in nude mice. *Melanoma Research*, *9*(2), 105–114. https://doi.org/10.1097/00008390-199904000-00001

Fulda, S., Galluzzi, L., & Kroemer, G. (2010). Targeting mitochondria for cancer therapy. *Nature Reviews Drug Discovery*, *9*(6), 447–464. https://doi.org/10.1038/nrd3137

Fulda, S., & Vucic, D. (2012). Targeting IAP proteins for therapeutic intervention in cancer. *Nature Reviews Drug Discovery*, *11*(2), 109–124. https://doi.org/10.1038/nrd3627

Fulda, S., Wick, W., Weller, M., & Debatin, K. M. (2002). Smac agonists sensitize for Apo2L/TRAIL-or anticancer drug-induced apoptosis and induce regression of malignant glioma in vivo. *Nature Medicine*, *8*(8), 808–815. https://doi.org/10.1038/nm735

Gaither, A., Porter, D., Yao, Y., Borawski, J., Yang, G., Donovan, J., Sage, D., Slisz, J., Tran, M., Straub, C., Ramsey, T., Iourgenko, V., Huang, A., Chen, Y., Schlegel, R., Labow, M., Fawell, S., Sellers, W. R., & Zawel, L. (2007). A Smac mimetic rescue screen reveals roles for inhibitor of apoptosis proteins in tumor necrosis factor-α signaling. *Cancer Research*, *67*(24), 11493–11498. https://doi.org/10.1158/0008-5472.CAN-07-5173

Galluzzi, L., Morselli, E., Kepp, O., Vitale, I., Rigoni, A., Vacchelli, E., Michaud, M., Zischka, H., Castedo, M., & Kroemer, G. (2010). Mitochondrial gateways to cancer. *Molecular Aspects of Medicine*, *31*(1), 1–20. https://doi.org/10.1016/j.mam.2009.08.002

Gao, Z., Tian, Y., Wang, J., Yin, Q., Wu, H., Li, Y. M., & Jiang, X. (2007). A dimeric Smac/Diablo peptide directly relieves caspase-3 inhibition by XIAP: Dynamic and cooperative regulation of XIAP by Smac/Diablo. *Journal of Biological Chemistry*, *282*(42), 30718–30727. https://doi.org/10.1074/jbc.M705258200

Garcia-Carbonell, R., Yao, S. J., Das, S., & Guma, M. (2019). Dysregulation of intestinal epithelial cell RIPK pathways promotes chronic inflammation in the IBD gut. *Frontiers in Immunology*, *10*(MAY), 1094. https://doi.org/10.3389/FIMMU.2019.01094/BIBTEX

Ghosh, S., & Hayden, M. S. (2012). Celebrating 25 years of NF-κB

Research. *Immunological Reviews*, *246*(1), 5. https://doi.org/10.1111/J.1600-065X.2012.01111.X

Giebeler, N., Schönefuß, A., Landsberg, J., Tüting, T., Mauch, C., & Zigrino, P. (2017). Deletion of ADAM-9 in HGF/CDK4 mice impairs melanoma development and metastasis. *Oncogene*, *36*(35), 5058–5067. https://doi.org/10.1038/onc.2017.162

Gijsbers, K., Gouwy, M., Struyf, S., Wuyts, A., Proost, P., Opdenakker, G., Penninckx, F., Ectors, N., Geboes, K., & Van Damme, J. (2005). GCP-2/CXCL6 synergizes with other endothelial cell-derived chemokines in neutrophil mobilization and is associated with angiogenesis in gastrointestinal tumors. *Experimental Cell Research*, *303*(2), 331–342. https://doi.org/10.1016/j.yexcr.2004.09.027

Goldar, S., Khaniani, M. S., Derakhshan, S. M., & Baradaran, B. (2015). Molecular mechanisms of apoptosis and roles in cancer development and treatment. *Asian Pacific Journal of Cancer Prevention*, *16*(6), 2129–2144. https://doi.org/10.7314/APJCP.2015.16.6.2129

Goncharov, T., Hedayati, S., Mulvihill, M. M., Fairbrother, W. J., Deshayes, K., Goncharov, T., Hedayati, S., Mulvihill, M. M., Izrael-tomasevic, A., Zobel, K., Jeet, S., Fedorova, A. V, Eidenschenk, C., Yu, K., Shaw, A. S., & Kirkpatrick, D. S. (2018). Disruption of XIAP-RIP2 Association Blocks NOD2- Mediated Inflammatory Signaling Article Disruption of XIAP-RIP2 Association Blocks NOD2-Mediated Inflammatory Signaling. *Molecular Cell*, *69*(4), 551-565.e7. https://doi.org/10.1016/j.molcel.2018.01.016

Goncharov, T., Hedayati, S., Mulvihill, M. M., Izrael-Tomasevic, A., Zobel, K., Jeet, S., Fedorova, A. V., Eidenschenk, C., deVoss, J., Yu, K., Shaw, A. S., Kirkpatrick, D. S., Fairbrother, W. J., Deshayes, K., & Vucic, D. (2018). Disruption of XIAP-RIP2 Association Blocks NOD2-Mediated Inflammatory Signaling. *Molecular Cell*, *69*(4), 551-565.e7. https://doi.org/10.1016/j.molcel.2018.01.016

Green, D. R., & Kroemer, G. (2004). The pathophysiology of mitochondrial cell death. *Science*, *305*(5684), 626–629. https://doi.org/10.1126/science.1099320

Gregory, A. D., & Houghton, A. M. G. (2011). Tumor-associated neutrophils: New targets for cancer therapy. *Cancer Research*, *71*(7), 2411–2416. https://doi.org/10.1158/0008-5472.CAN-10-2583

Günther, S. D., Fritsch, M., Seeger, J. M., Schiffmann, L. M., Snipas, S. J., Coutelle, M., Kufer, T. A., Higgins, P. G., Hornung, V., Bernardini, M. L., Höning, S., Krönke, M., Salvesen, G. S., & Kashkar, H. (2020). Cytosolic Gram-negative bacteria prevent apoptosis by inhibition of

effector caspases through lipopolysaccharide. *Nature Microbiology*, *5*(2). https://doi.org/10.1038/s41564-019-0620-5

Gyrd-Hansen, M., Darding, M., Miasari, M., Santoro, M. M., Zender, L., Xue, W., Tenev, T., da Fonseca, P. C. A., Zvelebil, M., Bujnicki, J. M., Lowe, S., Silke, J., & Meier, P. (2008). IAPs contain an evolutionarily conserved ubiquitin-binding domain that regulates NF-κB as well as cell survival and oncogenesis. *Nature Cell Biology*, *10*(11), 1309–1317. https://doi.org/10.1038/ncb1789

Gyrd-Hansen, M., & Meier, P. (2010). IAPs: From caspase inhibitors to modulators of NF-κB, inflammation and cancer. *Nature Reviews Cancer*, *10*(8), 561–574. https://doi.org/10.1038/nrc2889

Haas, T. L., Emmerich, C. H., Gerlach, B., Schmukle, A. C., Cordier, S. M., Rieser, E., Feltham, R., Vince, J., Warnken, U., Wenger, T., Koschny, R., Komander, D., Silke, J., & Walczak, H. (2009). Recruitment of the Linear Ubiquitin Chain Assembly Complex Stabilizes the TNF-R1 Signaling Complex and Is Required for TNF-Mediated Gene Induction. *Molecular Cell*, *36*(5), 831–844. https://doi.org/10.1016/j.molcel.2009.10.013

Haglund, K., & Dikic, I. (2005). Ubiquitylation and cell signaling. *EMBO Journal*, *24*(19), 3353–3359. https://doi.org/10.1038/sj.emboj.7600808

Hanahan, D., & Weinberg, R. A. (2011a). Hallmarks of cancer: The next generation. *Cell*, *144*(5), 646–674. https://doi.org/10.1016/j.cell.2011.02.013

Hanahan, D., & Weinberg, R. A. (2011b). Hallmarks of cancer: The next generation. *Cell*, *144*(5), 646–674. https://doi.org/10.1016/j.cell.2011.02.013

Harlin, H., Reffey, S. B., Duckett, C. S., & Lindsten, T. (2001). *Characterization of XIAP-Deficient Mice*. *21*(10), 3604–3608. https://doi.org/10.1128/MCB.21.10.3604

Hartman, M. L., & Czyz, M. (2013). Anti-apoptotic proteins on guard of melanoma cell survival. *Cancer Letters*, *331*(1), 24–34. https://doi.org/10.1016/j.canlet.2013.01.010

Hasegawa, M., Fujimoto, Y., Lucas, P. C., Nakano, H., Fukase, K., Núñez, G., & Inohara, N. (2008). A critical role of RICK/RIP2 polyubiquitination in Nod-induced NF-κB activation. *EMBO Journal*, *27*(2), 373–383. https://doi.org/10.1038/sj.emboj.7601962

Hatakeyama, S., Yada, M., Matsumoto, M., Ishida, N., & Nakayama, K. I. (2001). U Box Proteins as a New Family of Ubiquitin-Protein Ligases.

Journal of Biological Chemistry, *276*(35), 33111–33120. https://doi.org/10.1074/jbc.M102755200

Hayden, M. S., & Ghosh, S. (2011). NF-κB in immunobiology. *Cell Research*, *21*(2), 223–244. https://doi.org/10.1038/cr.2011.13

Heim, V. J., Dagley, L. F., Stafford, C. A., Hansen, F. M., Clayer, E., Bankovacki, A., Webb, A. I., Lucet, I. S., Silke, J., & Nachbur, U. (2020). A regulatory region on RIPK 2 is required for XIAP binding and NOD signaling activity . *EMBO Reports*, *21*(11), 1–14. https://doi.org/10.15252/embr.202050400

Hicke, L. (2001). Protein regulation by monoubiquitin. *Nature Reviews Molecular Cell Biology*, *2*(3), 195–201. https://doi.org/10.1038/35056583

Hicke, L., & Dunn, R. (2003). Regulation of Membrane Protein Transport by Ubiquitin and Ubiquitin-Binding Proteins. *Annual Review of Cell and Developmental Biology*, *19*, 141–172. https://doi.org/10.1146/annurev.cellbio.19.110701.154617

Hicke, L., Schubert, H. L., & Hill, C. P. (2005). Ubiquitin-binding domains. *Nature Reviews Molecular Cell Biology*, *6*(8), 610–621. https://doi.org/10.1038/nrm1701

Hinds, M. G., Norton, R. S., Vaux, D. L., & Day, C. L. (1999). Solution structure of a baculoviral inhibitor of apoptosis (IAP) repeat. *Nature Structural Biology*, *6*(7), 648–651. https://doi.org/10.1038/10701

Hiscutt, E. L., Hill, D. S., Martin, S., Kerr, R., Harbottle, A., Birch-Machin, M., Redfern, C. P. F., Fulda, S., Armstrong, J. L., & Lovat, P. E. (2010). Targeting X-linked inhibitor of apoptosis protein to increase the efficacy of endoplasmic reticulum stress-induced apoptosis for melanoma therapy. *Journal of Investigative Dermatology*, *130*(9), 2250–2258. https://doi.org/10.1038/jid.2010.146

Hoege, C., Pfander, B., Moldovan, G. L., Pyrowolakis, G., & Jentsch, S. (2002). RAD6-dependent DNA repair is linked to modification of PCNA by ubiquitin and SUMO. *Nature*, *419*(6903), 135–141. https://doi.org/10.1038/nature00991

Hofer-Warbinek, R., Schmid, J. A., Stehlik, C., Binder, B. R., Lipp, J., & De Martin, R. (2000). Activation of NF-κB by XIAP, the X chromosome-linked inhibitor of apoptosis, in endothelial cells involves TAK1. *Journal of Biological Chemistry*, *275*(29), 22064–22068. https://doi.org/10.1074/jbc.M910346199

Hölzel, M., & Tüting, T. (2016). Inflammation-Induced Plasticity in Melanoma Therapy and Metastasis. In *Trends in Immunology* (Vol.

37, Issue 6, pp. 364–374). https://doi.org/10.1016/j.it.2016.03.009

Honjo, H., Watanabe, T., Kamata, K., Minaga, K., & Kudo, M. (2021). RIPK2 as a New Therapeutic Target in Inflammatory Bowel Diseases. *Frontiers in Pharmacology*, *12*. https://doi.org/10.3389/FPHAR.2021.650403

Hörnle, M., Peters, N., Thayaparasingham, B., Vörsmann, H., Kashkar, H., & Kulms, D. (2011). Caspase-3 cleaves XIAP in a positive feedback loop to sensitize melanoma cells to TRAIL-induced apoptosis. *Oncogene*, *30*(5), 575–587. https://doi.org/10.1038/onc.2010.434

Hrdinka, M., & Gyrd-Hansen, M. (2017). The Met1-Linked Ubiquitin Machinery: Emerging Themes of (De)regulation. *Molecular Cell*, *68*(2), 265–280. https://doi.org/10.1016/J.MOLCEL.2017.09.001

Hrdinka, M., Schlicher, L., Dai, B., Pinkas, D. M., Bufton, J. C., Picaud, S., Ward, J. A., Rogers, C., Suebsuwong, C., Nikhar, S., Cuny, G. D., Huber, K. V., Filippakopoulos, P., Bullock, A. N., Degterev, A., & Gyrd-Hansen, M. (2018). Small molecule inhibitors reveal an indispensable scaffolding role of RIPK 2 in NOD 2 signaling . *The EMBO Journal*, *37*(17), 1–16. https://doi.org/10.15252/embj.201899372

Hsu, H., Huang, J., Shu, H. B., Baichwal, V., & Goeddel, D. V. (1996). TNF-dependent recruitment of the protein kinase RIP to the TNF receptor-1 signaling complex. *Immunity*, *4*(4), 387–396. https://doi.org/10.1016/S1074-7613(00)80252-6

Hsu, H., Shu, H. B., Pan, M. G., & Goeddel, D. V. (1996). TRADD-TRAF2 and TRADD-FADD interactions define two distinct TNF receptor 1 signal transduction pathways. *Cell*, *84*(2), 299–308. https://doi.org/10.1016/S0092-8674(00)80984-8

Hsu, H., Xiong, J., & Goeddel, D. V. (1995). The TNF receptor 1-associated protein TRADD signals cell death and NF-κB activation. *Cell*, *81*(4), 495–504. https://doi.org/10.1016/0092-8674(95)90070-5

Huang, Y., Park, Y. C., Rich, R. L., Segal, D., Myszka, D. G., & Wu, H. (2001). Structural basis of caspase inhibition by XIAP: Differential roles of the linker versus the BIR domain. *Cell*, *104*(5), 781–790. https://doi.org/10.1016/s0092-8674(01)00273-2

Hugot, J., Chamaillard, M., Zouali, H., Lesage, S., Ce, J., & Macry, J. (2001). *Letters to nuature*. 599–603. www.nature.com

Hunter, A. M., LaCasse, E. C., & Korneluk, R. G. (2007). The inhibitors of apoptosis (IAPs) as cancer targets. *Apoptosis*, *12*(9), 1543–1568.

https://doi.org/10.1007/s10495-007-0087-3

Hussain, A. R., Uddin, S., Ahmed, M., Bu, R., Ahmed, S. O., Abubaker, J., Sultana, M., Ajarim, D., Al-Dayel, F., Bavi, P. P., & Al-Kuraya, K. S. (2010). Prognostic significance of XIAP expression in DLBCL and effect of its inhibition on AKT signalling. *Journal of Pathology*, *222*(2), 180–190. https://doi.org/10.1002/path.2747

Ikeda, F., Deribe, Y. L., Skånland, S. S., Stieglitz, B., Grabbe, C., Franz-Wachtel, M., Van Wijk, S. J. L., Goswami, P., Nagy, V., Terzic, J., Tokunaga, F., Androulidaki, A., Nakagawa, T., Pasparakis, M., Iwai, K., Sundberg, J. P., Schaefer, L., Rittinger, K., MacEk, B., & Dikic, I. (2011). SHARPIN forms a linear ubiquitin ligase complex regulating NF-κB activity and apoptosis. *Nature*, *471*(7340), 637–641. https://doi.org/10.1038/nature09814

Inohara, N., Del Peso, L., Koseki, T., Chen, S., & Núñez, G. (1998). RICK, a novel protein kinase containing a caspase recruitment domain, interacts with CLARP and regulates CD95-mediated apoptosis. *Journal of Biological Chemistry*, *273*(20), 12296–12300. https://doi.org/10.1074/jbc.273.20.12296

Inohara, N., Koseki, T., Lin, J., Del Peso, L., Lucas, P. C., Chen, F. F., Ogura, Y., & Núñez, G. (2000). An Induced Proximity Model for NF-κB Activation in the Nod1/RICK and RIP Signaling Pathways *. *Journal of Biological Chemistry*, *275*(36), 27823–27831. https://doi.org/10.1074/JBC.M003415200

Ishigami, S., Natsugoe, S., Tokuda, K., Nakajo, A., Xiangming, C., Iwashige, H., Aridome, K., Hokita, S., & Aikou, T. (2000). Clinical impact of intratumoral natural killer cell and dendritic cell infiltration in gastric cancer. *Cancer Letters*, *159*(1), 103–108. https://doi.org/10.1016/S0304-3835(00)00542-5

Ivanov, V. N., Bhoumik, A., & Ronai, Z. (2003). Death receptors and melanoma resistance to apoptosis. *Oncogene*, *22*(20), 3152–3161. https://doi.org/10.1038/sj.onc.1206456

Jaafar, R. F., Ibrahim, Z., Ataya, K., Hassanieh, J., Ard, N., & Faraj, W. (2021). Receptor-Interacting Serine/Threonine-Protein Kinase-2 as a Potential Prognostic Factor in Colorectal Cancer. *Medicina 2021, Vol. 57, Page 709*, *57*(7), 709. https://doi.org/10.3390/MEDICINA57070709

Jaafar, R., Mnich, K., Dolan, S., Hillis, J., Almanza, A., Logue, S. E., Samali, A., & Gorman, A. M. (2018). RIP2 enhances cell survival by activation of NF-κB in triple negative breast cancer cells. *Biochemical and Biophysical Research Communications*, *497*(1), 115–121.

https://doi.org/10.1016/j.bbrc.2018.02.034

Jensen, T. O., Schmidt, H., Møller, H. J., Donskov, F., Høyer, M., Sjoegren, P., Christensen, I. J., & Steiniche, T. (2012). Intratumoral neutrophils and plasmacytoid dendritic cells indicate poor prognosis and are associated with pSTAT3 expression in AJCC stage I/II melanoma. *Cancer*, *118*(9), 2476–2485. https://doi.org/10.1002/cncr.26511

Jerrells, T. R., Dean, J. H., Richardson, G., Cannon, G. B., & Herberman, R. B. (1979). Increased monocyte-mediated cytostasis of lymphoid cell lines in breast and lung cancer patients. *International Journal of Cancer*, *23*(6), 768–776. https://doi.org/10.1002/ijc.2910230606

Jun, J. C., Cominelli, F., & Abbott, D. W. (2013). RIP2 activity in inflammatory disease and implications for novel therapeutics. *Journal of Leukocyte Biology*, *94*(5), 927–932. https://doi.org/10.1189/JLB.0213109

Kang, M. H., & Reynolds, C. P. (2009). Bcl-2 Inhibitors: Targeting mitochondrial apoptotic pathways in cancer therapy. *Clinical Cancer Research*, *15*(4), 1126–1132. https://doi.org/10.1158/1078-0432.CCR-08-0144

Kashkar, H. (2010). X-linked inhibitor of apoptosis: A chemoresistance factor or a hollow promise. *Clinical Cancer Research*, *16*(18), 4496–4502. https://doi.org/10.1158/1078-0432.CCR-10-1664

Keane, M. P., Belperio, J. A., Xue, Y. Y., Burdick, M. D., & Strieter, R. M. (2004). Depletion of CXCR2 Inhibits Tumor Growth and Angiogenesis in a Murine Model of Lung Cancer. *The Journal of Immunology*, *172*(5), 2853–2860. https://doi.org/10.4049/jimmunol.172.5.2853

Kerr, J. F. R., Wyllie, A. H., & Currie, A. R. (1972). Apoptosis: A Basic Biological Phenomenon with Wide-ranging Implications in Tissue Kinetics. *British Journal of Cancer*, *26*(4), 239. https://doi.org/10.1038/BJC.1972.33

Kluger, H. M., McCarthy, M. M., Alvero, A. B., Sznol, M., Ariyan, S., Camp, R. L., Rimm, D. L., & Mor, G. (2007). The X-linked inhibitor of apoptosis protein (XIAP) is up-regulated in metastatic melanoma, and XIAP cleavage by Phenoxodiol is associated with Carboplatin sensitization. *Journal of Translational Medicine*, *5*, 1–15. https://doi.org/10.1186/1479-5876-5-6

Kohrgruber, N., Halanek, N., Gröger, M., Winter, D., Rappersberger, K.,

Schmitt-Egenolf, M., Stingl, G., & Maurer, D. (1999). Survival, maturation, and function of CD11c- and CD11c+ peripheral blood dendritic cells are differentially regulated by cytokines. *Journal of Immunology (Baltimore, Md. : 1950)*, *163*(6), 3250–3259. http://www.ncbi.nlm.nih.gov/pubmed/10477594

Krieg, A., Correa, R. G., Garrison, J. B., Le Negrate, G., Welsh, K., Huang, Z., Knoefel, W. T., & Reed, J. C. (2009). XIAP mediates NOD signaling via interaction with RIP2. *Proceedings of the National Academy of Sciences of the United States of America*, *106*(34), 14524–14529. https://doi.org/10.1073/pnas.0907131106

Kuhns, M. S., Davis, M. M., & Garcia, K. C. (2006). Deconstructing the form and function of the TCR/CD3 complex. *Immunity*, *24*(2), 133–139. https://doi.org/10.1016/j.immuni.2006.01.006

Kulke, R., Bornscheuer, E., Schluter, C., Bartels, J., Rowert, J., Sticherling, M., & Christophers, E. (1998). The CXC receptor 2 is overexpressed in psoriatic epidermis. *Journal of Investigative Dermatology*, *110*(1), 90–94. https://doi.org/10.1046/j.1523-1747.1998.00074.x

LaCasse, E. C., Baird, S., Korneluk, R. G., & MacKenzie, A. E. (1998). The inhibitors of apoptosis (IAPs) and their emerging role in cancer. *Oncogene*, *17*(25), 3247–3259. https://doi.org/10.1038/sj.onc.1202569

LaCasse, E. C., Cherton-Horvat, G. G., Hewitt, K. E., Jerome, L. J., Morris, S. J., Kandimalla, E. R., Yu, D., Wang, H., Wang, W., Zhang, R., Agrawal, S., Gillard, J. W., & Durkin, J. P. (2006). Preclinical characterization of AEG35156/GEM 640, a second-generation antisense oligonucleotide targeting X-linked inhibitor of apoptosis. *Clinical Cancer Research*, *12*(17), 5231–5241. https://doi.org/10.1158/1078-0432.CCR-06-0608

Lakritz, J. R., Poutahidis, T., Mirabal, S., Varian, B. J., Levkovich, T., Ibrahim, Y. M., Ward, J. M., Teng, E. C., Fisher, B., Parry, N., Lesage, S., Alberg, N., Gourishetti, S., Fox, J. G., Ge, Z., & Erdman, S. E. (2015). Gut bacteria require neutrophils to promote mammary tumorigenesis. *Oncotarget*, *6*(11), 9387–9396. https://doi.org/10.18632/oncotarget.3328

Larisch, S., Yi, Y., Lotan, R., Kerner, H., Eimerl, S., Tony Parks, W., Gottfried, Y., Birkey Reffey, S., De Caestecker, M. P., Danielpour, D., Book-Melamed, N., Timberg, R., Duckett, C. S., Lechleider, R. J., Steller, H., Orly, J., Kim, S. J., & Roberts, A. B. (2000). A novel mitochondrial septin-like protein, ARTS, mediates apoptosis

dependent on its P-loop motif. *Nature Cell Biology*, *2*(12), 915–921. https://doi.org/10.1038/35046566

Lewis, J., Burstein, E., Reffey, S. B., Bratton, S. B., Roberts, A. B., & Duckett, C. S. (2004). Uncoupling of the Signaling and Caspase-inhibitory Properties of X-linked Inhibitor of Apoptosis. *Journal of Biological Chemistry*, *279*(10), 9023–9029. https://doi.org/10.1074/jbc.M312891200

Li, L., Thomas, R. M., Suzuki, H., De Brabander, J. K., Wang, X., & Harran, P. G. (2004). A small molecule smac mimic potentiates TRAIL- and TNFα-mediated cell death. *Science*, *305*(5689), 1471–1474. https://doi.org/10.1126/science.1098231

Li, P., Nijhawan, D., Budihardjo, I., Srinivasula, S. M., Ahmad, M., Alnemri, E. S., & Wang, X. (1997). Cytochrome c and dATP-Dependent Formation of Apaf-1/Caspase-9 Complex Initiates an Apoptotic Protease Cascade. *Cell*, *91*(4), 479–489. https://doi.org/10.1016/S0092-8674(00)80434-1

Liston, P., Fong, W. G., Kelly, N. L., Toji, S., Miyazaki, T., Conte, D., Tamai, K., Craig, C. G., McBurney, M. W., & Korneluk, R. G. (2001). Identification of XAF1 as an antagonist of XIAP anti-caspase activity. *Nature Cell Biology*, *3*(2), 128–133. https://doi.org/10.1038/35055027

Liston, P., Royt, N., Tamai, K., Lefebvre, C., Baird, S., Cherton-horvat, G., Farahani, R., Mclean, M., I, J. I. I., H, A. M., & Korneluk, R. G. (1996). *FIG. 1 Effect of NAIP on cell death induced by serum*. *379*(November 1995), 349–353.

Liu, Y., Chen, X. D., Yu, J., Chi, J. L., Long, F. W., Yang, H. W., Chen, K. L., Lv, Z. Y., Zhou, B., Peng, Z. H., Sun, X. F., Li, Y., & Zhou, Z. G. (2017). Deletion Of XIAP reduces the severity of acute pancreatitis via regulation of cell death and nuclear factor-κB activity. *Cell Death and Disease*, *8*(3), 1–11. https://doi.org/10.1038/cddis.2017.70

Löder, S., Fakler, M., Schoeneberger, H., Cristofanon, S., Leibacher, J., Vanlangenakker, N., Bertrand, M. J. M., Vandenabeele, P., Jeremias, I., Debatin, K. M., & Fulda, S. (2012). RIP1 is required for IAP inhibitor-mediated sensitization of childhood acute leukemia cells to chemotherapy-induced apoptosis. *Leukemia*, *26*(5), 1020–1029. https://doi.org/10.1038/leu.2011.353

Lorick, K. L., Jensen, J. P., Fang, S., Ong, A. M., Hatakeyama, S., & Weissman, A. M. (1999). RING fingers mediate ubiquitin-conjugating enzyme (E2)-dependent ubiquitination. *Proceedings of the National Academy of Sciences of the United States of America*, *96*(20), 11364–11369. https://doi.org/10.1073/pnas.96.20.11364

Lu, M., Lin, S. C., Huang, Y., Kang, Y. J., Rich, R., Lo, Y. C., Myszka, D., Han, J., & Wu, H. (2007). XIAP Induces NF-κB Activation via the BIR1/TAB1 Interaction and BIR1 Dimerization. *Molecular Cell*, *26*(5), 689–702. https://doi.org/10.1016/j.molcel.2007.05.006

Maloney, C., Kallis, M. P., Edelman, M., Tzanavaris, C., Lesser, M., Soffer, S. Z., Symons, M., & Steinberg, B. M. (2020). Gefitinib inhibits invasion and metastasis of osteosarcoma via inhibition of macrophage receptor interacting serine-threonine kinase 2. *Molecular Cancer Therapeutics*, *19*(6), 1340–1350. https://doi.org/10.1158/1535-7163.MCT-19-0903

Mantovani, A., Sozzani, S., Locati, M., Allavena, P., & Sica, A. (2002). Macrophage polarization: Tumor-associated macrophages as a paradigm for polarized M2 mononuclear phagocytes. *Trends in Immunology*, *23*(11), 549–555. https://doi.org/10.1016/S1471-4906(02)02302-5

Mantovani, A., Tagliabue, A., Dean, J. H., Jerrells, T. R., & Herberman, R. B. (1979). Cytolytic activity of circulating human monocytes on transformed and untransformed human fibroblasts. *International Journal of Cancer*, *23*(1), 28–31. https://doi.org/10.1002/ijc.2910230106

Massague, J. (2000). NEW EMBO MEMBERS REVIEW: Transcriptional control by the TGF-beta/Smad signaling system. *The EMBO Journal*, *19*(8), 1745–1754. https://doi.org/10.1093/emboj/19.8.1745

Masucci, M. T., Minopoli, M., & Carriero, M. V. (2019). Tumor Associated Neutrophils. Their Role in Tumorigenesis, Metastasis, Prognosis and Therapy. *Frontiers in Oncology*, *9*(November), 1–16. https://doi.org/10.3389/fonc.2019.01146

Matsumoto, M. L., Wickliffe, K. E., Dong, K. C., Yu, C., Bosanac, I., Bustos, D., Phu, L., Kirkpatrick, D. S., Hymowitz, S. G., Rape, M., Kelley, R. F., & Dixit, V. M. (2010). K11-linked polyubiquitination in cell cycle control revealed by a K11 linkage-specific antibody. *Molecular Cell*, *39*(3), 477–484. https://doi.org/10.1016/j.molcel.2010.07.001

McCarthy, J. V., Ni, J., & Dixit, V. M. (1998a). RIP2 is a novel NF-κB-activating and cell death-inducing kinase. *Journal of Biological Chemistry*, *273*(27), 16968–16975. https://doi.org/10.1074/jbc.273.27.16968

McCarthy, J. V., Ni, J., & Dixit, V. M. (1998b). RIP2 is a novel NF-κB-activating and cell death-inducing kinase. *Journal of Biological Chemistry*, *273*(27), 16968–16975.

https://doi.org/10.1074/jbc.273.27.16968

McKnight, A. J., Macfarlane, A. J., Dri, P., Turley, L., Willis, A. C., & Gordon, S. (1996). Molecular cloning of F4/80, a murine macrophage-restricted cell surface glycoprotein with homology to the G-protein-linked transmembrane 7 hormone receptor family. *Journal of Biological Chemistry*, *271*(1), 486–489. https://doi.org/10.1074/jbc.271.1.486

Medema, J. P., Scaffidi, C., Kischkel, F. C., Shevchenko, A., Mann, M., Krammer, P. H., & Peter, M. E. (1997). FLICE is activated by association with the CD95 death-inducing signaling complex (DISC). *EMBO Journal*, *16*(10), 2794–2804. https://doi.org/10.1093/emboj/16.10.2794

Micheau, O., Lens, S., Gaide, O., Alevizopoulos, K., & Tschopp, J. (2001). NF-κB Signals Induce the Expression of c-FLIP. *Molecular and Cellular Biology*, *21*(16), 5299–5305. https://doi.org/10.1128/mcb.21.16.5299-5305.2001

Miguel Martins, L., Iaccarino, I., Tenev, T., Gschmeissner, S., Totty, N. F., Lemoine, N. R., Savopoulos, J., Gray, C. W., Creasy, C. L., Dingwall, C., & Downward, J. (2002). The serine protease Omi/HtrA2 regulates apoptosis by binding XIAP through a Reaper-like motif. *Journal of Biological Chemistry*, *277*(1), 439–444. https://doi.org/10.1074/jbc.M109784200

Miller, L. K. (1999). *Pii: S0962-8924(99)01609-8*. *8924*(99), 6–9.

Murdoch, C., Muthana, M., Coffelt, S. B., & Lewis, C. E. (2008). The role of myeloid cells in the promotion of tumour angiogenesis. *Nature Reviews Cancer*, *8*(8), 618–631. https://doi.org/10.1038/nrc2444

Nachbur, U., Stafford, C. A., Bankovacki, A., Zhan, Y., Lindqvist, L. M., Fiil, B. K., Khakham, Y., Ko, H. J., Sandow, J. J., Falk, H., Holien, J. K., Chau, D., Hildebrand, J., Vince, J. E., Sharp, P. P., Webb, A. I., Jackman, K. A., Mühlen, S., Kennedy, C. L., … Silke, J. (2015). A RIPK2 inhibitor delays NOD signalling events yet prevents inflammatory cytokine production. *Nature Communications*, *6*. https://doi.org/10.1038/ncomms7442

Nath, D., & Shadan, S. (2009). The ubiquitin system. *Nature*, *458*(7237), 421. https://doi.org/10.1038/458421a

Ndubaku, C., Cohen, F., Varfolomeev, E., & Vucic, D. (2009). Targeting inhibitor of apoptosis proteins for therapeutic intervention. *Http://Dx.Doi.Org/10.4155/Fmc.09.116*, *1*(8), 1509–1525. https://doi.org/10.4155/FMC.09.116

Neil, J. R., & Schiemann, W. P. (2008). Altered TAB1:IκB kinase interaction promotes transforming growth factor β-mediated nuclear factor-κB activation during breast cancer progression. *Cancer Research*, *68*(5), 1462–1470. https://doi.org/10.1158/0008-5472.CAN-07-3094

Neil, J. R., Tian, M., & Schiemann, W. P. (2009). X-linked inhibitor of apoptosis protein and its E3 ligase activity promote transforming growth factor-β-mediated nuclear factor-κB activation during breast cancer progression. *Journal of Biological Chemistry*, *284*(32), 21209–21217. https://doi.org/10.1074/jbc.M109.018374

Noonan, F. P., Recio, J. A., Takayama, H., Duray, P., Anver, M. R., Rush, W. L., De Fabo, E. C., & Merlino, G. (2001). Neonatal sunburn and melanoma in mice. *Nature*, *413*(6853), 271–272. https://doi.org/10.1038/35095108

Ochs, H. D., Gambineri, E., & Torgerson, T. R. (2007). IPEX, FOXP3 and regulatory T-cells: A model for autoimmunity. *Immunologic Research*, *38*(1–3), 112–121. https://doi.org/10.1007/s12026-007-0022-2

Oeckinghaus, A., Hayden, M. S., & Ghosh, S. (2011). Crosstalk in NF-κB signaling pathways. *Nature Immunology*, *12*(8), 695–708. https://doi.org/10.1038/ni.2065

Ogura, Y., Bonen, D. K., Inohara, N., Nicolae, D. L., Chen, F. F., Ramos, R., Britton, H., Moran, T., Karaliuskas, R., Duerr, R. H., Achkar, J.-P., Brant, S. R., Bayless, T. M., S., K. B., Hanauer, S. B., Nunez, G., & Cho, J. H. (2001). Ogura 2001. *Nature*, *411*(May), 603–606.

Ola, M. S., Nawaz, M., & Ahsan, H. (2011). Role of Bcl-2 family proteins and caspases in the regulation of apoptosis. *Molecular and Cellular Biochemistry*, *351*(1–2), 41–58. https://doi.org/10.1007/s11010-010-0709-x

Oost, T. K., Sun, C., Armstrong, R. C., Al-Assaad, A. S., Betz, S. F., Deckwerth, T. L., Ding, H., Elmore, S. W., Meadows, R. P., Olejniczak, E. T., Oleksijew, A., Oltersdorf, T., Rosenberg, S. H., Shoemaker, A. R., Tomaselli, K. J., Zou, H., & Fesik, S. W. (2004). Discovery of potent antagonists of the antiapoptotic protein XIAP for the treatment of cancer. *Journal of Medicinal Chemistry*, *47*(18), 4417–4426. https://doi.org/10.1021/jm040037k

Opdenakker, G., & Van Damme, J. (2004). The countercurrent principle in invasion and metastasis of cancer cells. Recent insights on the roles of chemokines. *International Journal of Developmental Biology*, *48*(5–6), 519–527. https://doi.org/10.1387/ijdb.041796go

Pahl, H. L. (1999). Activators and target genes of Rel/NF-κB transcription factors. *Oncogene*, *18*(49), 6853–6866. https://doi.org/10.1038/sj.onc.1203239

Park, S. M., Yoon, J. B., & Lee, T. H. (2004). Receptor interacting protein is ubiquitinated by cellular inhibitor of apoptosis proteins (c-IAP1 and c-IAP2) in vitro. *FEBS Letters*, *566*(1–3), 151–156. https://doi.org/10.1016/j.febslet.2004.04.021

Pasparakis, M., & Vandenabeele, P. (2015). Necroptosis and its role in inflammation. *Nature*, *517*(7534), 311–320. https://doi.org/10.1038/nature14191

Paul Krimpenfort, Kim C. Quon, Wolter J. Mooi, A. L. & A. B. (2011). *Loss of p16 Ink4a confers susceptibility to metastatic melanoma in mice*. *1142*(2000), 83–86.

Payne, A. S., & Cornelius, L. A. (2002a). The role of chemokines in melanoma tumor growth and metastasis. *Journal of Investigative Dermatology*, *118*(6), 915–922. https://doi.org/10.1046/j.1523-1747.2002.01725.x

Payne, A. S., & Cornelius, L. A. (2002b). The role of chemokines in melanoma tumor growth and metastasis. *Journal of Investigative Dermatology*, *118*(6), 915–922. https://doi.org/10.1046/j.1523-1747.2002.01725.x

Pedersen, J., LaCasse, E. C., Seidelin, J. B., Coskun, M., & Nielsen, O. H. (2014). Inhibitors of apoptosis (IAPs) regulate intestinal immunity and inflammatory bowel disease (IBD) inflammation. *Trends in Molecular Medicine*, *20*(11), 652–665. https://doi.org/10.1016/j.molmed.2014.09.006

Philpott, D. J., Sorbara, M. T., Robertson, S. J., Croitoru, K., & Girardin, S. E. (2014). NOD proteins: Regulators of inflammation in health and disease. *Nature Reviews Immunology*, *14*(1), 9–23. https://doi.org/10.1038/nri3565

Pickart, C. M., & Fushman, D. (2004). Polyubiquitin chains: Polymeric protein signals. *Current Opinion in Chemical Biology*, *8*(6), 610–616. https://doi.org/10.1016/j.cbpa.2004.09.009

Prakash, H., Albrecht, M., Becker, D., Kuhlmann, T., & Rudel, T. (2010). Deficiency of XIAP leads to sensitization for Chlamydophila pneumoniae pulmonary infection and dysregulation of innate immune response in mice. *Journal of Biological Chemistry*, *285*(26), 20291–20302. https://doi.org/10.1074/jbc.M109.096297

Probst, B. L., Liu, L., Ramesh, V., Li, L., Sun, H., Minna, J. D., & Wang,

L. (2010). Smac mimetics increase cancer cell response to chemotherapeutics in a TNF-α-dependent manner. *Cell Death and Differentiation*, *17*(10), 1645–1654. https://doi.org/10.1038/cdd.2010.44

Qualai, J., Li, L. X., Cantero, J., Tarrats, A., Fernández, M. A., Sumoy, L., Rodolosse, A., McSorley, S. J., & Genescà, M. (2016). Expression of CD11c is associated with unconventional activated T cell subsets with high migratory potential. *PLoS ONE*, *11*(4), 1–22. https://doi.org/10.1371/journal.pone.0154253

Ramp, U., Krieg, T., Caliskan, E., Mahotka, C., Ebert, T., Willers, R., Gabbert, H. E., & Gerharz, C. D. (2004). XIAP expression is an independent prognostic marker in clear-cell renal carcinomas. *Human Pathology*, *35*(8), 1022–1028. https://doi.org/10.1016/j.humpath.2004.03.011

Ran, F., Hsu, P., Wright, J., & Agarwala, V. (2013). Genome engineering using the CRISPR-Cas9 system. *Nature Protocols*, *8*(11), 2281–2308. https://doi.org/10.1038/nprot.2013.143

Reffey, S. B., Wurthner, J. U., Parks, W. T., Roberts, A. B., & Duckett, C. S. (2001). X-linked Inhibitor of Apoptosis Protein Functions as a Cofactor in Transforming Growth Factor-β Signaling. *Journal of Biological Chemistry*, *276*(28), 26542–26549. https://doi.org/10.1074/jbc.M100331200

Rigaud, S., Fondanèche, M. C., Lambert, N., Pasquier, B., Mateo, V., Soulas, P., Galicier, L., Le Deist, F., Rieux-Laucat, F., Revy, P., Fischer, A., De Saint Basile, G., & Latour, S. (2006). XIAP deficiency in humans causes an X-linked lymphoproliferative syndrome. *Nature*, *444*(7115), 110–114. https://doi.org/10.1038/nature05257

RM, S., PJ, P., DA, A., & SL, K. (1995). The role of CXC chemokines as regulators of angiogenesis. *Shock (Augusta, Ga.)*, *4*(3), 155–160. https://doi.org/10.1097/00024382-199509000-00001

Rumble, J. M., & Duckett, C. S. (2008). Diverse functions within the IAP family. *Journal of Cell Science*, *121*(21), 3505–3507. https://doi.org/10.1242/jcs.040303

Sabio, G., & Davis, R. J. (2014). TNF and MAP kinase signalling pathways. *Seminars in Immunology*, *26*(3), 237–245. https://doi.org/10.1016/j.smim.2014.02.009

Saelens, X., Festjens, N., Vande Walle, L., Van Gurp, M., Van Loo, G., & Vandenabeele, P. (2004). Toxic proteins released from mitochondria in cell death. *Oncogene*, *23*(16 REV. ISS. 2), 2861–2874.

https://doi.org/10.1038/sj.onc.1207523

Safa, A. R., & Author, E. O. (2012). c-FLIP, A MASTER ANTI-APOPTOTIC REGULATOR HHS Public Access Author manuscript. *Exp Oncol*, *34*(3), 176–184. https://www.ncbi.nlm.nih.gov/pmc/articles/PMC4817998/pdf/nihms771427.pdf

Salghetti, S. E., Caudy, A. A., Chenoweth, J. G., & Tansey, W. P. (2001). Regulation of transcriptional activation domain function by ubiquitin. *Science*, *293*(5535), 1651–1653. https://doi.org/10.1126/science.1062079

Sayers, T. J. (2011). Targeting the extrinsic apoptosis signaling pathway for cancer therapy. *Cancer Immunology, Immunotherapy*, *60*(8), 1173–1180. https://doi.org/10.1007/s00262-011-1008-4

Schadendorf, D., Möller, A., Algermissen, B., Worm, M., Sticherling, M., & Czarnetzki, B. M. (1993). IL-8 produced by human malignant melanoma cells in vitro is an essential autocrine growth factor. *The Journal of Immunology*, *151*(5).

Schaider, H., Oka, M., Bogenrieder, T., Nesbit, M., Satyamoorthy, K., Berking, C., Matsushima, K., & Herlyn, M. (2003). Differential response of primary and metastatic melanomas to neutrophils attracted by IL-8. *International Journal of Cancer*, *103*(3), 335–343. https://doi.org/10.1002/ijc.10775

Scheuermann, R. H., & Racila, E. (1995). CD19 antigen in leukemia and lymphoma diagnosis and immunotherapy. *Leukemia and Lymphoma*, *18*(5–6), 385–397. https://doi.org/10.3109/10428199509059636

Schiffmann, L. M., Fritsch, M., Gebauer, F., Günther, S. D., Stair, N. R., Seeger, J. M., Thangarajah, F., Dieplinger, G., Bludau, M., Alakus, H., Göbel, H., Quaas, A., Zander, T., Hilberg, F., Bruns, C. J., Kashkar, H., & Coutelle, O. (2019). Tumour-infiltrating neutrophils counteract anti-VEGF therapy in metastatic colorectal cancer. *British Journal of Cancer*, *120*(1), 69–78. https://doi.org/10.1038/s41416-018-0198-3

Schiffmann, L. M., Göbel, H., Löser, H., Schorn, F., Werthenbach, J. P., Fuchs, H. F., Plum, P. S., Bludau, M., Zander, T., Schröder, W., Bruns, C. J., Kashkar, H., Quaas, A., & Gebauer, F. (2019). Elevated X-linked inhibitor of apoptosis protein (XIAP) expression uncovers detrimental prognosis in subgroups of neoadjuvant treated and T-cell rich esophageal adenocarcinoma. *BMC Cancer*, *19*(1), 1–8. https://doi.org/10.1186/s12885-019-5722-1

Schiffmann, L. M., Werthenbach, J. P., Heintges-Kleinhofer, F., Seeger, J. M., Fritsch, M., Günther, S. D., Willenborg, S., Brodesser, S., Lucas, C., Jüngst, C., Albert, M. C., Schorn, F., Witt, A., Moraes, C. T., Bruns, C. J., Pasparakis, M., Krönke, M., Eming, S. A., Coutelle, O., & Kashkar, H. (2020). Mitochondrial respiration controls neoangiogenesis during wound healing and tumour growth. *Nature Communications*, *11*(1), 1–13. https://doi.org/10.1038/s41467-020-17472-2

Schimmer, A. D., Dalili, S., Batey, R. A., & Riedl, S. J. (2006). Targeting XIAP for the treatment of malignancy. *Cell Death and Differentiation*, *13*(2), 179–188. https://doi.org/10.1038/sj.cdd.4401826

Schimmer, A. D., Herr, W., Hänel, M., Borthakur, G., Frankel, A., Horst, H. A., Martin, S., Kassis, J., Desjardins, P., Seiter, K., Fiedler, W., Noppeney, R., Giagounidis, A., Jacob, C., Jolivet, J., Tallman, M. S., & Koschmieder, S. (2011). Addition of AEG35156 XIAP antisense oligonucleotide in reinduction chemotherapy does not improve remission rates in patients with primary refractory acute myeloid leukemia in a randomized phase II study. *Clinical Lymphoma, Myeloma and Leukemia*, *11*(5), 433–438. https://doi.org/10.1016/j.clml.2011.03.033

Schmid, J. P., Canioni, D., Moshous, D., Touzot, F., Mahlaoui, N., Hauck, F., Kanegane, H., Lopez-Granados, E., Mejstrikova, E., Pellier, I., Galicier, L., Galambrun, C., Barlogis, V., Bordigoni, P., Fourmaintraux, A., Hamidou, M., Dabadie, A., Le Deist, F., Haerynck, F., … Latour, S. (2011). Clinical similarities and differences of patients with X-linked lymphoproliferative syndrome type 1 (XLP-1/SAP deficiency) versus type 2 (XLP-2/XIAP deficiency). *Blood*, *117*(5), 1522–1529. https://doi.org/10.1182/blood-2010-07-298372

Schulman, B. A., & Wade Harper, J. (2009). Ubiquitin-like protein activation by E1 enzymes: The apex for downstream signalling pathways. *Nature Reviews Molecular Cell Biology*, *10*(5), 319–331. https://doi.org/10.1038/nrm2673

Seeger, J. M., Brinkmann, K., Yazdanpanah, B., Haubert, D., Pongratz, C., Coutelle, O., Krönke, M., & Kashkar, H. (2010). Elevated XIAP expression alone does not confer chemoresistance. *British Journal of Cancer*, *102*(12), 1717–1723. https://doi.org/10.1038/sj.bjc.6605704

Seeger, J. M., Schmidt, P., Brinkmann, K., Hombach, A. A., Coutelle, O., Zigrino, P., Wagner-Stippich, D., Mauch, C., Abken, H., Krönke, M., & Kashkar, H. (2010). The proteasome inhibitor bortezomib sensitizes melanoma cells toward adoptive CTL attack. *Cancer*

Research, *70*(5), 1825–1834. https://doi.org/10.1158/0008-5472.CAN-09-3175

Sharpless, N. E., Bardeesy, N., Lee, K. H., Carrasco, D., Castrillon, D. H., Aguirre, A. J., Wu, E. A., Horner, J. W., & DePinho, R. A. (2001). Loss of p16Ink4a with retention of p19 predisposes mice to tumorigenesis. *Nature*, *413*(6851), 86–91. https://doi.org/10.1038/35092592

Shaw, T. J., Lacasse, E. C., Durkin, J. P., & Vanderhyden, B. C. (2008). Downregulation of XIAP expression in ovarian cancer cells induces cell death in vitro and in vivo. *International Journal of Cancer*, *122*(6), 1430–1434. https://doi.org/10.1002/ijc.23278

Sherwood, E. R., & Toliver-Kinsky, T. (2004). Mechanisms of the inflammatory response. *Best Practice and Research: Clinical Anaesthesiology*, *18*(3), 385–405. https://doi.org/10.1016/j.bpa.2003.12.002

Shi, Y. H., Ding, W. X., Zhou, J., He, J. Y., Xu, Y., Gambotto, A. A., Rabinowich, H., Fan, J., & Yin, X. M. (2008). Expression of X-linked inhibitor-of-apoptosis protein in hepatocellular carcinoma promotes metastasis and tumor recurrence. *Hepatology*, *48*(2), 497–507. https://doi.org/10.1002/hep.22393

Shiozaki, E. N., Chai, J., Rigotti, D. J., Riedl, S. J., Li, P., Srinivasula, S. M., Alnemri, E. S., Fairman, R., & Shi, Y. (2003). Mechanism of XIAP-Mediated Inhibition of Caspase-9. *Molecular Cell*, *11*(2), 519–527. https://doi.org/10.1016/S1097-2765(03)00054-6

Shortman, K., & Heath, W. R. (2010). The CD8+ dendritic cell subset. *Immunological Reviews*, *234*(1), 18–31. https://doi.org/10.1111/j.0105-2896.2009.00870.x

Shu, H. D., Takeuchi, M., & Goeddel, D. V. (1996). The tumor necrosis factor receptor 2 signal transducers TRAF2 and c-IAP1 are components of the tumor necrosis factor receptor 1 signaling complex. *Proceedings of the National Academy of Sciences of the United States of America*, *93*(24), 13973–13978. https://doi.org/10.1073/pnas.93.24.13973

Siddiqui, W. A., Ahad, A., & Ahsan, H. (2015). The mystery of BCL2 family: Bcl-2 proteins and apoptosis: an update. *Archives of Toxicology*, *89*(3), 289–317. https://doi.org/10.1007/s00204-014-1448-7

Silke, J., Ekert, P. G., Day, C. L., Hawkins, C. J., Baca, M., Chew, J., Pakusch, M., Verhagen, A. M., & Vaux, D. L. (2001). Direct inhibition

of caspase 3 is dispensable for the anti-apoptotic activity of XIAP. *EMBO Journal*, *20*(12), 3114–3123. https://doi.org/10.1093/emboj/20.12.3114

Silke, J., Hawkins, C. J., Ekert, P. G., Chew, J., Day, C. L., Pakusch, M., Verhagen, A. M., & Vaux, D. L. (2002). The anti-apoptotic activity of XIAP is retained upon mutation of both the caspase 3- and caspase 9-interacting sites. *Journal of Cell Biology*, *157*(1), 115–124. https://doi.org/10.1083/jcb.200108085

Singel, S. M., Batten, K., Cornelius, C., Jia, G., Fasciani, G., Barron, S. L., Wright, W. E., & Shay, J. W. (2014). Receptor-interacting protein kinase 2 promotes triple-negative breast cancer cell migration and invasion via activation of nuclear factor-kappaB and c-Jun N-terminal kinase pathways. *Breast Cancer Research*, *16*(2), 1–14. https://doi.org/10.1186/bcr3629

Soengas, M. S., & Lowe, S. W. (2003). Apoptosis and melanoma chemoresistance. *Oncogene*, *22*(20), 3138–3151. https://doi.org/10.1038/sj.onc.1206454

Speckmann, C., Lehmberg, K., Albert, M. H., Damgaard, R. B., Fritsch, M., Gyrd-Hansen, M., Rensing-Ehl, A., Vraetz, T., Grimbacher, B., Salzer, U., Fuchs, I., Ufheil, H., Belohradsky, B. H., Hassan, A., Cale, C. M., Elawad, M., Strahm, B., Schibli, S., Lauten, M., … Ehl, S. (2013). X-linked inhibitor of apoptosis (XIAP) deficiency: The spectrum of presenting manifestations beyond hemophagocytic lymphohistiocytosis. *Clinical Immunology*, *149*(1), 133–141. https://doi.org/10.1016/j.clim.2013.07.004

Srinivasula, S. M., Hegde, R., Saleh, A., Datta, P., Shiozaki, E., Chai, J., Lee, R. A., Robbins, P. D., Fernandes-Alnemri, T., Shi, Y., & Alnemri, E. S. (2001). Erratum: A conserved XIAP-interaction motif in caspase-9 and Smac/DIABLO regulates caspase activity and apoptosis (Nature (2001) 410 (112-116)). *Nature*, *411*(6841), 1081. https://doi.org/10.1038/35082622

Stafford, C. A., Lawlor, K. E., Heim, V. J., Bankovacki, A., Bernardini, J. P., Silke, J., & Nachbur, U. (2018). IAPs Regulate Distinct Innate Immune Pathways to Co-ordinate the Response to Bacterial Peptidoglycans. *Cell Reports*, *22*(6), 1496–1508. https://doi.org/10.1016/j.celrep.2018.01.024

Stennicke, H. R., Jürgensmeier, J. M., Shin, H., Deveraux, Q., Wolf, B. B., Yang, X., Zhou, Q., Ellerby, H. M., Ellerby, L. M., Bredesen, D., Green, D. R., Reed, J. C., Froelich, C. J., & Salvesen, G. S. (1998). Pro-caspase-3 is a major physiologic target of caspase-8. *Journal of*

Biological Chemistry, *273*(42), 27084–27090. https://doi.org/10.1074/jbc.273.42.27084

Suebsuwong, C., Dai, B., Pinkas, D. M., Duddupudi, A. L., Li, L., Bufton, J. C., Schlicher, L., Gyrd-Hansen, M., Hu, M., Bullock, A. N., Degterev, A., & Cuny, G. D. (2020). Receptor-interacting protein kinase 2 (RIPK2) and nucleotide-binding oligomerization domain (NOD) cell signaling inhibitors based on a 3,5-diphenyl-2-aminopyridine scaffold. *European Journal of Medicinal Chemistry*, *200*. https://doi.org/10.1016/j.ejmech.2020.112417

Sun, H., Nikolovska-Coleska, Z., Lu, J., Qiu, S., Yang, C. Y., Gao, W., Meagher, J., Stuckey, J., & Wang, S. (2006). Design, synthesis, and evaluation of a potent, cell-permeable, conformationally constrained second mitochondria derived activator of caspase (Smac) mimetic. *Journal of Medicinal Chemistry*, *49*(26), 7916–7920. https://doi.org/10.1021/jm061108d

Sun, S. C. (2011). Non-canonical NF-κB signaling pathway. *Cell Research*, *21*(1), 71–85. https://doi.org/10.1038/cr.2010.177

Szczerba, B. M., Castro-Giner, F., Vetter, M., Krol, I., Gkountela, S., Landin, J., Scheidmann, M. C., Donato, C., Scherrer, R., Singer, J., Beisel, C., Kurzeder, C., Heinzelmann-Schwarz, V., Rochlitz, C., Weber, W. P., Beerenwinkel, N., & Aceto, N. (2019). Neutrophils escort circulating tumour cells to enable cell cycle progression. *Nature*, *566*(7745), 553–557. https://doi.org/10.1038/s41586-019-0915-y

Takahashi, R., Deveraux, Q., Tamm, I., Welsh, K., Assa-Munt, N., Salvesen, G. S., & Reed, J. C. (1998). A single BIR domain of XIAP sufficient for inhibiting caspases. *Journal of Biological Chemistry*, *273*(14), 7787–7790. https://doi.org/10.1074/jbc.273.14.7787

Tedder, T. F., Inaoki, M., & Sato, S. (1997). The CD19-CD21 complex regulates signal transduction thresholds governing humoral immunity and autoimmunity. *Immunity*, *6*(2), 107–118. https://doi.org/10.1016/S1074-7613(00)80418-5

Teijeira, A., Garasa, S., Ochoa, M. C., Villalba, M., Olivera, I., Cirella, A., Eguren-Santamaria, I., Berraondo, P., Schalper, K. A., de Andrea, C. E., Sanmamed, M. F., & Melero, I. (2021). IL8, neutrophils, and NETs in a collusion against cancer immunity and immunotherapy. *Clinical Cancer Research*, *27*(9), 2383–2393. https://doi.org/10.1158/1078-0432.CCR-20-1319

Ting, A. T., Pimentel-Muiños, F. X., & Seed, B. (1996). RIP mediates tumor necrosis factor receptor 1 activation of NF-κB but not

Fas/APO-1-initiated apoptosis. *EMBO Journal*, *15*(22), 6189–6196. https://doi.org/10.1002/j.1460-2075.1996.tb01007.x

Tormo, D., Ferrer, A., Gaffal, E., Wenzel, J., Basner-Tschakarjan, E., Steitz, J., Heukamp, L. C., Gütgemann, I., Buettner, R., Malumbres, M., Barbacid, M., Merlino, G., & Tüting, T. (2006). Rapid growth of invasive metastatic melanoma in carcinogen-treated hepatocyte growth factor/scatter factor-transgenic mice carrying an oncogenic CDK4 mutation. *American Journal of Pathology*, *169*(2), 665–672. https://doi.org/10.2353/ajpath.2006.060017

Trapani, J. A. (2001). Granzymes: A family of lymphocyte granule serine proteases. *Genome Biology*, *2*(12), 1–7.

Travert, M., Ame-Thomas, P., Pangault, C., Morizot, A., Micheau, O., Semana, G., Lamy, T., Fest, T., Tarte, K., & Guillaudeux, T. (2008). CD40 Ligand Protects from TRAIL-Induced Apoptosis in Follicular Lymphomas through NF-κB Activation and Up-Regulation of c-FLIP and Bcl-x L . *The Journal of Immunology*, *181*(2), 1001–1011. https://doi.org/10.4049/jimmunol.181.2.1001

Tu, H., & Costa, M. (2020). Xiap's profile in human cancer. *Biomolecules*, *10*(11), 1–15. https://doi.org/10.3390/biom10111493

Vakkila, J., & Lotze, M. T. (2004). Tumour Growth. *Immunology*, *4*(August), 1–8.

Varfolomeev, E., Blankenship, J. W., Wayson, S. M., Fedorova, A. V., Kayagaki, N., Garg, P., Zobel, K., Dynek, J. N., Elliott, L. O., Wallweber, H. J. A., Flygare, J. A., Fairbrother, W. J., Deshayes, K., Dixit, V. M., & Vucic, D. (2007). IAP Antagonists Induce Autoubiquitination of c-IAPs, NF-κB Activation, and TNFα-Dependent Apoptosis. *Cell*, *131*(4), 669–681. https://doi.org/10.1016/j.cell.2007.10.030

Varfolomeev, E., Goncharov, T., Fedorova, A. V., Dynek, J. N., Zobel, K., Deshayes, K., Fairbrother, W. J., & Vucic, D. (2008). c-IAP1 and c-IAP2 are critical mediators of tumor necrosis factor α (TNFα)-induced NF-κB activation. *Journal of Biological Chemistry*, *283*(36), 24295–24299. https://doi.org/10.1074/jbc.C800128200

Varfolomeev, E., & Vucic, D. (2008). (Un)expected roles of c-IAPs in apoptotic and NFκB signaling pathways. *Cell Cycle*, *7*(11), 1511–1521. https://doi.org/10.4161/cc.7.11.5959

Vaux, D. L., & Silke, J. (2005). IAPs, RINGs and ubiquitylation. *Nature Reviews Molecular Cell Biology*, *6*(4), 287–297. https://doi.org/10.1038/nrm1621

Vince, J. E., Pantaki, D., Feltham, R., Mace, P. D., Cordier, S. M., Schmukle, A. C., Davidson, A. J., Callus, B. A., Wong, W. W. L., Gentle, I. E., Carter, H., Lee, E. F., Walczak, H., Day, C. L., Vaux, D. L., & Silke, J. (2009). TRAF2 must bind to cellular inhibitors of apoptosis for tumor necrosis factor (TNF) to efficiently activate NF-κB and to prevent TNF-induced apoptosis. *Journal of Biological Chemistry*, *284*(51), 35906–35915. https://doi.org/10.1074/jbc.M109.072256

Vince, J. E., Wong, W. W. L., Khan, N., Feltham, R., Chau, D., Ahmed, A. U., Benetatos, C. A., Chunduru, S. K., Condon, S. M., McKinlay, M., Brink, R., Leverkus, M., Tergaonkar, V., Schneider, P., Callus, B. A., Koentgen, F., Vaux, D. L., & Silke, J. (2007). IAP Antagonists Target cIAP1 to Induce TNFα-Dependent Apoptosis. *Cell*, *131*(4), 682–693. https://doi.org/10.1016/j.cell.2007.10.037

Vucic, D. (2018). XIAP at the crossroads of cell death and inflammation. *Oncotarget*, *9*(44), 27319–27320. https://doi.org/10.18632/oncotarget.25363

Vucic, D., Deshayes, K., Ackerly, H., Pisabarro, M. T., Kadkhodayan, S., Fairbrother, W. J., & Dixit, V. M. (2002). SMAC negatively regulates the anti-apoptotic activity of melanoma inhibitor of apoptosis (ML-IAP). *Journal of Biological Chemistry*, *277*(14), 12275–12279. https://doi.org/10.1074/jbc.M112045200

Vucic, D., Dixit, V. M., & Wertz, I. E. (2011). Ubiquitylation in apoptosis: A post-translational modification at the edge of life and death. *Nature Reviews Molecular Cell Biology*, *12*(7), 439–452. https://doi.org/10.1038/nrm3143

Vucic, D., & Fairbrother, W. J. (2007). The inhibitor of apoptosis proteins as therapeutic targets in cancer. *Clinical Cancer Research*, *13*(20), 5995–6000. https://doi.org/10.1158/1078-0432.CCR-07-0729

Wajant, H., & Siegmund, D. (2019). TNFR1 and TNFR2 in the control of the life and death balance of macrophages. *Frontiers in Cell and Developmental Biology*, *7*(May), 1–14. https://doi.org/10.3389/fcell.2019.00091

Waters, J. P., Pober, J. S., & Bradley, J. R. (2013). Tumour necrosis factor and cancer. *Journal of Pathology*, *230*(3), 241–248. https://doi.org/10.1002/path.4188

Witt, A., Seeger, J. M., Coutelle, O., Zigrino, P., Broxtermann, P., Andree, M., Brinkmann, K., Jüngst, C., Schauss, A. C., Schüll, S., Wohlleber, D., Knolle, P. A., Krönke, M., Mauch, C., & Kashkar, H. (2015). IAP antagonization promotes inflammatory destruction of

vascular endothelium . *EMBO Reports*, *16*(6), 719–727. https://doi.org/10.15252/embr.201439616

Witt, A., & Vucic, D. (2017). Diverse ubiquitin linkages regulate RIP kinases-mediated inflammatory and cell death signaling. *Cell Death and Differentiation*, *24*(7), 1160–1171. https://doi.org/10.1038/cdd.2017.33

Wölfel, T., Hauer, M., Schneider, J., Serrano, M., Wölfel, C., Klehmann-Hieb, E., De Plaen, E., Hankeln, T., Meyer Zum Büschenfelde, K. H., & Beach, D. (1995). A p16INK4a-insensitive CDK4 mutant targeted by cytolytic T lymphocytes in a human melanoma. *Science*, *269*(5228), 1281–1284. https://doi.org/10.1126/science.7652577

Wrana, J. L. (2000). (smad-atf2) Regulation of Smad Activity Minireview. *Cell*, *100*, 189–192.

Wu, G., Chai, J., Suber, T. L., Wu, J., & Du, C. (2000). *35050012*. *408*(December), 1–5.

Xiang, G., Wen, X., Wang, H., Chen, K., & Liu, H. (2009). Expression of X-linked inhibitor of apoptosis protein in human colorectal cancer and its correlation with prognosis. *Journal of Surgical Oncology*, *100*(8), 708–712. https://doi.org/10.1002/jso.21408

Yamaguchi, K., Nagai, S. I., Ninomiya-Tsuji, J., Nishita, M., Tamai, K., Irie, K., Ueno, N., Nishida, E., Shibuya, H., & Matsumoto, K. (1999). XIAP, a cellular member of the inhibitor of apoptosis protein family, links the receptors to TAB1-TAK1 in the BMP signaling pathway. *EMBO Journal*, *18*(1), 179–187. https://doi.org/10.1093/emboj/18.1.179

Yan, Y., Mahotka, C., Heikaus, S., Shibata, T., Wethkamp, N., Liebmann, J., Suschek, C. V., Guo, Y., Gabbert, H. E., Gerharz, C. D., & Ramp, U. (2004). Disturbed balance of expression between XIAP and Smac/DIABLO during tumour progression in renal cell carcinomas. *British Journal of Cancer*, *91*(7), 1349–1357. https://doi.org/10.1038/sj.bjc.6602127

Yang, L., Mashima, T., Sato, S., Mochizuki, M., Sakamoto, H., Yamori, T., Oh-hara, T., & Tsuruo, T. (2003). Predominant suppression of apoptosome by inhibitor of apoptosis protein in non-small cell lung cancer H460 cells: Therapeutic effect of a novel polyarginine-conjugated Smac peptide. *Cancer Research*, *63*(4), 831–837.

Yang, Y., Fang, S., Jensen, J. P., Weissman, A. M., & Ashwell, J. D. (2000). Ubiquitin protein ligase activity of IAPs and their degradation in proteasomes in response to apoptotic stimuli. *Science*, *288*(5467),

874–877. https://doi.org/10.1126/science.288.5467.874

Zakeri, Z. F., Quaglino, D., Latham, T., & Lockshin, R. A. (1993). Delayed internucleosomal DNA fragmentation in programmed cell death. *The FASEB Journal*, *7*(3), 470–478. https://doi.org/10.1096/FASEBJ.7.5.8462789

Zamoyska, R. (1994). The CD8 coreceptor revisited: One chain good, two chains better. *Immunity*, *1*(4), 243–246. https://doi.org/10.1016/1074-7613(94)90075-2

Zeise, E., Weichenthal, M., Schwarz, T., & Kulms, D. (2004). Resistance of human melanoma cells against the death ligand TRAIL is reversed by ultraviolet-B radiation via downregulation of FLIP. *Journal of Investigative Dermatology*, *123*(4), 746–754. https://doi.org/10.1111/j.0022-202X.2004.23420.x

Zhang, H., Ma, Y., Zhang, Q., Liu, R., Luo, H., & Wang, X. (2022). A pancancer analysis of the carcinogenic role of receptor - interacting serine / threonine protein kinase - 2 (RIPK2) in human tumours. *BMC Medical Genomics*, 1–14. https://doi.org/10.1186/s12920-022-01239-3

Zhang, L., Conejo-Garcia, J. R., Katsaros, D., Gimotty, P. A., Massobrio, M., Regnani, G., Makrigiannakis, A., Gray, H., Schlienger, K., Liebman, M. N., Rubin, S. C., & Coukos, G. (2003). Intratumoral T Cells, Recurrence, and Survival in Epithelial Ovarian Cancer. *New England Journal of Medicine*, *348*(3), 203–213. https://doi.org/10.1056/NEJMOA020177/SUPPL_FILE/NEJM_ZHANG_203SA1-4.PDF

Zhang, X. D., Wu, J. J., Gillespie, S., Borrow, J., & Hersey, P. (2006). Human melanoma cells selected for resistance to apoptosis by prolonged exposure to tumor necrosis factor-related apoptosis-inducing ligand are more vulnerable to necrotic cell death induced by cisplatin. *Clinical Cancer Research*, *12*(4), 1355–1364. https://doi.org/10.1158/1078-0432.CCR-05-2084

Zhu, J., Li, Q., He, J. T., & Liu, G. Y. (2015). Expression of TAK1/TAB1 expression in non-small cell lung carcinoma and adjacent normal tissues and their clinical significance. *International Journal of Clinical and Experimental Pathology*, *8*(12), 15801–15807.

Zigrino, P., Mauch, C., Fox, J. W., & Nischt, R. (2005). ADAM-9 expression and regulation in human skin melanoma and melanoma cell lines. *International Journal of Cancer*, *116*(6). https://doi.org/10.1002/ijc.21087

Zou, H., Henzel, W. J., Liu, X., Lutschg, A., & Wang, X. (1997). Apaf-1, a Human Protein Homologous to C. elegans CED-4, Participates in Cytochrome c–Dependent Activation of Caspase-3. *Cell*, *90*(3), 405–413. https://doi.org/10.1016/S0092-8674(00)80501-2

Zuo, L., Weger, J., Yang, Q., Goldstein, A. M., Tucker, M. A., Walker, G. J., Hayward, N., & Dracopoli, N. C. (1996). Germline mutations in $p16^{INK4a}$ binding domain of CDK4 in familial melanoma. *Nature Genetics*, *12*(january), 97–99.

6 Appendix

Target	B16 XIAP^{KO} (clone 1) Normalized Expression	B16 WT Normalized Expression	B16 WT Regulation	Compared to Regulation Threshold
Adipoq	N/A	N/A	N/A	No change
Areg	N/A	N/A	N/A	No change
Bmp2	N/A	N/A	N/A	No change
Bmp4	N/A	N/A	N/A	No change
Bmp7	N/A	N/A	N/A	No change
Ccl11	N/A	N/A	N/A	No change
Ccl12	N/A	N/A	N/A	No change
Ccl17	N/A	N/A	N/A	No change
Ccl20	N/A	N/A	N/A	No change
Ccl21c	N/A	N/A	N/A	No change
Ccl22	N/A	N/A	N/A	No change
Ccl4	N/A	N/A	N/A	No change
Ccl5	0.05087	0.19657	3.8641	Up regulated
Cd40lg	N/A	N/A	N/A	No change
Cntf	0.00025	0.00077	3.04209	Up regulated
Csf1	0.00024	N/A	N/A	No change
Csf2	N/A	N/A	N/A	No change
Csf3	N/A	N/A	N/A	No change
Cx3cl1	N/A	N/A	N/A	No change
Cxcl1	0.00709	0.00116	-6.1298	Down regulated
Cxcl10	0.02612	0.01029	-2.53831	Down regulated
Cxcl12	N/A	N/A	N/A	No change
Cxcl3	N/A	N/A	N/A	No change
Cxcl9	N/A	N/A	N/A	No change
Edn1	N/A	N/A	N/A	No change
Fasl	N/A	N/A	N/A	No change
Fgf2	N/A	N/A	N/A	No change
Gapdh	N/A	N/A	N/A	No change
Gdf10	N/A	N/A	N/A	No change
Gdf15	N/A	N/A	N/A	No change
gDNA	N/A	N/A	N/A	No change
Gm12597	N/A	N/A	N/A	No change
Gm13280	N/A	N/A	N/A	No change
Gpi1	0.6667	1.73443	2.60153	Up regulated
Grn	0.00021	0.00078	3.68691	Up regulated
Hmgb1	0.00453	0.01352	2.98386	Up regulated
Hprt	N/A	N/A	N/A	No change
Ifna1	N/A	N/A	N/A	No change
Ifna12	N/A	N/A	N/A	No change
Ifna13	N/A	N/A	N/A	No change
Ifna14	N/A	N/A	N/A	No change
Ifna2	N/A	N/A	N/A	No change
Ifna6	N/A	N/A	N/A	No change
Ifna7	N/A	N/A	N/A	No change
Ifna9	N/A	N/A	N/A	No change
Ifnab	0.00184	N/A	N/A	No change
Ifnb1	N/A	N/A	N/A	No change
Ifng	N/A	N/A	N/A	No change
Il10	N/A	N/A	N/A	No change
Il11	N/A	N/A	N/A	No change
Il12a	N/A	N/A	N/A	No change
Il13	N/A	N/A	N/A	No change
Il15	0.00053	0.00058	1.09331	No change
Il17a	N/A	N/A	N/A	No change
Il17f	N/A	N/A	N/A	No change
Il18	0.00472	0.00411	-1.14901	No change
Il1a	N/A	N/A	N/A	No change
Il1b	N/A	N/A	N/A	No change
Il2	N/A	N/A	N/A	No change
Il21	N/A	N/A	N/A	No change
Il23a	0.00098	0.00281	2.87043	Up regulated
Il3	N/A	N/A	N/A	No change
Il4	N/A	N/A	N/A	No change
Il5	N/A	N/A	N/A	No change
Il6	N/A	N/A	N/A	No change
Il7	N/A	N/A	N/A	No change
Il9	N/A	N/A	N/A	No change
Kitl	N/A	N/A	N/A	No change
Lep	N/A	N/A	N/A	No change
Lif	0.00036	0.00118	3.2704	Up regulated
Lta	0.00041	0.00116	2.83778	Up regulated
Mif	0.43959	0.3781	-1.16264	No change
Mstn	N/A	N/A	N/A	No change
Nrg1	0.00042	N/A	N/A	No change
Osm	N/A	N/A	N/A	No change
PCR	2.831	5.4409	1.9219	No change
Pf4	N/A	N/A	N/A	No change
Ppbp	N/A	N/A	N/A	No change
RQ1	0.00172	0.0044	2.56236	Up regulated
RQ2	N/A	N/A	N/A	No change
RT	N/A	N/A	N/A	No change
Scg2	N/A	N/A	N/A	No change
Sectm1a	N/A	N/A	N/A	No change
Slurp1	N/A	N/A	N/A	No change
Spp1	0.00089	0.00053	-1.68551	No change
Tbp	0.00084	0.00154	1.82148	No change
Tgfb2	0.0009	0.00085	-1.05287	No change
Thpo	N/A	N/A	N/A	No change
Tnf	N/A	N/A	N/A	No change
Tnfrsf11b	N/A	N/A	N/A	No change
Tnfsf10	N/A	N/A	N/A	No change
Tnfsf11	N/A	N/A	N/A	No change
Tnfsf13b	0.00047	0.00113	2.4113	Up regulated
Vegfa	0.10353	0.38516	3.72034	Up regulated
Wnt1	N/A	N/A	N/A	No change
Wnt5a	N/A	N/A	N/A	No change

6.1 Appendix Table 1: Cytokine/chemokine transcripts in B16 WT *vs* B16-XIAP^{KO} (clone 1)

The table shows all the cytokines and chemokine presented in **Figure 3.3A**. Unchanged Cytokine/chemokine transcripts were plotted as black dots. Cytokine/chemokine transcripts, which showed 2-fold up-regulation were plotted as red dots. Cytokine/chemokine transcripts, which showed 2-fold down-regulation were plotted as green dots.

Target	B16 XIAP^{KO} (clone 2) Normalized Expression	B16 WT Normalized Expression	B16 WT Regulation	Compared to Regulation Threshold
Adipoq				No change
Areg				No change
Bmp2				No change
Bmp4				No change
Bmp7				No change
Ccl11				No change
Ccl12				No change
Ccl17				No change
Ccl20				No change
Ccl21c				No change
Ccl22				No change
Ccl4				No change
Ccl5	0.00268	0.19657	73.38654	Up regulated
Cd40lg				No change
Cntf	0.00144	0.00077	-1.87539	No change
Csf1				No change
Csf2				No change
Csf3				No change
Cx3cl1				No change
Cxcl1	0.00329	0.00116	-2.84641	Down regulated
Cxcl10	0.01976	0.01029	-1.92035	No change
Cxcl12				No change
Cxcl3				No change
Cxcl9				No change
Edn1				No change
Fasl				No change
Fgf2				No change
Gapdh				No change
Gdf10				No change
Gdf15				No change
gDNA				No change
Gm12597	0.00070			No change
Gm13280				No change
Gpi1	0.40120	1.73443	4.32312	Up regulated
Grn		0.00097		No change
Hmgb1	0.00440	0.01352	3.07307	Up regulated
Hprt				No change
Ifna1				No change
Ifna12				No change
Ifna13				No change
Ifna14				No change
Ifna2				No change
Ifna6				No change
Ifna7				No change
Ifna9				No change
Ifnab	0.00083			No change
Ifnb1				No change
Ifng				No change
Il10				No change
Il11				No change
Il12a				No change
Il13				No change
Il15	0.00186	0.00058	-3.17238	Down regulated
Il17a				No change
Il17f				No change
Il18	0.00233	0.00411	1.76196	No change
Il1a				No change
Il1b				No change
Il2				No change
Il21				No change
Il23a	0.00213	0.00281	1.32442	No change
Il3				No change
Il4				No change
Il5				No change
Il6				No change
Il7				No change
Il9				No change
Kitl				No change
Lep				No change
Lif		0.00119		No change
Lta	0.00105	0.00116	1.09702	No change
Mif	0.39175	0.37810	-1.03612	No change
Mstn				No change
Nrg1	0.00110			No change
Osm				No change
PCR	7.97213	5.44090	-1.46522	No change
Pf4				No change
Ppbp				No change
RQ1	0.00146	0.00440	3.01870	Up regulated
RQ2				No change
RT				No change
Scg2				No change
Sectm1a				No change
Slurp1	0.00059			No change
Spp1	0.00114	0.00053	-2.16586	Down regulated
Tbp		0.00137		No change
Tgfb2	0.00349	0.00085	-4.09559	Down regulated
Thpo				No change
Tnf				No change
Tnfrsf11b				No change
Tnfsf10				No change
Tnfsf11				No change
Tnfsf13b	0.00145	0.00113	-1.28486	No change
Vegfa	0.18454	0.38516	2.08711	Up regulated
Wnt1				No change
Wnt5a				No change

6.2 Appendix Table 2: Cytokine/chemokine transcripts in B16 WT *vs* B16-XIAP^{KO} (clone 2)

The table shows all the cytokines and chemokine presented in **Figure 3.3A**. Unchanged Cytokine/chemokine transcripts were plotted as black dots. Cytokine/chemokine transcripts, which showed 2-fold up-regulation were plotted as red dots. Cytokine/chemokine transcripts, which showed 2-fold down-regulation were plotted as green dots.

No.	Sex M(1)F(0)	Age (Y)	Localisation	TD in mm	XIAP	CD177
1	0	80	foot	-	+	-
2	0	78	foot	0.49	-	-
3	1	69	n.i.	1.71	++	-
4	1	70	torso	-	-	-
5	0	71	leg	4.55	+	-
6	0	72	n.i.	-	++	+
7	0	73	foot	3.91	++	-
8	0	84	head	-	++	+
9	1	75	hand	37	++	+
10	1	74	n.i.	1.1	++	+
11	1	44	leg	1.46	+++	+
12	1	70	torso	9.6	+++	+
14	1	74	foot	6.8	+++	+++
15	1	84	head	11	++	+
18	0	46	torso	1.75	+++	++
19	0	72	leg	2	++	-
20	1	87	head	4.6	++	-
22	1	76	torso	3	+++	-
23	1	67	torso	1.1	++	-
24	1	50	torso	6.75	+++	-
25	1	58	torso	1.67	+++	-
26	0	70	leg	5.4	+	-
27	0	85	head	-	++	-
29	1	77	torso	6.2	+++	+++
30	1	65	torso	5.7	+++	+
31	1	77	head	2.28	+++	++
32	1	46	torso	1.1	+++	++
33	0	69	head	2.5	+++	+++
34	0	67	arm	2.2	++++	+
35	1	82	head	4	+++	++
36	1	82	arm	2.9	+++	-
37	1	75	torso	2.6	++	++
38	0	91	torso	3.6	++	-
39	1	74	head	4.5	++	++
40	1	76	arm	4	+++	++
41	1	82	head	3.4	++	++
42	1	81	arm	4.8	++	++
43	1	76	leg	11	+++	-
44	1	69	arm	2.5	++++	+
46	1	73	torso	1.5	++++	+++
47	0	72	torso	1.2	+++	+
48	1	46	torso	2.9	+++	++
49	1	52	foot	3.77	++	-
50	1	80	leg	2	+++	+++
51	1	80	torso	3.2	+++	++++
52	0	37	neck	4.5	+++	++++
53	1	72	torso	1.3	+++	++
54	1	45	head	2.1	+++	++
55	0	82	foot	6.5	+++	+++

6.3 Appendix Table 3: Intensities of CD177 and XIAP immunostainings in tumour samples derived from melanoma patients

The table shows detailed patients data used in **Figure 3.10.** Intensities of CD177 and XIAP immunostainings were qualitatively estimated in the same human melanoma. Specific staining intensity for XIAP and CD177, corresponding to relative amounts of infiltrated neutrophils, was arbitrarily set as the following: -, not expressed; +, low; ++, moderate; and +++, strong expression. The sex, age, localization and the thickness (TD) of the tumour are shown for every patient.

Target	*XIAP*^{KO} mouse 1 Normalized Expression	*XIAP*$^{fl/fl}$ Normalized Expression	*XIAP*$^{fl/fl}$ Regulation	Compared to Regulation Threshold
Adipoq				No change
Areg	0.01460	0.00684	-2.13474	Down regulated
Bmp2				No change
Bmp4				No change
Bmp7				No change
Ccl11	0.00281	0.00113	-2.48004	Down regulated
Ccl12	0.00404	0.00207	-1.95010	No change
Ccl17	0.00540	0.00366	-1.47544	No change
Ccl20	0.00142	0.00111	-1.28127	No change
Ccl21c	0.92999	0.10779	-8.62779	Down regulated
Ccl22	0.00127			No change
Ccl4				No change
Ccl5	0.00645	0.00160	-4.02320	Down regulated
Cd40lg				No change
Cntf	0.00437	0.00557	1.27384	No change
Csf1				No change
Csf2				No change
Csf3				No change
Cx3cl1				No change
Cxcl1	0.19287	0.06391	-3.01766	Down regulated
Cxcl10	0.00333	0.00098	-3.39250	Down regulated
Cxcl12	0.00612	0.00952	1.55695	No change
Cxcl3				No change
Cxcl9				No change
Edn1				No change
Fasl				No change
Fgf2	0.00095			No change
Gapdh				No change
Gdf10				No change
Gdf15				No change
gDNA				No change
Gm12597	0.00144	0.00099	-1.45817	No change
Gm13280				No change
Gpi1	0.46971	0.60460	1.28716	No change
Grn				No change
Hmgb1	0.09846	0.08009	-1.22950	No change
Hprt	0.00339	0.00525	1.55023	No change
Ifna1	0.00353	0.01084	3.07321	Up regulated
Ifna12		0.00169		No change
Ifna13		0.00081		No change
Ifna14	0.00055	0.01068	19.34575	Up regulated
Ifna2	0.00133	0.00379	2.84496	Up regulated
Ifna6	0.00066	0.01102	16.72450	Up regulated
Ifna7				No change
Ifna9				No change
Ifnab	0.00958	0.01159	1.20939	No change
Ifnb1				No change
Ifng				No change
Il10				No change
Il11	0.00054	0.00125	2.31267	Up regulated
Il12a				No change
Il13				No change
Il15	0.00718	0.00753	1.04774	No change
Il17a				No change
Il17f				No change
Il18	0.01914	0.00433	-4.41623	Down regulated
Il1a	0.01563	0.00703	-2.22401	Down regulated
Il1b	0.03223	0.00672	-4.79254	Down regulated
Il2				No change
Il21				No change
Il23a	0.00404	0.00344	-1.17416	No change
Il3		0.00353		No change
Il4				No change
Il5				No change
Il6				No change
Il7				No change
Il9				No change
Kitl				No change
Lep				No change
Lif	0.01450	0.01363	-1.06420	No change
Lta	0.02236	0.00664	-3.36869	Down regulated
Mif	0.37555	0.08553	-4.39108	Down regulated
Mstn	0.00680	0.01188	1.74730	No change
Nrg1	0.00376	0.00552	1.46714	No change
Osm	0.00273			No change
PCR	13.03694	18.64120	1.42988	No change
Pf4	0.03025	0.01151	-2.62801	Down regulated
Ppbp	0.00764	0.01282	1.67832	No change
RQ1	0.00348	0.00425	1.21926	No change
RQ2				No change
RT				No change
Scg2				No change
Sectm1a	0.00783	0.00226	-3.46252	Down regulated
Slurp1	0.03191	0.00189	-16.91603	Down regulated
Spp1	0.03558	0.00837	-4.25279	Down regulated
Tbp		0.00080		No change
Tgfb2	0.01168	0.00912	-1.28002	No change
Thpo	0.00139	0.00172	1.23952	No change
Tnf	0.00095			No change
Tnfrsf11b				No change
Tnfsf10				No change
Tnfsf11				No change
Tnfsf13b	0.00157	0.00157	-1.00015	No change
Vegfa	0.75780	0.70239	-1.07889	No change
Wnt1	0.00081	0.00622	7.66397	Up regulated
Wnt5a				No change

6.4 Appendix Table 4: Cytokine/chemokine transcripts in *Hgf-Cdk4*^{R24C} *Xiap*^{KO} (mouse 1) *vs Hgf-Cdk4*^{R24C} *Xiap*$^{fl/fl}$

The table shows all the cytokines and chemokine presented in **Figure 3.13D**. Unchanged Cytokine/chemokine transcripts were plotted as black dots. Cytokine/chemokine transcripts, which showed 2-fold up-regulation were plotted as red dots. Cytokine/chemokine transcripts, which showed 2-fold down-regulation were plotted as green dots.

Target	*XIAP*^{KO} mouse 2 Normalized Expression	*XIAP*$^{fl/fl}$ Normalized Expression	*XIAP*$^{fl/fl}$ Regulation	Compared to Regulation Threshold
Adipoq				No change
Areg	0.01203	0.00684	-1.76012	No change
Bmp2				No change
Bmp4				No change
Bmp7				No change
Ccl11	0.00084	0.00113	1.34926	No change
Ccl12	0.00241	0.00207	-1.16423	No change
Ccl17	0.00184	0.00366	1.98856	No change
Ccl20	0.00193	0.00111	-1.74113	No change
Ccl21c	0.20904	0.10779	-1.93937	No change
Ccl22				No change
Ccl4				No change
Ccl5	0.00078	0.00160	2.04868	Up regulated
Cd40lg				No change
Cntf	0.00274	0.00557	2.02957	Up regulated
Csf1				No change
Csf2				No change
Csf3				No change
Cx3cl1				No change
Cxcl1	0.03907	0.06391	1.63578	No change
Cxcl10	0.00306	0.00098	-3.11356	Down regulated
Cxcl12	0.00311	0.00952	3.06271	Up regulated
Cxcl3				No change
Cxcl9				No change
Edn1				No change
Fasl				No change
Fgf2				No change
Gapdh				No change
Gdf10				No change
Gdf15				No change
gDNA				No change
Gm12597		0.00099		No change
Gm13280				No change
Gpi1	0.21809	0.60460	2.77225	Up regulated
Grn				No change
Hmgb1	0.04569	0.08009	1.75272	No change
Hprt	0.00215	0.00525	2.44017	Up regulated
Ifna1	0.00811	0.01084	1.33703	No change
Ifna12	0.00059	0.00169	2.87717	Up regulated
Ifna13		0.00081		No change
Ifna14	0.00786	0.01068	1.35989	No change
Ifna2	0.00150	0.00379	2.52254	Up regulated
Ifna6	0.01591	0.01102	-1.44273	No change
Ifna7				No change
Ifna9				No change
Ifnab	0.00655	0.01159	1.76856	No change
Ifnb1	0.00090			No change
Ifng				No change
Il10				No change
Il11	0.00115	0.00125	1.08755	No change
Il12a				No change
Il13				No change
Il15	0.00254	0.00753	2.96019	Up regulated
Il17a				No change
Il17f				No change
Il18	0.01238	0.00433	-2.85668	Down regulated
Il1a	0.00311	0.00703	2.25699	Up regulated
Il1b	0.00081	0.00672	8.32979	Up regulated
Il2				No change
Il21				No change
Il23a	0.00415	0.00344	-1.20643	No change
Il3	0.00224	0.00353	1.57567	No change
Il4				No change
Il5				No change
Il6				No change
Il7				No change
Il9				No change
Kitl				No change
Lep				No change
Lif	0.00614	0.01363	2.21882	Up regulated
Lta	0.00551	0.00664	1.20539	No change
Mif	0.18045	0.08553	-2.10985	Down regulated
Mstn	0.00712	0.01188	1.66936	No change
Nrg1		0.00552		No change
Osm	0.00103			No change
PCR	14.18229	18.64120	1.31440	No change
Pf4	0.00506	0.01151	2.27531	Up regulated
Ppbp	0.00082	0.01282	15.71206	Up regulated
RQ1	0.00144	0.00425	2.95247	Up regulated
RQ2				No change
RT				No change
Scg2				No change
Sectm1a	0.00268	0.00226	-1.18549	No change
Slurp1	0.04966	0.00189	-26.32911	Down regulated
Spp1	0.00557	0.00837	1.50158	No change
Tbp		0.00080		No change
Tgfb2	0.00713	0.00912	1.27956	No change
Thpo	0.00096	0.00172	1.78615	No change
Tnf				No change
Tnfrsf11b				No change
Tnfsf10				No change
Tnfsf11				No change
Tnfsf13b	0.00321	0.00157	-2.04405	Down regulated
Vegfa	0.26227	0.70239	2.67807	Up regulated
Wnt1	0.00264	0.00622	2.35159	Up regulated
Wnt5a				No change

6.5 Appendix Table 5: Cytokine/chemokine transcripts in *Hgf-Cdk4*^{R24C} *Xiap*^{KO} (mouse 2) *vs Hgf-Cdk4*^{R24C} *Xiap*$^{fl/fl}$

The table shows all the cytokines and chemokine presented in **Figure 3.13D**. Unchanged Cytokine/chemokine transcripts were plotted as black dots. Cytokine/chemokine transcripts, which showed 2-fold up-regulation were plotted as red dots. Cytokine/chemokine transcripts, which showed 2-fold down-regulation were plotted as green dots.

Target	*XIAP*^{KO} mouse 3 Normalized Expression	*XIAP*$^{fl/fl}$ Normalized Expression	*XIAP*$^{fl/fl}$ Regulation	Compared to Regulation Threshold
Adipoq	0.82939	0.28074	-2.95428	Down regulated
Areg	0.35451	0.04815	-7.36222	Down regulated
Bmp2				No change
Bmp4				No change
Bmp7				No change
Ccl11	0.03503	0.00797	-4.39573	Down regulated
Ccl12	0.04376	0.01460	-2.99759	Down regulated
Ccl17	0.06833	0.02576	-2.65262	Down regulated
Ccl20	0.01510	0.00782	-1.93051	No change
Ccl21c	2.96278	0.75912	-3.90292	Down regulated
Ccl22	0.00895			No change
Ccl4				No change
Ccl5	0.00974	0.01129	1.15929	No change
Cd40lg				No change
Cntf	0.04942	0.03923	-1.25979	No change
Csf1				No change
Csf2				No change
Csf3				No change
Cx3cl1				No change
Cxcl1	0.58693	0.45011	-1.30397	No change
Cxcl10	0.03417	0.00691	-4.94106	Down regulated
Cxcl12	0.07292	0.06708	-1.08705	No change
Cxcl3				No change
Cxcl9				No change
Edn1				No change
Fasl				No change
Fgf2	0.00609			No change
Gapdh				No change
Gdf10				No change
Gdf15				No change
gDNA				No change
Gm12597	0.02155	0.00695	-3.10240	Down regulated
Gm13280	0.00469			No change
Gpi1	3.22818	4.25791	1.31898	No change
Grn				No change
Hmgb1	0.54329	0.56401	1.03813	No change
Hprt	0.02512	0.03696	1.47142	No change
Ifna1	0.16540	0.07637	-2.16577	Down regulated
Ifna12	0.00956	0.01187	1.24123	No change
Ifna13	0.01213	0.00569	-2.13198	Down regulated
Ifna14	0.11114	0.07524	-1.47712	No change
Ifna2	0.04135	0.02669	-1.54948	No change
Ifna6	0.21176	0.07764	-2.72738	Down regulated
Ifna7				No change
Ifna9	0.00729			No change
Ifnab	0.14092	0.08160	-1.72702	No change
Ifnb1	0.00885			No change
Ifng				No change
Il10				No change
Il11	0.03002	0.00878	-3.42096	Down regulated
Il12a	0.00918			No change
Il13	0.00306			No change
Il15	0.02225	0.05300	2.38137	Up regulated
Il17a				No change
Il17f				No change
Il18	0.16634	0.03052	-5.45046	Down regulated
Il1a	0.07070	0.04949	-1.42867	No change
Il1b	0.00611	0.04736	7.74876	Up regulated
Il2				No change
Il21				No change
Il23a	0.05475	0.02423	-2.25912	Down regulated
Il3	0.03091	0.02488	-1.24263	No change
Il4				No change
Il5				No change
Il6				No change
Il7				No change
Il9				No change
Kitl				No change
Lep				No change
Lif	0.10747	0.09598	-1.11970	No change
Lta	0.16616	0.04674	-3.55509	Down regulated
Mif	2.03607	0.60233	-3.38033	Down regulated
Mstn	0.21373	0.08366	-2.55477	Down regulated
Nrg1	0.01166	0.03884	3.33174	Up regulated
Osm				No change
PCR	77.52858	131.28207	1.69334	No change
Pf4	0.06715	0.08106	1.20703	No change
Ppbp	0.03270	0.09031	2.76174	Up regulated
RQ1	0.01926	0.02991	1.55279	No change
RQ2				No change
RT				No change
Scg2				No change
Sectm1a	0.09634	0.01593	-6.04653	Down regulated
Slurp1	0.36167	0.01328	-27.22643	Down regulated
Spp1	0.08312	0.05892	-1.41054	No change
Tbp				No change
Tgfb2	0.08505	0.06424	-1.32397	No change
Thpo	0.02046	0.01211	-1.68861	No change
Tnf	0.00531			No change
Tnfrsf11b				No change
Tnfsf10				No change
Tnfsf11				No change
Tnfsf13b	0.03105	0.01107	-2.80601	Down regulated
Vegfa	7.05005	4.94660	-1.42523	No change
Wnt1	0.04710	0.04380	-1.07542	No change
Wnt5a				No change

6.6 Appendix Table 6: Cytokine/chemokine transcripts in *Hgf-Cdk4*^{R24C} *Xiap*^{KO} (mouse 3) *vs Hgf-Cdk4*^{R24C} *Xiap*$^{fl/fl}$

The table shows all the cytokines and chemokine presented in **Figure 3.13D**. Unchanged Cytokine/chemokine transcripts were plotted as black dots. Cytokine/chemokine transcripts, which showed 2-fold up-regulation were plotted as red dots. Cytokine/chemokine transcripts, which showed 2-fold down-regulation were plotted as green dots.

7 Abbreviation

°C	Degree Celsius	**DNA**	Deoxyribonucleic acid
µg	Microgram	**EDTA**	Ethylenediamine-tetraacetic acid
µl	Microliter	***et al.***	et alteri /-a /-um (and others)
µM	Micromolar	**FCS**	fetal calf serum
BSA	Bovine serum albumin	**GFP**	Enhanced green fluorescent protein
cIAP	Cellular IAP	**IAP**	Inhibitors of apoptosis protein
kDa	Kilodalton	**IBM**	IAP-binding motif
DMSO	Dimethylsulfoxid	**IF**	Immunofluorescence
IP	Immunoprecipitation	**L18-MDP**	L18- Muramyl dipeptide
NFκB	Nuclear Factor κB	**MAPK**	Mitogen activated protein Kinase
MOMP	Mitochondrial outer membrane permeabilisation	**PBS**	Phosphate buffered saline
PCR	Polymerase chain reaction	**pH**	potential hydrogen (lat.)
RIPK	Receptor-interacting serine/threonine-protein kinase	**rpm**	Revolutions per minute
RT	Room temperature	**SD**	standard deviation
SDS	Sodium dodecylsulfate	**SEM**	Standard error of the mean
SMAC	Second mitochondrial derived activator of caspases	**TNF**	Tumour necrosis factor
WB	Western Blot	**XIAP**	X-linked inhibitor of apoptosis
%	Percent sign	**ANOVA**	One-way analysis of variance
min	Minute(s)	**H&E**	Haematoxylin&Eosin

8 Acknowledgements

I would like to thank Prof. Dr. Hamid Kashkar for his supervision during my PhD thesis, for his support and all his advices, which have built my scientific career.

I would like to thank Prof. Manolis Pasparakis and Prof. Jan Riemer for accepting to be part of my PhD defence committee.

I would like to thank all my colleagues in AG Kashkar and AG Krönke for the nice working atmosphere and for all the support they gave me to keep going hard. I would like to thank especially Dr. Melanie Fritsch, Dr. Alina Farid and Dr. Fabian Schorn for reading my thesis. Additionally, I would like to thank Dr. Jens Seeger for the tumour measurement and for accepting taking my defence minutes. Furthermore, I would like to thank Ali Manav for the technical support.

I would like to thank also Dr. Paola Zigrino and Jan Zamek for all the support and help during the paper revision.

Finally, I would like to thank my family for encouraging me to follow my dreams. I would like to thank them for all their prayers and their support. Last and not least, I would like to thank all my friends for being always there for me in the sad and happy moments.

9 Declaration

„Hiermit versichere ich an Eides statt, dass ich die vorliegende Dissertation selbstständig und ohne die Benutzung anderer als der angegebenen Hilfsmittel und Literatur angefertigt habe. Alle Stellen, die wörtlich oder sinngemäß aus veröffentlichten und nicht veröffentlichten Werken dem Wortlaut oder dem Sinn nach entnommen wurden, sind als solche kenntlich gemacht. Ich versichere an Eides statt, dass diese Dissertation noch keiner anderen Fakultät oder Universität zur Prüfung vorgelegen hat; dass sie - abgesehen von unten angegebenen Teilpublikationen und eingebundenen Artikeln und Manuskripten - noch nicht veröffentlicht worden ist sowie, dass ich eine Veröffentlichung der Dissertation vor Abschluss der Promotion nicht ohne Genehmigung des Promotionsausschusses vornehmen werde. Die Bestimmungen dieser Ordnung sind mir bekannt. Darüber hinaus erkläre ich hiermit, dass ich die Ordnung zur Sicherung guter wissenschaftlicher Praxis und zum Umgang mit wissenschaftlichem Fehlverhalten der Universität zu Köln gelesen und sie bei der Durchführung der Dissertation zugrundeliegenden Arbeiten und der schriftlich verfassten Dissertation beachtet habe und verpflichte mich hiermit, die dort genannten Vorgaben bei allen wissenschaftlichen Tätigkeiten zu beachten und umzusetzen. Ich versichere, dass die eingereichte elektronische Fassung der eingereichten Druckfassung vollständig entspricht."

Teilpublikationen: Teile dieser Doktorarbeit wurden in folgender Publikation veröffentlicht:

Daoud, M., Broxtermann, P. N., Schorn, F., Werthenbach, J. P., Seeger, J. M., Schiffmann, L. M., Brinkmann, K., Vucic, D., Tüting, T., Mauch, C., Kulms, D., Zigrino, P., & Kashkar, H. (2022). XIAP promotes melanoma growth by inducing tumour neutrophil infiltration. *EMBO Reports*, e53608. https://doi.org/10.15252/EMBR.202153608

03.06.2022, Mila Daoud

Report

SOURCE DATA | TRANSPARENT PROCESS | OPEN ACCESS

EMBO reports

XIAP promotes melanoma growth by inducing tumour neutrophil infiltration

Mila Daoud[1,2,3,†], Pia Nora Broxtermann[1,2,3,†], Fabian Schorn[1,2,3], J Paul Werthenbach[1,2,3], Jens Michael Seeger[1,2,3], Lars M Schiffmann[1,3,4], Kerstin Brinkmann[5], Domagoj Vucic[6], Thomas Tüting[7], Cornelia Mauch[8], Dagmar Kulms[9,10], Paola Zigrino[8] & Hamid Kashkar[1,2,3,*]

Abstract

Elevated expression of the X-linked inhibitor of apoptosis protein (XIAP) has been frequently reported in malignant melanoma suggesting that XIAP renders apoptosis resistance and thereby supports melanoma progression. Independent of its anti-apoptotic function, XIAP mediates cellular inflammatory signalling and promotes immunity against bacterial infection. The pro-inflammatory function of XIAP has not yet been considered in cancer. By providing detailed *in vitro* analyses, utilising two independent mouse melanoma models and including human melanoma samples, we show here that XIAP is an important mediator of melanoma neutrophil infiltration. Neutrophils represent a major driver of melanoma progression and are increasingly considered as a valuable therapeutic target in solid cancer. Our data reveal that XIAP ubiquitylates RIPK2, involve TAB1/RIPK2 complex and induce the transcriptional up-regulation and secretion of chemokines such as IL8, that are responsible for intra-tumour neutrophil accumulation. Alteration of the XIAP-RIPK2-TAB1 inflammatory axis or the depletion of neutrophils in mice reduced melanoma growth. Our data shed new light on how XIAP contributes to tumour growth and provides important insights for novel XIAP targeting strategies in cancer.

Keywords melanoma; neutrophil; RIPK2; TAB1; XIAP
Subject Categories Cancer; Immunology; Signal Transduction
DOI 10.15252/embr.202153608 | Received 12 July 2021 | Revised 21 March 2022 | Accepted 31 March 2022
EMBO Reports (2022) e53608

Introduction

Cutaneous melanoma is a devastatingly aggressive malignancy arising through the transformation of melanocytes. If detected early, surgical excision with appropriate margins yields a favourable prognosis. Undetected tumour lesions however can grow and progress to invasive disease with a much less favourable course. Genetic, functional and biochemical studies suggested apoptosis resistance as one of the major drivers of melanoma progression (Soengas & Lowe, 2003). Elevated expression of the X-linked inhibitor of apoptosis protein (XIAP) has been frequently associated with melanoma progression in patients (Emanuel *et al*, 2008; Hiscutt *et al*, 2010; Ayachi *et al*, 2019) and several previous studies indicated that XIAP targeting can promote susceptibility to apoptosis in melanoma cells (Lecis *et al*, 2010; Seeger *et al*, 2010b; Hornle *et al*, 2011). Together, these studies highlighted the therapeutic value of XIAP targeting strategies in melanoma treatments.

X-linked inhibitor of apoptosis protein consists of three Baculovirus IAP Repeat (BIR 1–3) motifs promoting protein–protein interaction and a Really Interesting New Gene (RING) domain (Liston *et al*, 1996; Uren *et al*, 1996; Farahani *et al*, 1997) which confers ubiquitin ligase (E3) activity (Yang *et al*, 2000; Nakatani *et al*, 2013). Initial studies identified BIR2, BIR3 and the linker element between BIR1 and BIR2 domains as the responsible caspase binding/inhibitory elements of XIAP rendering apoptosis resistance (Eckelman *et al*, 2006). Independently, XIAP has been long known to induce NFκB activation and MAP kinase signalling by involving TGFβ-activated kinase 1 (TAK1) (Yamaguchi *et al*, 1999) upon direct interaction with the TAK1 binding protein (TAB1) via its BIR1 domain (Lu *et al*, 2007). Further studies showed that XIAP interacts via its BIR2 domain with the kinase domain of the receptor-interacting protein kinase 2 (RIPK2), an adaptor of the NOD

1 Faculty of Medicine and University Hospital of Cologne, Institute for Molecular Immunology, University of Cologne, Cologne, Germany
2 Faculty of Medicine and University Hospital of Cologne, Center for Molecular Medicine Cologne (CMMC), University of Cologne, Cologne, Germany
3 Cologne Excellence Cluster on Cellular Stress Responses in Aging-Associated Diseases (CECAD), University of Cologne, Cologne, Germany
4 Faculty of Medicine and University Hospital of Cologne, Department of General, Visceral, Cancer and Transplant Surgery, University of Cologne, Cologne, Germany
5 The Walter & Eliza Hall Institute of Medical Research (WEHI) and Department of Medical Biology, University of Melbourne, Melbourne, Vic., Australia
6 Department of Early Discovery Biochemistry, Genentech, South San Francisco, CA, USA
7 Laboratory of Experimental Dermatology, Department of Dermatology, University Hospital Magdeburg, Magdeburg, Germany
8 Faculty of Medicine and University Hospital of Cologne, Department of Dermatology and Venereology, University of Cologne, Cologne, Germany
9 Department of Dermatology, Experimental Dermatology, TU-Dresden, Dresden, Germany
10 National Center for Tumor Diseases Dresden, TU-Dresden, Dresden, Germany
*Corresponding author. Tel: +49 221 47884091; E-mail: h.kashkar@uni-koeln.de
†These authors contributed equally to this work

© 2022 The Authors. Published under the terms of the CC BY NC ND 4.0 license

10 CV

Personal Information

Name	Mila Daoud
E-Mail	mila.daoud@uk-koeln.de
Telephone	+49 157 590 19040
Date of birth	24.12.1990
Nationality	Syrian

Higher Education

2018 – Present	**PhD Candidate** at the University Hospital Cologne CECAD Center, Germany XIAP promotes melanoma growth by inducing tumour neutrophil infiltration
2015 – 2017	**MSc in Biomedical Sciences** Bonn- Rhein-Sieg University of Applied Sciences, Germany Optimizing CRISPaint (CRISPR/Cas9 based system) for Endogenous Gene Tagging in Melanoma Cells. Final grade 1.4.
2016 – 2017	**Leadership for Syria Program** at Konstanz University, Germany
2014 – 2015	Second year master in laboratory Diagnosis Tishreen University, Syria
2008 – 2013	**BSc in Pharmacology and Pharmaceutical Chemistry** at Tishreen University, Syria. GPA 1.9 with an excellent esteem.
2007 – 2008	**Baccalaureate of Science Degree** with GPA 1.2.

Awards and Achievements

2021	Poster prize at the 18th International TNF Conference, Switzerland
2021 – Present	Member of the Cell death RTG Graduate School
2019 – Present	Member of the Graduate School for Biological Sciences
2018 – 2021	Pharmacology and Experimental Therapeutics Program fellowship (funded by Bayer)
2015 – 2017	German Academic Exchange Service (DAAD) Scholarship
2011 – 2013	One of the top three students. Certificate of Martyr Basil Al-Assad for academic at Tishreen University, Syria

Publication

2022	XIAP promotes melanoma growth by inducing tumour neutrophil infiltration- **Embo Report** 202153608 Mila Daoud, Pia Nora Broxtermann, ……..., Hamid Kashkar
2020	Adoptive T Cell Therapy Targeting Different Gene Products Reveals Diverse and Context-Dependent Immune Evasion in Melanoma- **Immunity** 53(3), 564-580.e9 Maike Effern, Nicole Glodde,....., Mila Daoud,....., Michael Hölzel

Work Experience

2017	Student assistant at the Clinical Chemistry and Clinical Pharmacology Institute, University Hospital Bonn
2014 – 2015	Laboratory assistant at the Department of Laboratory Diagnosis Al Assad University Hospital, Syria

2014 – 2015	Teaching assistant in the practical sessions Tishreen University, Syria
2014 – 2015	Medical representative, Syria

Languages

Arabic	Native language
English	Fluent both in Spoken & Written
German	B2 level (telc certificate)

Computer Skills

Standard	Windows, Word, Excel, Power Point, Photoshop
Research related Programs	Snap Gene Viewer, Mendeley, Adobe Illustrator,GraphPad Prism, Flowjo ImageJ, Adobe Photoshop

Volunteer Works and Communication Skills

2018	Helping old people at Rosental Haus, Bonn
2016 – 2017	Supporting the integration of new students as Study Buddy at Bonn- Rhein –Sieg University of Applied Sciences, Bonn
2016 - 2017	A member of DAAD-Freundeskreis Bonn, meeting with a host family through the program "Germany behind the scenes".
2016 - Present	A member of DAAD-Freundeskreis Köln-Bonn, meeting with international DAAD scholarship students.
2016 - Present	Participation in a Tandem-Program together with students of the German Academic Scholarship Foundation (the Studienstiftung des deutschen Volkes).

Organizational Skills

2021- Present	PhD Career Perspective Events Organizing Committee Member Organizing career seminars for PhD and Post.doc students
2021	Holding a master lab course for one week at the University of Cologne
2020- Present	CECAD Committee Member Organizing annual retreat and soft skills courses for PhD students

Referees

Prof. Hamid Kashkar Email: h.kashkar@uni-koeln.de

Cologne, June 2022